ornl

OAK RIDGE NATIONAL LABORATORY

MARTIN MARIETTA

ORNL/TM-11577

MARTIN MARIETTA ENERGY SYSTEMS LIBRARIES

3 4456 0314795 8

Determination of the Solubility of Solid CCl_4 in Supercritical CF_4 Subambient Temperature

T. A. Barber
P. R. Bienkowski
H. D. Cochran

OAK RIDGE NATIONAL LABORATORY
CENTRAL RESEARCH LIBRARY
CIRCULATION SECTION
4500N ROOM 175
LIBRARY LOAN COPY
DO NOT TRANSFER TO ANOTHER PERSON
If you wish someone else to see this report, send in name with report and the library will arrange a loan.

OPERATED BY
MARTIN MARIETTA ENERGY SYSTEMS, INC.
FOR THE UNITED STATES
DEPARTMENT OF ENERGY

This report has been reproduced directly from the best available copy.

Available to DOE and DOE contractors from the Office of Scientific and Technical Information, P.O. Box 62, Oak Ridge, TN 37831; prices available from (615) 576-8401, FTS 626-8401.

Available to the public from the National Technical Information Service, U.S. Department of Commerce, 5285 Port Royal Rd., Springfield, VA 22161.
NTIS price codes—Printed Copy: A07 Microfiche A01

This report was prepared as an account of work sponsored by an agency of the United States Government. Neither the United States Government nor any agency thereof, nor any of their employees, makes any warranty, express or implied, or assumes any legal liability or responsibility for the accuracy, completeness, or usefulness of any information, apparatus, product, or process disclosed, or represents that its use would not infringe privately owned rights. Reference herein to any specific commercial product, process, or service by trade name, trademark, manufacturer, or otherwise, does not necessarily constitute or imply its endorsement, recommendation, or favoring by the United States Government or any agency thereof. The views and opinions of authors expressed herein do not necessarily state or reflect those of the United States Government or any agency thereof.

ORNL/TM-11577

Chemical Technology Division

DETERMINATION OF THE SOLUBILITY OF SOLID CCl_4 IN SUPERCRITICAL CF_4 SUBAMBIENT TEMPERATURE

T. A. Barber*
P. R. Bienkowski*
H. D. Cochran

*Department of Chemical Engineering, University of Tennessee, Knoxville, Tennessee 37916.

This report was prepared as a dissertation and submitted to the faculty of the Graduate School of the University of Tennessee in partial fulfillment of the degree of Master of Science in Chemical Engineering. This work was supported, in part, by the Division of Chemical Sciences, USDOE, under subcontract with the University of Tennessee. The work was performed at ORNL.

Date Published–July 1990

Prepared by the
OAK RIDGE NATIONAL LABORATORY
Oak Ridge, Tennessee 37831
operated by
MARTIN MARIETTA ENERGY SYSTEMS, INC.
for the
U.S. DEPARTMENT OF ENERGY
under contract DE-AC05-84OR21400

MARTIN MARIETTA ENERGY SYSTEMS LIBRARIES

3 4456 0314795 8

ABSTRACT

A dynamic experimental apparatus developed for supercritical fluid studies was used to determine the solubility of solid CCl_4 in supercritical CF_4. An on-line quadrupole mass spectrometer was utilized for analysis of the effluent. The direct coupling of supercritical extraction with mass spectrometry offers a quantitative method for the direct determination of the solute mole fraction in the supercritical fluid. Valid data were obtained for two isotherms at 244K and 249K. Solubilities were found to range from 5.1×10^{-4} to 2.58×10^{-2} mole fraction. These data will broaden the data base to support the testing of new theoretical models for predicting supercritical behavior. This study successfully correlated the data by two different computational approaches: the compressed gas model and the Kirkwood-Buff fluctuation integral model. As the critical point for CF_4 is 227.6 K, these data are among the few supercritical solubility data available at subambient temperature.

TABLE OF CONTENTS

CHAPTER		PAGE
I.	INTRODUCTION	1
	1.1 Objectives	2
II.	BACKGROUND	3
	2.1 Industrial Applications	3
	2.2 SCFE Advantages	4
III.	THEORY	7
	3.1 Phase Behavior	7
	3.2 Modeling Solubility	10
	3.2.1 Compressed Gas Model	12
	3.2.2 Kirkwood-Buff LC Model	18
	3.2.3 Other Models	22
	3.2.4 Model Summary	24
IV.	EXPERIMENTAL	25
	4.1 Experimental Overview	25
	4.2 Equipment and Operations	30
	4.2.1 Materials	30
	4.2.2 Pressurizing System and Extraction Column	31
	4.2.3 Expansion and Analysis	33
	4.3 Calibration and Interpretation	35

V. RESULTS AND DISCUSSION 40

5.1 CF_4 - CCl_4 Solubility Data 40

5.2 Modeling 45

5.3 Data Reliability 53

5.3.1 Summary of Error Analysis 53

5.3.2 Summary of Data Validation 53

VI. CONCLUSIONS AND RECOMMENDATIONS 54

6.1 Conclusions 54

6.2 Recommendations 55

6.2.1 Future Solubility Studies 55

6.2.2 Future Modeling 55

LIST OF REFERENCES 57

APPENDICES 65

APPENDIX A RAW DATA 66

APPENDIX B ERROR ANALYSIS 75

APPENDIX C COMPUTER PROGRAMS 80

APPENDIX D DATA VALIDATION 107

VITA 118

LIST OF TABLES

TABLE		PAGE
2.1	Properties of Gas, Supercritical, and Liquid Phases	5
4.1	Pressure Correction Data	37
5.1	Solubility Isotherms of CCl_4 in Supercritical CF_4 at 244K and 249K	41
5.2	P-R CG Modeling Correlations	47
5.3	K-B LC Modeling Correlations	49
5.4	Model Correlation Comparison	52
D.1	Solubility Isotherms of CCl_4 in Supercritical CF_4 at 234K and 239K	109
D.2	Flow Rate Experiment Results	111
D.3	Column Velocities at Different Pressures	113

LIST OF FIGURES

FIGURE PAGE

3.1 Phase Diagram of CO_2 Showing Supercritical Region 8

3.2 Six Categories of Phase Behavior in Binary Fluid Systems 9

3.3 Simple Category I Solid-SCF P-T and P-T-x Phase Diagrams 10

4.1 Schematic Diagram of Constant-Composition View-Cell Apparatus 26

4.2 Schematic Diagram of a Capillary SFC-MS Apparatus 29

4.3 Schematic Diagram of SFC-MS Interface 29

4.4 Direct Coupled SCFE-MS Apparatus 32

4.5 Equilibrium Flow Rate 34

4.6 Double Orifice Sample Inlet to MS 34

4.7 Mass Spectrometer Calibration Curve 35

4.8 MS Pressure Correction Curve 37

4.9 Linearized MS Pressure Correction Curve 38

4.10 Mass Spectra of CCl_4 and CF_4 39

5.1 Mole Fraction of CCl_4 vs. Pressure at 244K and 249K 42

5.2 CF_4 Density vs. Pressure 42

5.3 Mole Fraction of CCl_4 vs. Density at 244K and 249K 43

5.4 ln E vs. Density at 249K 44

FIGURE PAGE

5.5 ln E vs. Density at 244K 45

5.6 P-R Modeling at 249K 47

5.7 P-R Modeling at 244K 48

5.8 K-B Modeling at 249K 50

5.9 K-B Modeling at 244K 50

D.1 Mole Fraction of CCl_4 vs. Pressure at 234K and 239K 110

D.2 I/P vs. Superficial Velocity Results 112

D.3 Column Mean Velocity Profile 114

D.4 P-R Modeling at 239K 116

D.5 Temperature Dependence of k_{ij} 116

D.6 P-R Modeling at 234K 117

NOMENCLATURE

A	Dimensionless constant defined by equation (3-18)
a	Peng-Robinson parameter, $bar-cm^3/gmol^2$ (section 3.2.1)
AAD	Objective function defined by equation (5-4)
B	Dimensionless constant defined by equation (3-19)
b	Peng-Robinson parameter, $cm^3/gmol$
f	Fugacity, bar
G	Kirkwood-Buff fluctuation integral, $cm^3/gmol$
I	Ion current (10^{-6} amp)
K	Characteristic parameter defined by equation (3-11)
K_T	Isothermal compressibility, $-bar^{-1}$ (section 3.2.2)
k_{ij}	Peng-Robinson binary interaction parameter
N	Number of experimental data
P	Pressure, bar
R	Gas constant, $bar-cm^3/gmolK$
T	Temperature, K
v^s	Solid molar volume, $cm^3/gmol$
$\bar{v}_0$	Superficial velocity, cm/min
$\bar{v}$	Mean velocity, cm/min
y	Mole fraction
Z	Compressibility factor

Greek Letters

α Parameter defined by equation (3-11)

γ Activity coefficient

ϕ Fugacity coefficient

ω Acentric factor

Superscript

cal Calculation

exp Experimental

f Fluid phase

s Solid phase

sat Saturation

∞ Infinite solute dilution

Subscript

c Critical point

i i component

j j component

r Reduced

corr Corrected

CHAPTER I

INTRODUCTION

Applications of supercritical fluid technology have come to the forefront of technological research including supercritical fluid extraction (SCFE), supercritical fluid chromatography, chemical reactions in supercritical fluids, and polymer fractionation. As a result of high energy costs and the demand for stringent health and safety standards, SCFE has become increasingly important as an alternative process for conventional separations in commercial processes.

Most systems for which supercritical solubility data exist are large heavy organic compounds in small, simple solvent molecules such as the naphthalene-CO_2 system. In comparison the molecular size of CCl_4 is small, approximately 1.3 times the diameter of CF_4 while the intermolecular attraction (i.e. Lennard-Jones ε parameter) is uncharacteristically large, about 2.4 times that of CF_4. This particular solute-solvent system was chosen because both molecules can be approximated reasonably well as spherically symmetric easing the theoretical interpretation of the results.

In order to measure solubility, an extraction device with a means to analyze the effluent or a constant composition device must be developed. Many SCFE devices are described in the literature and are classified as either dynamic (flow-type) or static apparatuses. Since in this study only the equilibrium composition of the solute-rich supercritical gas phase was measured, a flow-type apparatus was chosen. Direct coupling of SCFE to a mass spectrometer was utilized to analyze the effluent providing a method of on-line analysis.

As commercial processes are developed, the understanding of SCFE behavior through thermodynamic models and molecular models by statistical mechanics has taken on considerable importance. Though advances in modeling solubilities have been made in the past decade, challenges remain in the testing of new theoretical models for correlating and predicting supercritical behavior. Two models are examined in this study to correlate the data. The compressed gas model utilizing the Peng-Robinson equation of state with conventional mixing rules was investigated and compared to results from the Kirkwood-Buff local composition model which is based on the Kirkwood-Buff solution theory.

This study provides a data base for current and future supercritical modeling. In addition, this study is among the few supercritical solubility studies at subambient temperature.

1.1 Objectives

To evaluate the supercritical fluid extraction of solid CCl_4 with CF_4, experimental solid-vapor equilibrium on the system are needed. The objectives of this study were:

(1) to modify the apparatus originally built for high pressure MoF_6-- CF_4 solid-vapor equilibrium measurements utilizing direct-coupled mass spectrometry.

(2) to measure solid-vapor equilibrium data for the CCl_4–CF_4 system as a function of temperature and pressure

(3) to correlate the solubility data from the compressed gas model using a cubic equation of state and a Kirkwood-Buff model.

CHAPTER II

BACKGROUND

Observation of enhanced solubility in a supercritical gases at high density occurred over a century ago when Hannay and Hogarth (1879) first reported the solubilities of inorganic salts in supercritical ethanol to the Royal Society of London in 1879. Though researchers such as Villard (1896) and Buchner (1906) in the late 1800's and early 1900's made significant additions to the experimental base, interest waned until nearly a half century later. In 1955 Todd and Elgin (1955) studied the high pressure phase equilibria of several liquid and solid solutes in supercritical ethylene. They and others proposed exploiting supercritical fluid solubilities as an extraction scheme for solid-fluid systems. Since that time supercritical fluids have offered an alterative process for separation in commercial processes.

2.1 Industrial Applications

Distillation and liquid extraction have long been the conventional separation and purification techniques to separate binary and multicomponent mixtures in the petroleum, chemical, and food industries. Some of the current applications of SCFE are: the decaffeination of coffee and tea (*Zosel*, 1978); the deoiling of potato chips (*Wolkomir*, 1984); the recovery of vegetable oils from crushed seeds (*Stahl* et al., 1980); and the deasphalting of heavy oils with supercritical propane (*Zhuze*, 1960). Other potential commercial applications for SCFE are: the removal of nicotine from tobacco (*Hubert* and *Vitzthum*,

1978); the molecular weight fractionation of polymer mixtures (*McHugh* and *Krukonis*, 1986); and the removal of organic chemicals from fermentation broths (*Willson* and *Cooney*, 1985).

Perhaps the greatest potential of SCFE lies in the recovery of valuable products produced from bioprocesses. These products are often present in low concentrations. Product recovery is cost-intensive and technically difficult accounting for as much as 80% of the expense of an antibiotic production operation (*Bienkowski* et al., 1988). For example, many antibiotic or biological compound separations require:

(1) 60-100 processing stages using liquid-liquid extraction (LLE)

(2) a difficult precipitation or an expensive distillation to recover the antibiotic from the solvent

(3) many toxic LLE solvents necessitate extensive and expensive washing procedures for safety before use

In addition many biological compounds are thermally labile, degrading when exposed to high temperature. The operating temperature of a supercritical fluid extraction is controlled by the critical temperature of the solvent selected. Many supercritical solvents have critical temperatures near ambient temperature, thus protecting heat sensitive compounds and making SCFE less energy intensive.

2.2 SCFE Advantages

SCFE offers considerable flexibility for an effective separation through controlling pressure, temperature, and choice of solvents. A supercritical solvent that could extract the compound of interest directly and allow recovery with a drop in pressure and/or temperature

would offer distinct advantages over conventional separation methods.

Supercritical fluid solvents exploit the physical properties of the critical region to offer advantages over conventional solvents. These advantages can be summarized (*McHugh* and *Krukonis*, 1986) as follows:

(1) combines gas-like transport properties with liquid-like solvent powers;

(2) offers moderate operating temperature;

(3) utilizes non-toxic gases as solvents;

(4) dissolves non-volatiles; and

(5) provides for efficient product recovery.

From Table 2.1 (*Schneider*, 1988) one can compare the physico-chemical properties of supercritical fluid phases to those of gases and liquids. The enhanced solvent power of up to ten orders of magnitude in supercritical fluids is quite similar to that of liquids. The density of the supercritical fluid phase is much closer to that of a liquid; however, the binary diffusion coefficients and viscosities resemble those of compressed gases.

Table 2.1. Properties of Gas, Supercritical, and Liquid Phases

Properties	Gas(1atm)	SCF Phase	Liquid
density (g/cm^3)	10^{-3}	0.3	1.0
diffusivity (cm^2/s)	10^{-1}	10^{-3} to 10^{-4}	$<10^{-5}$
viscosity (g/cm·s)	10^{-4}	10^{-3} to 10^{-4}	10^{-2}

Most of these phenomena are favorable for SCFE with respect to mass transfer. However, even with a well chosen solvent, SCFE is not without disadvantages (*McHugh* and *Krukonis*, 1986) which include:

(1) relatively high pressures are involved

(2) the existence of baratropic states where the coexisting phases have the same densities

(3) convection effects

(4) the slowing down of equilibration near the critical state

For SCFE to reach its maximum potential, its theory and practical application must be well understood.

CHAPTER III

THEORY

Increased emphasis on the application of supercritical fluids has resulted in the need for accurate knowledge concerning the phase equilibrium of multi-component mixtures. Excellent discussion of supercritical fluid solubility exists in literature. Among the many reviews, several recent papers provide abbreviated but accurate discussion of SCFE theory (*Lira*, 1988; *Johnston*, 1989). Several books offer discussions on supercritical solubility and phase behavior (*Squires* and *Paulaitis*, 1987; *Johnston* and *Penninger*, 1989) with the book by McHugh and Krukonis (1986) as perhaps the best introduction into the field.

3.1 Phase Behavior

Supercritical fluid extraction exploits the pressure-density relationships of the critical region to allow fluids like CF_4 to function as solvents. Figure 3.1 is a phase diagram of reduced density vs. reduced pressure for CO_2 discussed by many authors, e.g. Williams (1981), Giddings et al. (1968) and Schneider (1978).

The shaded area is the critical region where the densities are acceptable for SCFE. This region lies just above the critical temperature, $T_c = 304.4K$ ($T_r = 1.0$ isotherm), and below moderate temperatures, $T = 334.6K$ ($T_r = 1.1$ isotherm). Here in this region the isotherm curves flatten out and small changes in pressure result in large changes of volume or density. The increase in density towards liquid-like density allows a supercritical fluid to be an effective solvent.

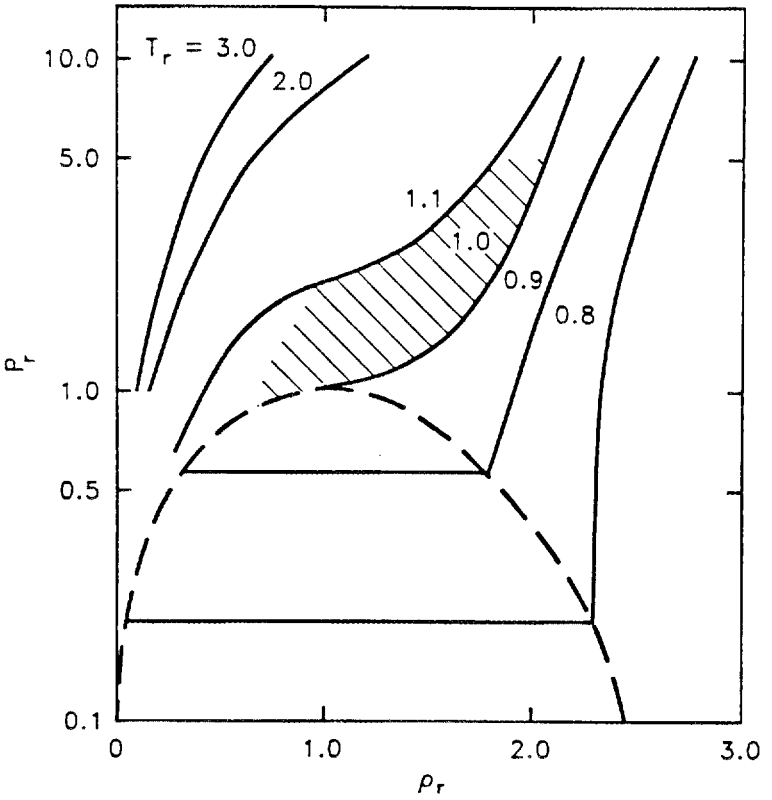

Fig. 3.1. Phase diagram of CO_2 showing supercritical region.

Although SCFE in a commercial process could involve multicomponent mixtures, the essential features of the phase equilibrium behavior at elevated pressures can be illustrated by considering only binary mixtures. Classifications are usually based on PT projections of mixture critical curves and three-phase equilibrium lines.

Figure 3.2 (*Prausnitz* et al., 1986) is a representation of the six major cases of binary phase diagrams representing regions of multiple phases in pressure-temperature-composition (P-T-x) space projected onto a two dimensional pressure-temperature (P-T) diagram. These regions are composed of two-phase areas of liquid-vapor (LV), solid-vapor (SV) or liquid-liquid (LL) equilibria; three-phase lines of liquid-liquid-vapor (LLV), solid-liquid-vapor (SLV) or solid-solid-vapor (SSV).

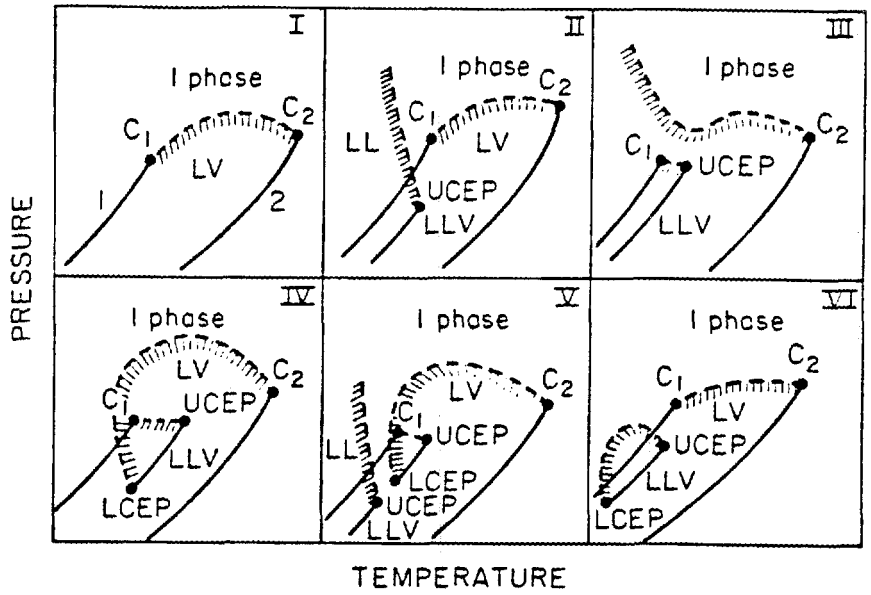

Fig. 3.2. Six categories of phase behavior in binary fluid systems. C = critical point; L = liquid; V = vapor; UCEP = upper critical end point; LCEP = lower critical end point. Dashed curves are critical lines and heterogeneous regions marked by hatching (*Prausnitz* et al., 1986).

As an example, Figure 3.3 (*McHugh* and *Krukonis*, 1986) is the simplest P-T diagram of a solid-SCF system which make up a large and important category of binary mixtures. The melting point of the solid is greater than the critical temperature of the supercritical fluid. Curves CD and MH are the pure-component vapor-pressure curves of the SCF and the solid component respectively. Curve MN is the pure solid component melting curve, and the EM curve is the solid component sublimation curve. Points D and H represent pure component critical points.

The distinguishing feature of this simple system is the continuous curve between the critical points of the pure components and the three-phase solid-liquid-vapor (SLV) line.

Freezing point depression is observed as pressure increases and more gas dissolves in the heavy liquid phase.

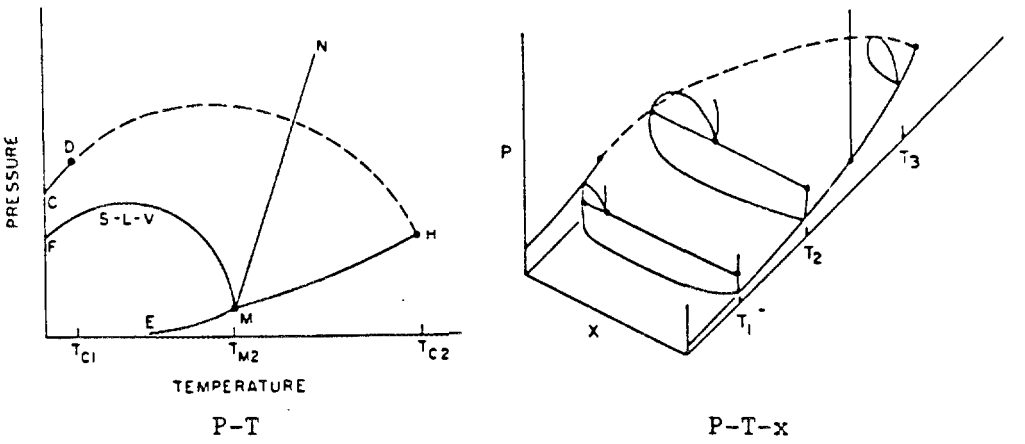

Fig. 3.3 Simple category I solid-SCF P-T and P-T-x phase diagrams.

Many other examples exist in the literature (e.g. *Paulaitis* et al., 1983) for all categories. CO_2 and n-octane is an example of a category II binary mixture (see Figure 3.2) where a continuous mixture critical curve similar to category I is observed; however, at lower temperatures a second critical curve exists for liquid-liquid equilibrium. The lower bound on this critical curve is the intersection with the three phase LLV line and the upper bound (not shown) will be the intersection with a three-phase SLL line at very high pressures (*Street*, 1974). Descriptions of the other categories as well as discussions on ternary mixtures can be found in previously cited literature.

3.2 Modeling Solubility

The solvent strength of a supercritical fluid may be manipulated over a wide range with a small change in temperature or pressure. This ability to fine tune the solvent strength

of a supercritical fluid is its most unique feature. The solutions are often highly nonideal and far from the ideal gas reference states where fugacity coefficients for solutes, ϕ_i^s, may be many orders of magnitude below unity. Primarily four problems exist in predicting phase equilibria in the SCF state (*Johnston* et al., 1989), they are:

(1) the vapor pressure is the most important indicator of a solute's solubility as the greater the vapor pressure the greater the solubility; however, the vapor pressure is often unavailable for relatively nonvolatile solids;

(2) the equation of state (EOS) must predict densities accurately in the critical region, which is not a serious problem for dilute systems, since accurate equations of state are available for pure fluid densities (*Reynolds*, 1979);

(3) SCF solutions are often highly asymmetric in that there are huge differences in the sizes and energies of the components. As a result, binary interaction constants must be correlated from data such as when using conventional corresponding states theory based on critical properties; and

(4) The solutions are highly compressible, which leads to solvent condensation or clustering about the solute even in nonpolar systems.

To understand the influence of vapor pressure on the solubility of a solute in a supercritical solvent, it is convenient to define an enhancement factor, E. The enhancement factor ($E = y_{exp}P/p^{sat}$) is the extent to which pressure enhances the solubility of a solid in the gas compared to the solubility calculated from the ideal gas expression $y_{ideal} = p^{sat}/P$. This factor provides a means to focus on interactions in the SCF phase.

The structure of SCF solutions is unusual because of the large compressibility and larger free volume when compared to a liquid solution. This allows attractive forces to move molecules into energetically favorable positions to form clusters. Evidence of

clustering was initially given by observation that the partial molar volume of a solute, such as naphthalene reaches negative values thousands of $cm^3/gmol$ at infinite dilution (*Eckert* et al., 1983). The small, highly compressed solvent condenses or clusters about the attractive solute. A recent review (*Johnston* et al., 1989) explained the use of UV-vis and fluorescent probes to study the clustering in greater detail. Some of the advanced models include this clustering phenomenon.

3.2.1 Compressed Gas Model

The more common and general approaches to supercritical modeling are the solubility parameter approach by Czubryt et al (1970), the expanded liquid approach by Mackay and Paulaitis (1979) and the compressed gas approach by Prausnitz et al. (1986).

Though the treatment by the virial equation of state is rigorous, it is of limited utility because of difficulties in evaluating higher virial coefficients and series convergence problems at higher pressures. The solubility parameter approach uses approximate methods for applying solubility parameter concepts to supercritical fluids since the density of a SCF is 0.3 to 0.9 times the equivalent liquid density. The key approximations are:

(1) the solubility parameter, δ_g, is a function only of density, ρ, and is approximated by the linear relationship below

$$\delta_g = \delta_{liq}\,[\rho/\rho_{liq}] \tag{3-1}$$

(2) the solubility enhancement is related by

$$\ln E = (v_0\delta_o^2/RT)(\delta_r)(2-\delta_r) \tag{3-2}$$

where v_0 - solute molar volume

δ_0 - solute solubility parameter

δ_r - reduced solubility parameter (δ_g/δ_0)

This method showed excellent qualitative agreement but did not adequately allow for density-dependent entropy effects, pressure-volume effects, and the various molecular subtleties which render regular solution theory inexact (*Czubryt* et al., 1970).

The expanded liquid approach treats the supercritical fluid as an expanded liquid. In stead of expressing $f_2^f = y_2\phi_2 P$ as shown below in the compressed gas model, at a fixed temperature T, the fluid-phase fugacity is expressed as a function of pressure P and mole fraction y_2

$$f_2^f = y_2\gamma_2(y_2,P^0)f_2^{0l}(P^0)\exp\int_{P^0}^{P}\bar{v}_2\frac{dP}{RT} \tag{3-3}$$

where f_2^{0L} - fugacity of pure liquid

P^0 - arbitrary fixed reference pressure

γ_2 - activity coefficient as a function of composition only

$\bar{v}_2$ - solute partial molar volume

A convenient choice for P^0 was the critical pressure, P_c, of the solvent where the solubility of the solute is negligible. Then the activity coefficient is essentially the activity coefficient at infinite dilution, γ_2^∞, and $\bar{v}_2 = \bar{v}_2^\infty$. Equation (3-3) can be rewritten as

$$f_2^f = y_2\gamma_2^\infty(P_c)f_2^{0l}(P_c)\exp\int_{P_c}^{P}\bar{v}_2^\infty\frac{dP}{RT} \tag{3-4}$$

The expanded liquid approach was used to correlate the solubility of naphthalene in supercritical CO_2 and ethylene (*Mackay* and *Paulaitis*, 1979). Though a better quantitative and qualitative agreement compared to results from the compressed gas model was obtained, two mixture parameters are required - an activity coefficient at infinite dilution for the heavy solute (γ_i^∞) and a binary interaction parameter (k_{ij}). Few techniques have been developed to calculate the reference activity coefficient, although Eckert et al. (1986) have developed a

method to correlate this parameter with the heat of vaporization of the solute (*Johnston* et al., 1989).

The simplest computational approach is the compressed gas model which utilizes a cubic equation of state. Cubic equations of state have been frequently used because of their simplicity and relative accuracy over a broad range compared to more complex equations. A cubic equation such as the Peng-Robinson equation of state requires only critical properties (T_c,P_c) and the acentric factor ω for application to a fluid system. The compressed gas model offers the computational advantage of only one single fitted parameter (k_{ij}) which accounts for binary interaction in mixtures. However, it should be noted that the solubility calculations are sensitive to the empirical mixing rules which are required for these equations of state.

The solubility of a non-volatile solute in a supercritical solvent is determined from standard thermodynamic relationships by equating the condensed-phase and fluid-phase fugacities for the heavy component i where at equilibrium

$$f_i^s = f_i^f \tag{3-5}$$

The fugacity of component i in the fluid phase can be expressed as

$$f_i^f = \phi_i^f \, y_i \, P \tag{3-6}$$

where ϕ_i^f - fugacity coefficient of the fluid phase

y_i - mole fraction

P - pressure

The fugacity of component i in the condensed phase can be expressed (assuming no

solvent is dissolved in the solute) as

$$f_i^f = p_i^{sat}\,\phi_i^{sat}\exp\int_{p_i^{sat}}^{P}\frac{v_i^s}{RT}\,dP \tag{3-7}$$

where p_i^{sat} - saturated vapor pressure

ϕ_i^{sat} - fugacity coefficient of the condensed phase at saturation pressure

v_i^s - molar volume of the solid

T - temperature

R - gas constant

Equating equation (3-6) to (3-7) and assuming the solid is incompressible, the solubility of solute in the supercritical fluid can be expressed as

$$y_i = \frac{p_i^{sat}}{P}\,\frac{\phi_i^{sat}}{\phi_i^f}\exp\left[\frac{v_i^s\left(P-p_i^{sat}\right)}{RT}\right] \tag{3-8}$$

By assuming the fugacity coefficient for the solid at saturation condition is unity (sublimation pressures are typically low, therefore, ϕ_i^f=1.0, equation (3-8) is further simplified to

$$y_i = \frac{p_i^{sat}}{P}\,\frac{1}{\phi_i^f}\exp\left[\frac{v_i^s\left(P-p_i^{sat}\right)}{RT}\right] \tag{3-9}$$

where the exponential term is the Poynting correction for the fugacity of the pure solid.

The fugacity coefficient, ϕ_i^f, is obtained from an equation of state using an exact thermodynamic relationship (*Prausnitz* et al., 1986). In pressure-explicit terms (P = {T,V, n_1, n_2 ...}) the fugacity coefficient is expressed as

$$\ln\phi_i^f = \frac{1}{RT}\int_V^{\infty}\left[\left(\frac{\partial P}{\partial n_i}\right)_{T,V,n_j} - \frac{RT}{V}\right]dV - \ln Z \tag{3-10}$$

where the key term is $(\partial P/\partial n_i)_{T,V,n_j}$ which is not a partial molar quantity. The accurate calculation of $(\partial P/\partial n_i)_{T,V,n_j}$ and hence the fugacity coefficient is required for estimation of the solute's solubility in the supercritical fluid. Haselow et al. (1985) evaluated nine equations of state on 31 binary mixture systems for their ability to describe supercritical extraction. In many of the cases, the Peng- Robinson equation of state (*Peng* and *Robinson*, 1976) offers the best fit to the experimental data with a 26% average absolute deviation (AAD) between calculated and experimental data when physical properties are known. The Peng-Robinson EOS is expressed as

$$P = \frac{RT}{V-b} - \frac{a(T)}{V(V-b) + b(V-b)} \tag{3-11}$$

where a(T) accounts for the attractive forces between molecules and parameter, b, represents the repulsive interaction force, which is related to the size of hard spheres. Pure component parameters a_i(T) and b_i are determined from the corresponding states theory, based on the critical states. The parameter a_i(T) is expressed as

$$a_i(T) = a_i(T_c) \cdot \alpha(T_{ri}, \omega_i) \tag{3-12}$$

where the a_i(T) at the critical point is

$$a_i(T_c) = 0.45724 \cdot \left[\frac{R^2 T_{ci}^2}{P_{ci}}\right] \tag{3-13}$$

and the variation of α with temperature is expressed as a function of reduced temperature (T_r) and the acentric factor,

$$\alpha(T_{ri}, \omega_i) = \left[1 + K_i\left[1 - \sqrt{T_{ri}}\right]\right]^2 \tag{3-14}$$

where a constant characteristic of each component, K_i, is

$$K_i = 0.37464 + 1.542260\omega_i - 0.26992\omega_i^2 \tag{3-15}$$

The parameter $b_i(T)$ is expressed as

$$b_i(T) = b_i(T_c) \tag{3-16}$$

where $b_i(T_c)$ at the critical point is

$$b_i(T_c) = 0.07780\left[\frac{RT_{ci}}{P_{ci}}\right] \tag{3-17}$$

In order to solve the Peng-Robinson equation for the fugacity coefficient, it is necessary to establish mixing rules for the parameters $a_i(T)$ and $b_i(T)$. The following conventional mixing rules have proven suitable

$$a = \sum_{i=1}^{n}\sum_{j=1}^{n} y_i\ y_j\ a_{ij} \tag{3-18}$$

$$b = \sum_{i=1}^{n} y_i\ b_i \tag{3-19}$$

where

$$a_{ij} = (1 - k_{ij})\sqrt{a(T)_i\, a(T)_j} \tag{3-20}$$

where k_{ij} is the binary interaction parameter which is obtained empirically by regressing the mixture data of interest.

The Peng-Robinson equation (3-11) can be rewritten in terms of the compressibility factor, Z as

$$Z^3 - (1 - B)Z^2 + (A - 3B^2 - 2B)Z - (AB - B^2 - B^3) = 0 \tag{3-21}$$

where

$$A = \frac{aP}{R^2T^2} \tag{3-22}$$

$$B = \frac{bP}{RT} \tag{3-23}$$

$$Z = \frac{Pv}{RT} \tag{3-24}$$

Equation (3-21) yields three roots with the largest root being the compressibility factor of vapor while the smallest root is that of the liquid.

Substituting equation (3-21) into equation (3-10) yields the fugacity coefficient

$$\ln \phi_i^f = \frac{b_i}{b}(Z - 1) - \ln (Z - B) - \frac{A}{2\sqrt{2}B}\left[\frac{2\sum y_i\, a_{ij}}{a} - \frac{b_i}{b}\right]\ln\left[\frac{Z + 2.414B}{Z - 0.414B}\right] \tag{3-25}$$

The solubility of a component i is determine by setting the range of k_{ij}; calculating the largest root Z from equation (3-21); calculating the fugacity coefficient (ϕ_i) from equation (3-10) and finally obtaining mole fraction (y_i) from equation (3-9). These calculations were run with an iterative Fortran program (see Appendix C) until the optimum value of k_{ij} was obtained by minimizing the average absolute deviation (AAD). With the optimized k_{ij} determined, the program was also used to generate P-x isotherms.

3.2.2 Kirkwood-Buff LC Model

The following rigorous expression was derived (*Cochran* et al., 1987) from the Kirkwood-Buff theory of solutions (*Kirkwood* and *Buff*, 1951) relating the variation of the inverse molar volume of a solute molecule i, dV_i^{-1}, to the variation in pressure, dP, and in the chemical potential, $d\mu_k$ of the c species in solution in solvent j:

$$RT\, dV_i^{-1} = V_i^{-1}G_{ij}\, dP + \sum_{k \neq j}^{c}\left[V_i^{-1}V_k^{-1}(G_{ik} - G_{ij}) + \delta_{ik}V_i^{-1}\right]d\mu_k. \tag{3-26}$$

The quantities $G_{\alpha\beta}$ are called the Kirkwood fluctuation integrals and relate the bulk

solution properties to the microscopic structure of the solution at a molecular level,

$$G_{\alpha\beta} = \int_0^\infty dr\, 4\pi r^2 [g_{\alpha\beta} - 1], \tag{3-27}$$

where $g_{\alpha\beta}$ is the pair corrrelation function. The fluctuation integral, $G_{\alpha\beta}$ divided by the solution molar volume, V, represents the excess above the bulk average concentration of molecules of type α surrounding a molecule of type β and is sometimes called the affinity of β for α. Equation (3-26) has been investigated for multicomponent systems including added co-solvents and multiple solutes (*Cochran* et al., 1990). In the present work we shall consider only the common case of a single pure, incompressible solid i at equilibrium with a supercritical solvent j. In this case the chemical potentials $d\mu_k$, can be replaced by $v_k^s\, dP$

$$RT\, dV_i^{-1} = V_i^{-1} G_{ij}\, dP + \left[V_i^{-1} V_i^{-1} (G_{ii} - G_{ij}) + V_i^{-1} \right] v_i^s\, dP. \tag{3-28}$$

A second simplification, applicable in modeling most supercritical solubility data is to assume the solution is dilute; then, Eq. (3-28) simplifies to

$$RT\, dV_i^{-1} = V_i^{-1} G_{ij}^0\, dP + v_i^s\, dP \tag{3-29}$$

where the superscript zero indicates the value of the quantity at infinite solute dilution. Equation (3-29) is an exact expression for the variation with pressure of the molar volume of solute i in a dilute solution in solvent j at equilibrium with a pure, incompressible solid i.

To be useful, Eq. (3-29) requires some way of evaluating the infinite dilution solvent-solute affinity, G_{ij}^0. Pfund et al. (1988) showed that the infinite dilution solvent-solute affinity, G_{ij}^0, can be related to the solvent-solvent affinity for the pure solvent, G_{jj}^0 by two simple solution models. If the molecules in the solution are assumed to repel one another at close distance and to attract one another at longer distances, like van der Waals' molecules,

a simple relation may be constructed between G_{ij}^0 and G_{jj}^0:

$$G_{ij}^0 + V_{ij} = \alpha_{ij}(G_{jj}^0 + V_{jj}) \tag{3-30}$$

where V_{ij} and V_{jj} are the excluded volumes of the solvent-solute and solvent-solvent interactions which could be estimated from critical volumes,

$$V_{ij} \approx (V_{c,i} + V_{c,j})/2 \tag{3-31}$$

for example, and α_{ij} is a scaling factor like van der Waals' a_{ij} which could also be estimated from critical point properties,

$$\alpha_{ij} \approx \frac{(T_{c,i}T_{c,j})^{1/2}(V_{c,i} + V_{c,j})/2}{T_{c,j}V_{c,j}}. \tag{3-32}$$

Such a model, called the excluded volume or EV model, was shown (*Cochran* et al., 1987) to have reasonable predictive capabilities for supercritical solutions and (*Pfund* et al., 1988) good correlative capabilities for supercritical solutions. If the solvent-solute excluded volume, V_{ij}, and the scaling parameter α_{ij} were fitted to each isotherm, the correlation of supercritical solubility data was excellent, but, if temperature-independent parameters were required, the fit was not so good as could be obtained with the compressed gas Peng-Robinson model.

Pfund et al. (1988) developed another model similar to the EV model but one in which the temperature effects were accounted for according to the local composition concept of Renon and Prausnitz (1968). The local composition or LC model is

$$G_{ij}^0 + V_{ij} = \alpha_{ij}[G_{jj}^0 - (V_{ij}/\alpha_{ij})\exp(b_0 + b_1/T)] \tag{3-33}$$

where b_0 and b_1 are local composition parameters. The LC model was found to be superior to both the compressed gas Peng-Robinson model and the Kirkwood-Buff EV model with temperature-independent parameters for correlating supercritical solubility data from a

number of systems (*Pfund* et al., 1988).

In Eq. (3-30) and (3-33) the solvent-solvent affinity for the pure solvent, G_{jj}^0, can be obtained from an accurate equation of state for the pure solvent.

$$G_{jj}^0 = V(K_T RT/V - 1) \tag{3-34}$$

where K_T is the isothermal compressibility of the pure solvent. For many common supercritical solvents (including the solvent used in this work) very accurate equations of state are available.

When Eq. (3-34) is substituted into Eq. (3-30) or (3-33) and the latter are substituted into Eq. (3-29) simple algebraic expressions can be obtained for the solubility in terms of the parameters of the models (V_{ij} and α_{ij} for the EV model; V_{ij}, b_0, and b_1 for the LC model) and properties of the pure solvent. For the EV model

$$\ln E = \ln(y_i P/p_i^{sat}) = \ln Z_j^0 - \alpha_{ij}\ln(f_j^0 V_j^0/RT) + (v_i^s + \alpha_{ij}V_{jj} - V_{ij})(P - p_i^{sat})/RT, \tag{3-35}$$

and for the LC model

$$\ln E = \ln Z_j^0 - \alpha_{ij}\ln(f_j^0 V_j^0/RT) + (v_i^s + V_{ij}\exp(b_0 + b_1/T) - V_{ij})(P - p_i^{sat})/RT \tag{3-36}$$

where f_j^0 is the pure solvent fugacity.

In addition to their use in predicting or correlating solubility data for dilute solutions of a pure incompressible solid in a supercritical solvent, the Kirkwood-Buff EV and LC models have been used to predict partial molar volume of solutes in supercritical solvents (*Cochran* et al., 1988), to predict the effect of solute concentration on the infinite dilution solute fugacity coefficient for dilute supercritical solutions (*Cochran* and *Lee*, 1987, 1988), and to model ternary supercritical solutions (*Cochran* et al., 1990). Because of the rigorous molecular basis for the Kirkwood-Buff models, they may prove to be more reliable than, for example, the compressed-gas Peng-Robinson model for predicting or extrapolating supercrit-

ical solubility or for extensions to modeling other properties of supercritical solutions.

In this study the K-B LC model was used to model the data. V_{12}, b_0, and b_1 are the three parameters to be fitted by experimental data. As with the compressed gas model, the parameters were fitted with an iterative Fortran program (see Appendix C) until the optimum value of the parameters was obtained by minimizing the average absolute deviation (AAD). P-x isotherms are also generated with the program.

3.2.3 Other Models

Other complex models have been proposed in literature. Johnston et al. (1989) provides an excellent review of these models including the two previously described. Hard sphere perturbation theory has been applied to supercritical systems by several authors e.g. Wong et al. (1986); and Dimitrelis and Prausnitz (1986).

In hard sphere models the attractive and repulsive parameters have more physical meaning than they do in cubic equations of state. The heart of hard sphere theory is the treatment of the free volume, V_f, which can be expressed as

$$V_f = V\exp\left[\frac{\xi(3\xi - 4)}{(1-\xi)^2}\right] \tag{3-37}$$

where ξ - $0.74(v_0/v)$

v_o - $(\sigma^3/\sqrt{2})N_A$

is valid at low and high densities. Then, Nv_0/N_A is the smallest possible volume that can be occupied by N hard spherical molecules of diameter σ. In the Carnahan-Starling equation of state for hard spheres where no attractive forces are present, the resulting equation of state

is expressed as

$$z^{HS} = \frac{Pv}{RT} = \frac{1 + \xi + \xi^2 - \xi^3}{(1 - \xi)^3} \tag{3-38}$$

When attractive forces are exerted by molecules, the Carnahan-Starling van der Waals (CSVDW) equation of state is expressed as

$$z = z^{HS} - \frac{a}{RTv} \tag{3-39}$$

where z^{HS} is the hard-sphere contribution. Equations of state which combine an accurate expression for the hard-sphere repulsive forces with the standard van der Waals attractive term, are termed hard-sphere van der Waals (HSVDW) equations of state. Johnston and Eckert (1981) used the CSVDW model to predict the solubilities of nonvolatile solids in supercritical ethylene and carbon dioxide. Improvement of the repulsive term in the equation of state can be made with the use of a model for a mixture of hard spheres (*Mansoori* et al., 1971). Wong et al (1985) had greater success with a mixed hard sphere van der Waals (HSVDW) model in predicting the solubility of relatively nonpolar solutes. The HSVDW model also includes a solute-solute attraction parameter which was observed to be necessary for mole fractions above 10^{-3}. The importance of solute-solute interaction has been observed with fluorescence measurements (*Brennecke* and *Eckert*, 1989). A recent paper by Cochran and coworkers (1990) describes such structures in terms of molecular distribution functions. Other variations of perturbed hard sphere models exist but are not discussed.

Another statistical mechanical approach is the lattice models. These lattice models are useful for modeling complex phase behavior, for example, multiphase behavior with critical end points. As with many models, accuracy is greatly decreased near the critical region (*Kumar* et al., 1987; *Bamberger* et al., 1988).

The Monte Carlo Simulation has been used to predict solubilities in supercritical solvents (*Shing* and *Chung*, 1987). It allows the calculation of phase behavior from intermolecular potentials such as the Lennard-Jones potential without the kinds of assumptions required in equation of state models. Its use is not warrented if a correlating model works well in predicting solubilities (*Johnston* et al., 1989).

The underlying molecular theory behind a model determines its ability to predict supercritical solubility. Models such as the HSVDW equations of state and the Kirkwood-Buff models are predictive in nature but yield better results when correlating the molecular interaction parameters from data. On the other hand, models such as the compressed gas model based on an empirical EOS and empirical mixing rules, are solely correlative models.

3.2.4 Model Summary

At present, no single model can treat all cases. The model of choice will be determined by the analysis objective, computational difficulty, and the known physical properties of the system. Because supercritical behavior is highly nonideal and the chemical potential values are highly variable, prediction and even correlations especially near the critical end points can be extremely difficult.

CHAPTER IV

EXPERIMENTAL

4.1 Experimental Overview

When considering experimental techniques for measuring solubility of a heavy solute in an SCF, one makes a choice between two basic types - a dynamic apparatus where the solute is continually swept with the SCF or a static apparatus where both solute and solvent are loaded into the same cell. One must weigh the objective of the study against the pros and cons of each type.

Examining the latter, McHugh et al. (1984) presented a static apparatus (see Figure 4.1) capable of determining the location of phase-border curves in P-T space and the solubility of a heavy solute in the SCF. The main component of the system is a high-pressure, variable-volume view-cell. The description of the operations is found in the literature. What is important are the advantages and disadvantages (*McHugh* and *Krukonis*, 1986) of a variable-volume view-cell listed below:

Advantages:

(1) equilibrium phases are determined visually;

(2) phase transition are visually detected, including phase inversions;

(3) solubilities in binary mixtures are obtained without sampling;

(4) heavy solids, liquids, or polymers can be studied;

(5) minimum amounts of material are used; and

(6) pressure is adjusted at fixed composition and temperature

Disadvantages:

(1) stripping data are not easily obtained;

(2) windows can fail at high pressures;

(3) even small leaks invalidate the experiment

(4) ensuring thorough equilibration/good contacting is difficult

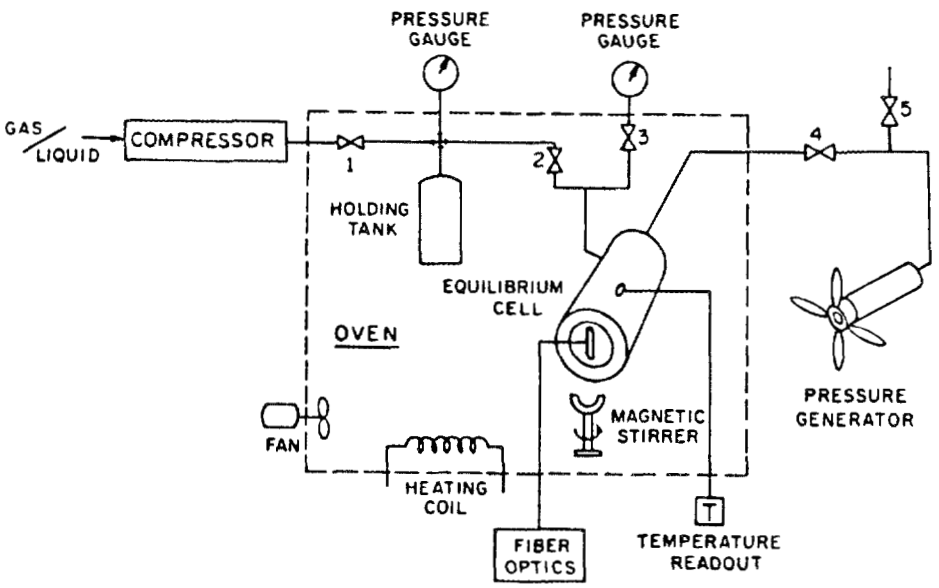

Fig. 4.1. Schematic diagram of a constant-composition view-cell apparatus. Used to obtain solid and liquid solubilities in a supercritical fluid (*McHugh* et al., 1984).

A static apparatus may not be well suited to meet the objective of an experiment particularly if it is an extraction of organics from an aqueous solution such as a fermentation broth. By far the most common apparatus is a flow-type apparatus used to determine the solubility of a heavy liquid or solid in a SCF by absorption. In this experiment we were interested only in the equilibrium composition of the solute-rich supercritical gas phase.

Thus a flow-type apparatus was chosen which embodies all the main features of other flow methods described in the literature (*Van Leer* and *Paulaitis*, 1980; *Simnick* et al., 1977).

The advantages and disadvantages (*McHugh* and *Krukonis*, 1986) common to this type of apparatus are listed below:

Advantages:

(1) off-the-shelf equipment may be used;

(2) a straight forward sampling procedure may be used; and

(3) reasonably large amounts of solubility data can be obtained rapidly and reproducibly.

Disadvantages:

(1) heavy solid or liquid can clog the metering valve which leads to measurement errors;

(2) if a liquid phase is present, entrainment of the liquid can occur;

(3) undetected phase changes can occur

(4) high pressure can cause the density of the SCF-rich phase to become greater than the density of the solute-rich liquid phase;

(5) solubility of the SCF in the liquid phase cannot be measured; and

(6) depletion of one or more components can occur during the experiment.

To meet the primary objective of this study, an apparatus was assembled where:

(1) CF_4 was charged with a high pressure booster compressor to the desired operating pressure;

(2) CF_4 flowed through a constant temperature bath before reaching the extraction column;

(3) CF_4 flowed slowly through a packed column of solid CCl_4, reaching saturation before exiting;

(4) the saturated CF_4 was expanded to atmospheric pressure across a metering value;

(5) a mass spectrometer was utilized for on-line analysis; and

(6) a flow meter controled the metering valve.

The physical properties of the solute(s) studied determine the type of analysis best suited to measure the solubility. Most extraction devices are provided with a trap allowing quantitative recovery of solute during a measured extraction time. The usual methods for determining solubility are to weigh trapped material (*McHugh* and *Paulaitis*, 1980; *Johnston* and *Eckert*, 1981; *Adachi* and *Benjamin*, 1983; *Moradinia* and *Teja*, 1986; *Mitra* et al., 1988) or to dissolve and analyze the trapped material (*Schneiderman* et al., 1987). More elegant methods of on-line analysis exist. Direct coupling of SCFE to gas chromatography (*Hawthorne* and *Miller*, 1987) and to HPLC (*Billoni* et al., 1988) have been described. This study presents another alternative of on-line analysis — mass spectrometry.

Direct coupling of supercritical fluid chromatography (SFC) to mass spectrometry has received considerable interest in the 1980's. An excellent introduction to this field is the review article by Smith et al. (1987a) describing the interfacing and applications of SFC-MS. Later reviews (*Smith* et al., 1988) exist but do not cover any new major techniques. In 1987 Smith and coworkers (1987b) described a method, an apparatus (see Figure 4.2), and the results of the application of SFC techniques to an SCFE study. The method is suitable for heavy, relatively non-volatile solutes such as aromatic hydrocarbons. Because of the proximity of the expansion orifice (resistor) to the mass spectrometer high vacuum chamber, a major design concern is whether the solvent-solute clusters have sufficiently dissipated to give representative sampling. Figure 4.3 (*Smith* et al., 1988) illustrates one of the current style of interface being investigated.

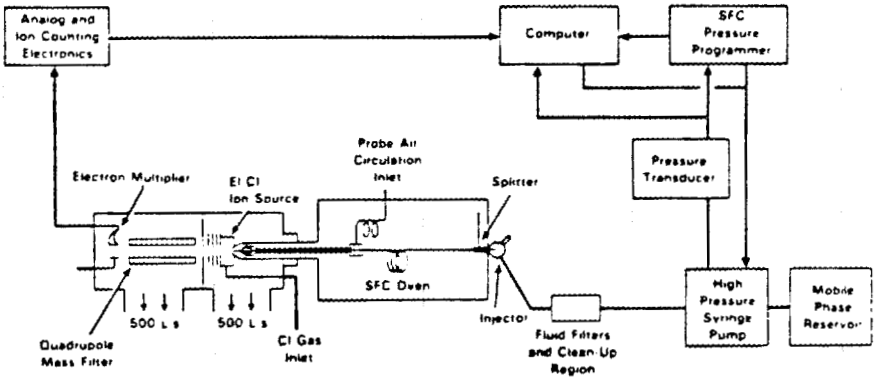

Fig. 4.2. Schematic diagram of a capillary SFC-MS apparatus (*Smith* et al., 1987a).

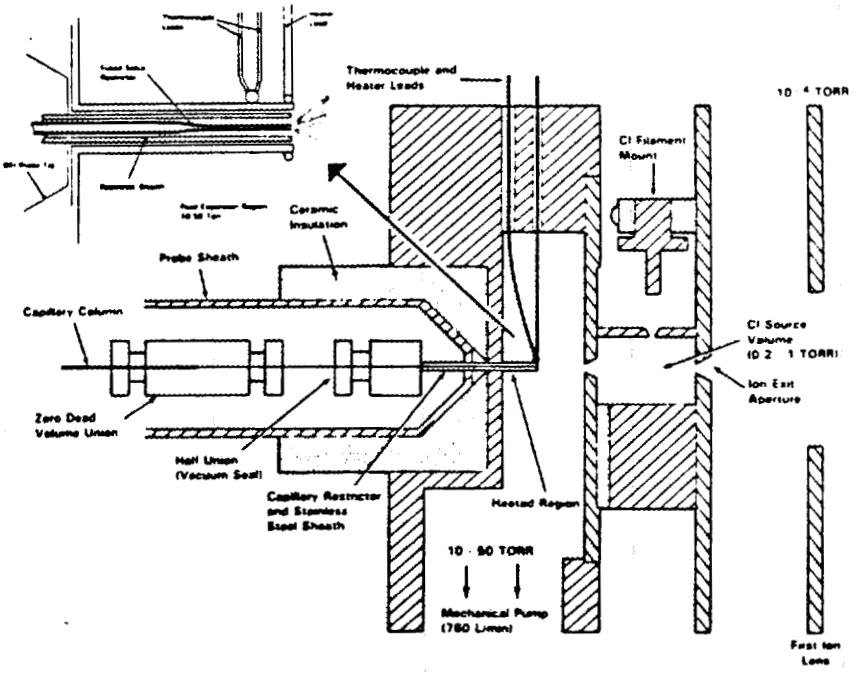

Fig. 4.3. Schematic diagram of SFC-MS interface. Inset: detail of probe tip heater and expansion region (*Smith* et al., 1987a).

In the present work the method of introducing the sample through a controllable low pressure chamber is altogether different and considerably downstream from the expansion valve to ensure representative sampling. To interpret the experimental results, the mole fraction of CCl_4 was calculated by comparing the ratio of the ion current from the mass spectrometer (corrected for MS pressure) to calibration standards of known mole fractions. Calibration and interpretation are described in detail later.

One physical limitation to the experiment was that the difference in the critical temperature of CF_4 (T_c = 226.7K) and the melting point of CCl_4 ($T_{m.p.}$ = 250.2K) provides only a narrow window of 23.5K for solid-vapor supercritical extraction. Thus, four isotherms in five degree increments at subambient temperature were chosen: 234, 239, 244, and 249K. In general, data points were taken along an isotherm by increasing or decreasing pressure in 34.5 bar (500 psi) increments from 33 to 290 bar.

4.2 Equipment and Operations

4.2.1 Materials

Tetrafluoromethane, CF_4, was obtained from Air Products and Chemicals, Inc. in standard cylinders with stated purity of 99.9%; the CF_4 was used without further processing. Tetrachloromethane, CCl_4, was obtained from Fisher Scientific as Certified A. C. S. grade. The CCl_4 was frozen with liquid nitrogen, crushed, and loaded as a solid into the cold equilibrium cell which was then closed and maintained near liquid nitrogen temperature until installation in the apparatus. Handling of CCl_4 from the bottle to the closed equilibrium cell was performed in a dry-box to prevent contamination by moisture.

4.2.2 Pressurizing System and Extraction Column

The apparatus used in this study was a single pass flow system shown schematically in Figure 4.4. CF_4 from a standard cylinder was compressed with a Sprague air-driven booster compressor and held in a 300 cm^3 Autoclave Engineers, Inc. vessel. CF_4 flowed from this supply via a high pressure regulator, R1, to equipment within a temperature-controlled enclosure.

The maximum extraction pressure was limited to 415 bar by the booster compressor, BC, and the extraction temperature could be varied from ambient temperature to about 210 K. Normal operating conditions were between 15 and 315 bar and 250.2 K (m.p. of CCl_4) to 226.7 K (critical temperature of CF_4). The outlet pressure gauge was a 0-5000 psig Bourden-tube Heise pressure gauge accurate to ± 5 psi (0.345 bar). The inlet pressure gauge was a digital 0-6000 psia Heise gauge calibrated to ± 19 psi at 6000 psia.

The temperature-controlled enclosure was an insulated, doubled-walled box cooled by vaporized liquid nitrogen. A small internal blower circulated the cold nitrogen within the enclosure. A Foxboro control unit regulated the amount of cold nitrogen entering the enclosure from an input signal provided by a thermocouple suspended in the air bath.

The CF_4 equilibrated to the enclosure temperature by passing through 20 feet of coiled 1/8 inch tubing prior to entering the column. The CF_4 then passed through the column at a flow rate slow enough to ensure equilibrium (approximately 0.8 cm/min at moderate pressures, 140 bar, at a discharge flow rate of 0.05 l/min.). The extraction column was a stainless steel tube (19 cm long, 0.84 cm ID) containing a packed bed of solid CCl_4. At each end and every 3.75 cm a glass wool pad was placed to prevent entrainment and channeling.

A split, cylindrical copper block of 12 cm OD was placed around the column to ensure temperature uniformity. Column temperature was monitored by two chromel/gold

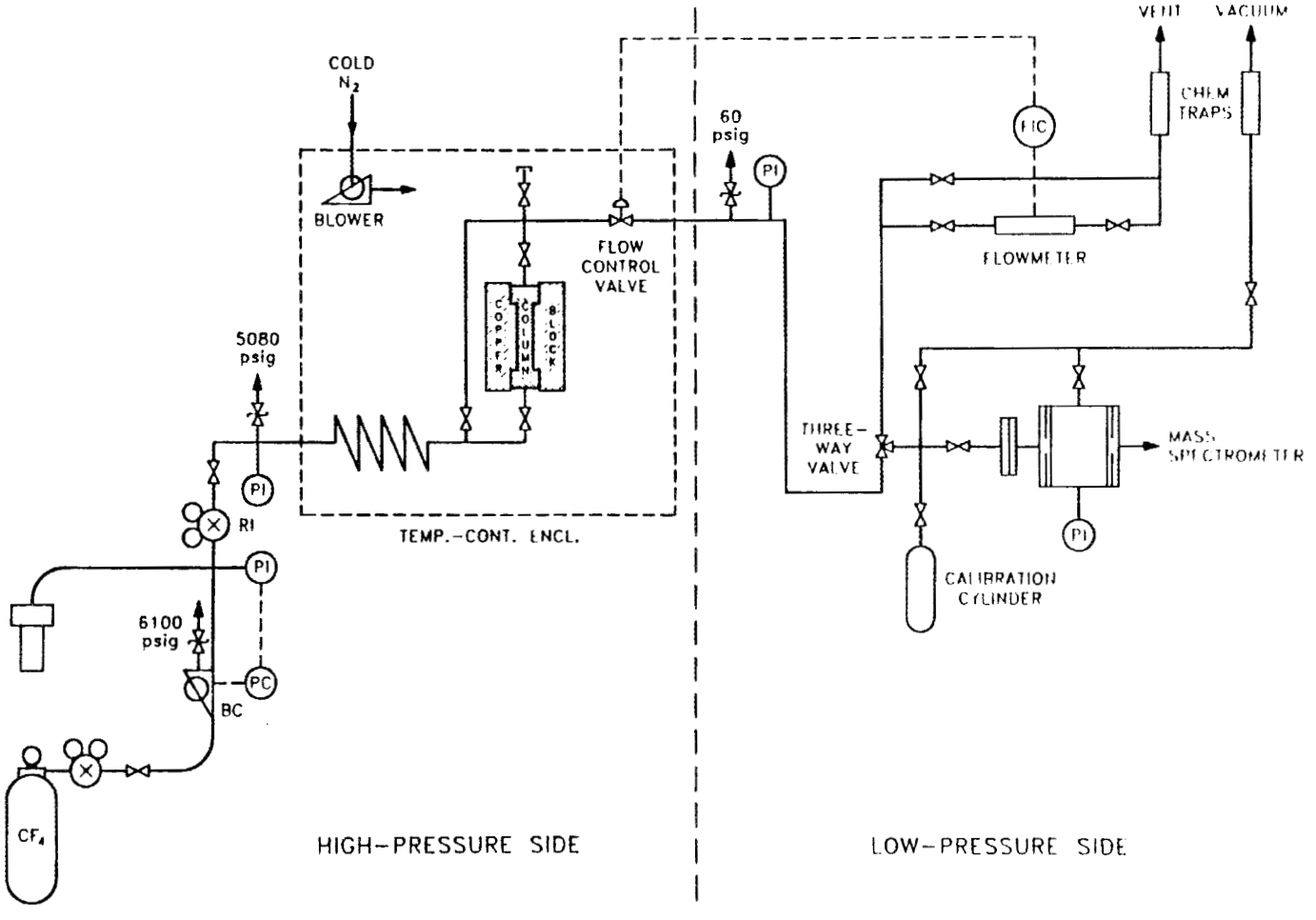

Fig 4.4. Direct coupled SCFE-MS apparatus.

(0.07 wt% iron) thermocouples inserted in the ends of the block. These thermocouples were accurate to ±0.1 K. They were calibrated repeatedly at the normal boiling point of nitrogen and the melting point of ice.

4.2.3 Expansion and Analysis

The solute-rich CF_4 was expanded to atmospheric pressure across a flow control valve, FCV. Heat was applied to the valve to prevent clogging of the valve by frozen CCl_4 or solute precipitation. The flow rate was observed on a Hastings flow meter, FM, which controls the FCV. Typical flow rates were between 0.02 to 0.06 standard liters per minute to ensure column equilibrium (see Figure 4.5). The critical importance of the flow rate is described in greater detail in Appendix D.2.

The analysis principle was simple. When the equilibrium of supercritical CF_4- CCl_4 was reached, the effluent was diverted to the mass spectrometer. In order to ensure that CCl_4 did not condense in the low pressure tubing, heating tape was wrapped around the tubing to maintain a temperature above the boiling point of CCl_4, 349.7 K. The effluent was admitted through a double orifice assembly (see Figure 4.6). The first orifice reduced the pressure to approximately 3 Torr. This was to ensure laminar flow, hence representative sampling, prior to entering the HVC of the quadrupole mass spectrometer through the second orifice. A UTI Model 100C quadrupole mass spectrometer was utilized in this experiment with the following optimized instrument settings: emission current- 2.20 ma, focus voltage- 20 v, ion energy- 15 v, electron energy- 70 v, and emission current (Total Pressure mode)- 0.41 ma.

Typical MS operational settings were Faraday Cup mode at 10^{-12} amps full scale and a MS pressure of 1.4×10^{-6} Torr. Data were recorded on a strip chart recorder.

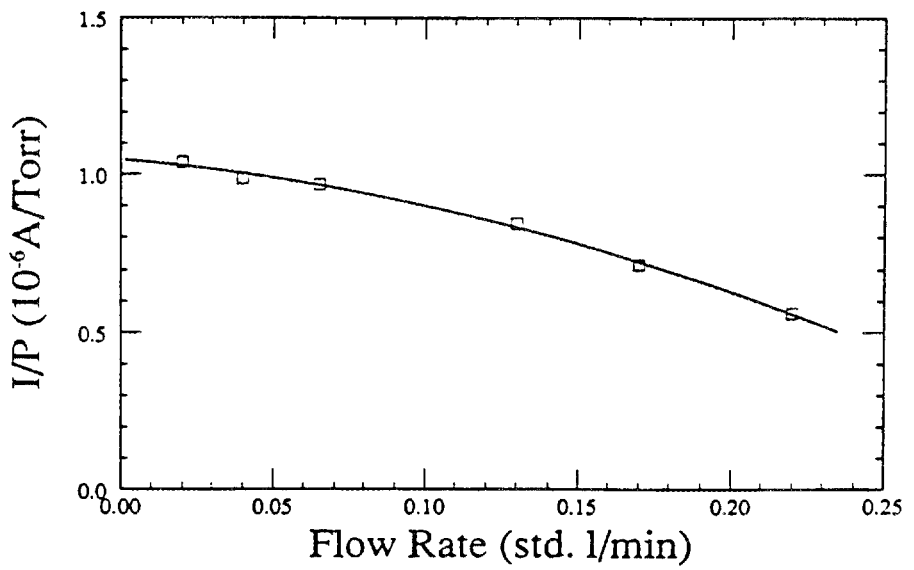

Fig. 4.5. Equilibrium flow rate. To test for adequate fluid/solid contact and equilibration, CF_4 flow rate was varied. Equilibrium at 136 bar was achieved at a flow rate ≤ 0.06 std. l/min. where the superficial velocity was ≈ 0.2 cm/min. for the 244K and 249K isotherms.

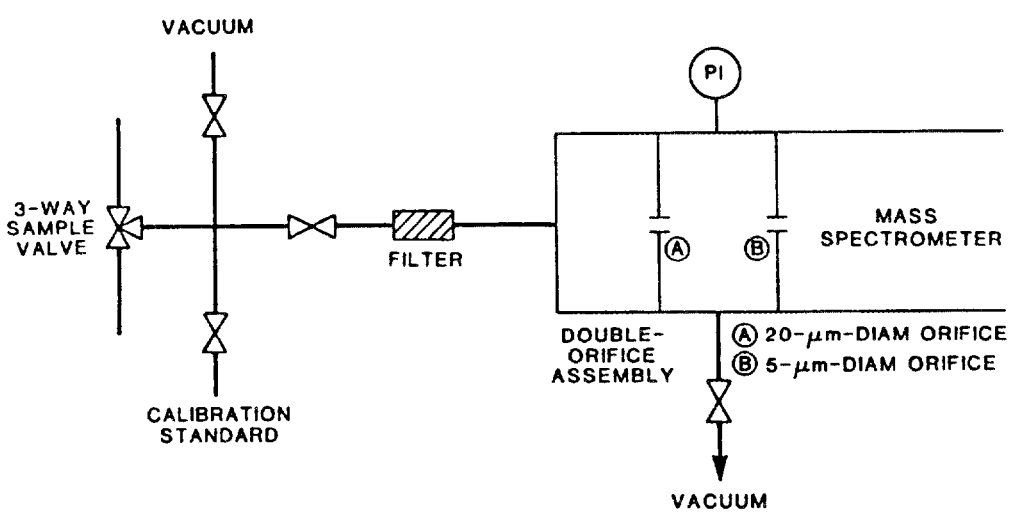

Fig. 4.6. Double orifice sample inlet to MS.

4.3 Calibration and Interpretation

A 303.4 ml cylinder was evacuated and flushed three times with CF_4. The cylinder was then charged to 2.6±0.1 psig. Using a gas chromatograph syringe a precise amount of CCl_4 (5–20μl) was injected. After heating to ensure no CCl_4 was in a liquid phase and thermal mixing for ≥ 24 h, the cylinder was opened to the evacuated low pressure side of the apparatus. MS data were taken directly. The 1.40×10^{-12} amp point was repeated and found to be within 1.0%.

If the detector signal is linear, the mole fraction y is given by the relation $y = (I/P)\times(C/(I/P))$ where I/P is the ion current normalized by the MS pressure and $C/(I/P)$ is a constant. Figure 4.7 is the calibration curve for the system at 1.38×10^{-6} Torr. Although it is essentially linear in the region where $y > 0.005$, an excellent fit for $0 < y < .014$ is provided by the cubic polynomial equation (4-1).

$$y = a_0 + a_1(I/P) + a_2(I/P)^2 + a_3(I/P)^3 \tag{4-1}$$

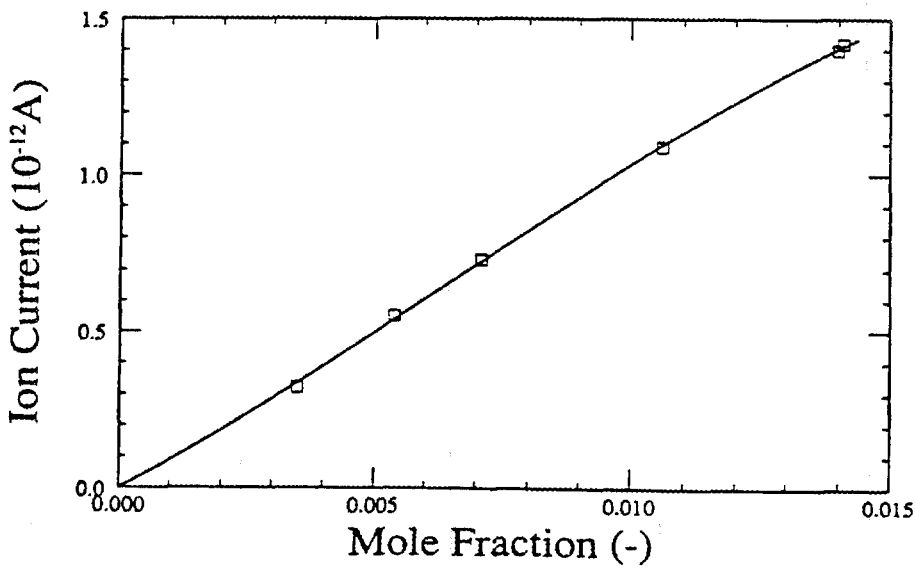

Fig. 4.7. Mass spectrometer calibration curve.

At $\leq 10^{-5}$ Torr the ion current of the MS was expected to be linear with respect to pressure; however, it was found to be nonlinear such that a 3-fold increase in pressure resulted in a 5-fold increase in ion current. Because of the nonlinearity, a simple (I/P) ratio could not be applied to the data in order to use the calibration curve. Therefore, the experimentally observed ion current, I_{exp}, required adjustment to the MS pressure of the calibration curve, 1.38^{-6} Torr. This adjusted ion current was termed I_{corr}, expressed as

$$I_{corr} = I_{exp} \times (correction\ factor) \tag{4-2}$$

where the correction factor is the ratio - $(I_{P=1.38\times10^{-6}}/I_P)$.

Figure 4.8 from Table 4.1 was used to correct ion current at any operating pressure to the pressure of the calibration curve. For the region between $1\times10^{-6} < P < 2\times10^{-6}$ Torr, a smooth curve fit the data with little error. In that region, the ion currents were read directly from the graph and the correction factor applied without a rigorous treatment for error. At $P > 2\times10^{-6}$ Torr the data was scattered and a large error was noticeably evident. With the assumption that as P approaches 0, I also approaches 0, the data was linearized as shown in Figure 4.9 and in equations (4-3) and (4-4). It was then tested for the significance level of correlation.

$$I = a + bP + cP^2 \tag{4-3}$$

where $a = 0$, equation (4-3) can then be expressed as

$$I/P = b + cP \tag{4-4}$$

Utilizing a spread sheet (see Appendix C), I_{corr} was calculated for $P > 2\times10^{-6}$ Torr with an error as great as ± 36% for $P > 4.0\times10^{-6}$ Torr. With a correlation coefficient of 0.826 and 5 degrees of freedom, the confidence level of correlation for the data was an excellent 95% (*Brownlee*, 1948).

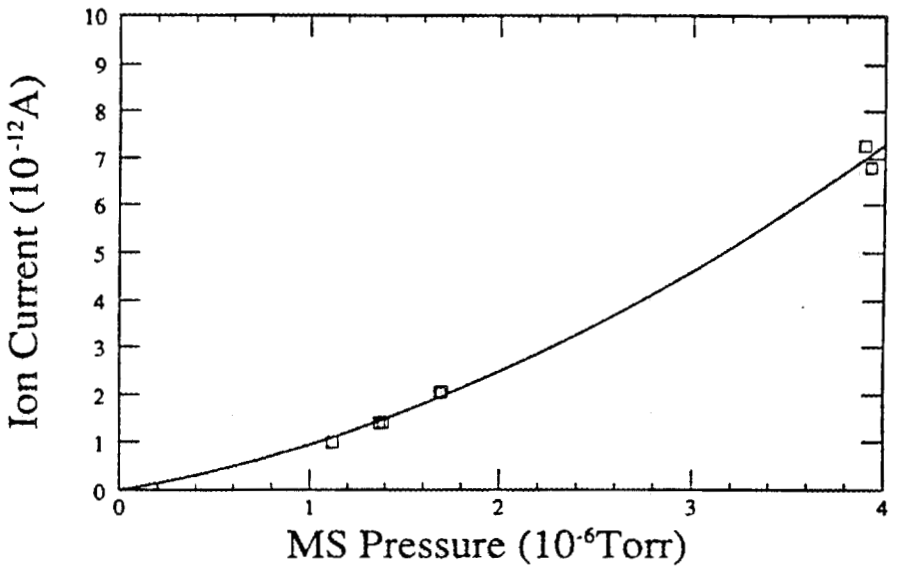

Fig. 4.8. MS pressure correction curve.

Table 4.1. Pressure Correction Data

Date (M/D/Y)	I (10^{-12} A)	P (10^{-6} Torr)	I/P (10^{-6} A/Torr)
08/11/89	1.00	1.120	0.89286
08/10/89	1.40	1.370	1.02190
08/11/89	1.42	1.390	1.02158
08/10/89	2.05	1.700	1.20588
08/11/89	2.03	1.690	1.20118
08/10/89	7.27	3.900	1.86410
08/11/89	6.80	3.930	1.73028

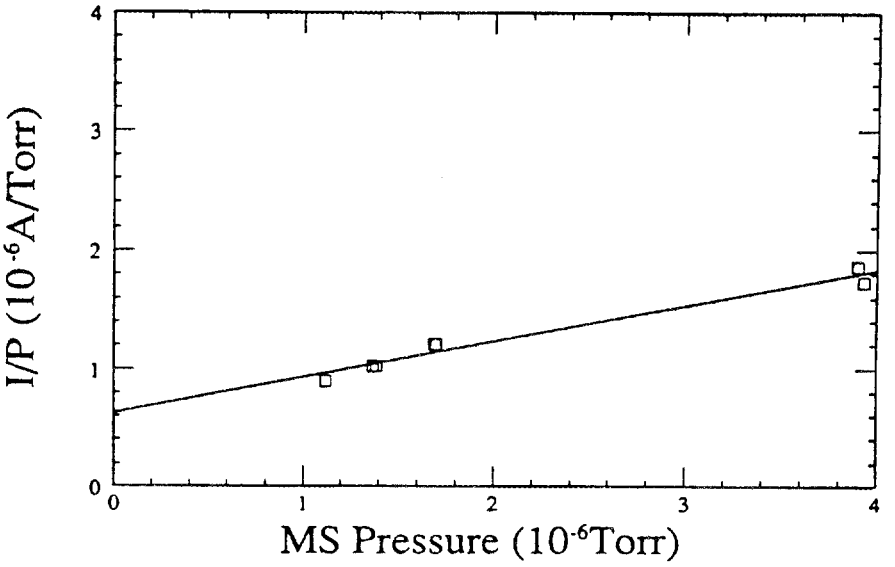

Fig. 4.9. Linearized MS pressure correction curve. Used for determining the correction factor at $P > 2\times10^{-6}$ Torr.

The CCl_4—CF_4 system proved very easy to interpret. (*Cornu* and *Massot*, 1975) Figure 4.10 is the mass spectrum of CCl_4 overlayed on that of CF_4. The distinct triplet at AMU's 117, 119, and 121 provided the fingerprint for determining the mole fraction of the solute. Of the three peaks the 117 AMU was the largest from the splitting pattern of the MS, and calculations were based on its amplitude.

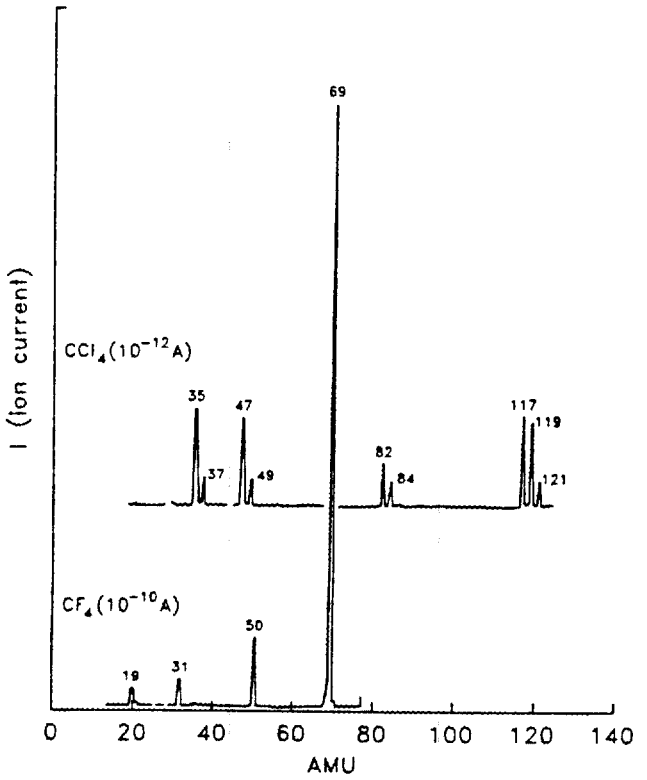

Fig. 4.10. Mass spectra of CCl_4 and CF_4.

CHAPTER V

RESULTS AND DISCUSSION

5.1 CF_4–CCl_4 Solubility Data

The solubility of solid CCl_4 in supercritical CF_4 was successfully measured at 244K to 249K and the data are presented in Table 5.1. The solubility data at 234K and 239K were inconsistent and are discussed in Appendix D. For the study the pressure varied from 13.0 bar to 310.0 bar. On-line mass spectrometry was used for analysis of the effluent. The MS ion current, I_{exp}, was corrected for the MS high vacuum chamber pressure to the pressure of the calibration curve (1.38×10^{-6} Torr). The mole fraction was calculated from the corrected ion current, I_{corr}, by a computer program in Appendix C if I_{corr} was < 1.38×10^{-12} A and by the use of a constant 0.01 ($-/1\times10^{-12}$ A) if I_{corr} was > 1.38×10^{-12} A.

The solubilities were found to range from 5.1×10^{-4} to 2.58×10^{-2} mole fraction. Figure 5.1 is a plot of the mole fraction of CCl_4 vs. pressure. It is observed that there is some scatter in the low pressure region of the 244K isotherm.

Some general comments can be drawn from Figure 5.1. For the pressure above the critical pressure of CF_4 , 37.4, up to 120 bar, the solubility of CCl_4 increases dramatically due to a rapid increase in density with increasing pressure. Figure 5.2 is a plot of CF_4 density (*Rubio* et al., 1985) vs. pressure at each of the isotherms.

Figure 5.2 not only illustrates the rapid change of density due to pressure increase but aids in explaining why the data do not exhibit a clear temperature-solubility crossover point

Table 5.1. Solubility Isotherms of CCl_4 in Supercritical CF_4 at 244K and 249K

249K				244K			
P (bar)	y (-)	ρ (gmol/l)	E (-)	P (bar)	y (-)	ρ (gmol/l)	E (-)
34.49	0.00163	2.30	5.74	12.96	0.00051	0.71	0.97
68.95	0.00574	8.13	40.42	23.78	0.00043	1.45	1.50
103.76	0.01329	10.93	140.84	33.78	0.00051	2.36	2.52
136.51	0.02101	11.98	292.93	50.67	0.00141	5.08	10.48
137.27	0.02200	12.00	308.44	61.02	0.00220	7.99	19.69
137.55	0.02100	12.01	295.02	67.58	0.00299	9.17	29.64
137.89	0.02100	12.02	295.78	69.70	0.00495	9.44	50.61
171.68	0.02250	12.70	394.53	84.81	0.00500	10.71	61.70
204.77	0.02380	13.22	497.76	100.32	0.00740	11.41	108.98
206.49	0.02360	13.24	497.72	103.08	0.01063	11.51	160.74
239.24	0.02490	13.64	608.40	136.86	0.01461	12.41	293.72
274.06	0.02550	14.01	713.77	137.55	0.01448	12.43	292.17
307.85	0.02580	14.32	813.84	138.24	0.01429	12.44	289.78
				171.33	0.01667	13.05	418.96
				210.98	0.01831	13.60	566.65
				240.90	0.01938	13.94	684.85
				276.13	0.02006	14.28	812.55

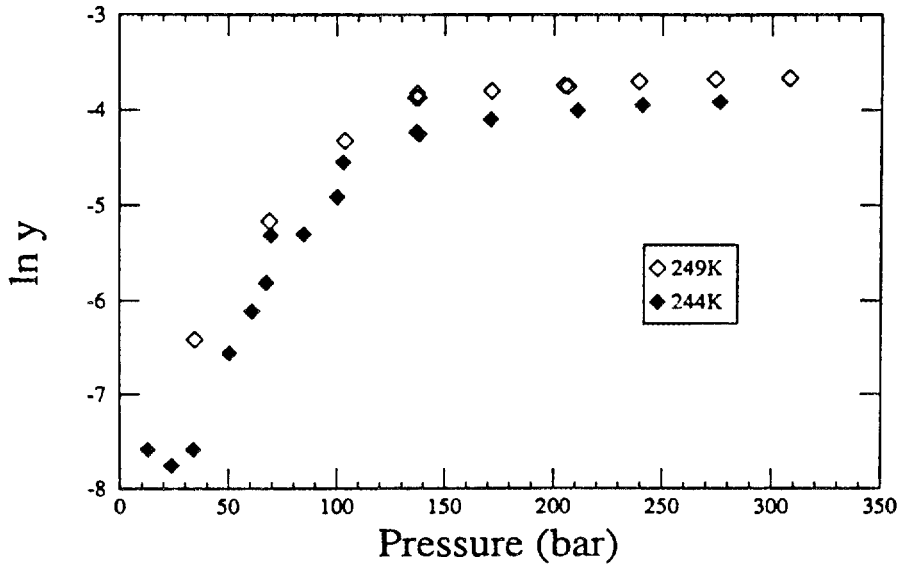

Fig. 5.1. Mole fraction of CCl_4 vs. pressure at 244K and 249K.

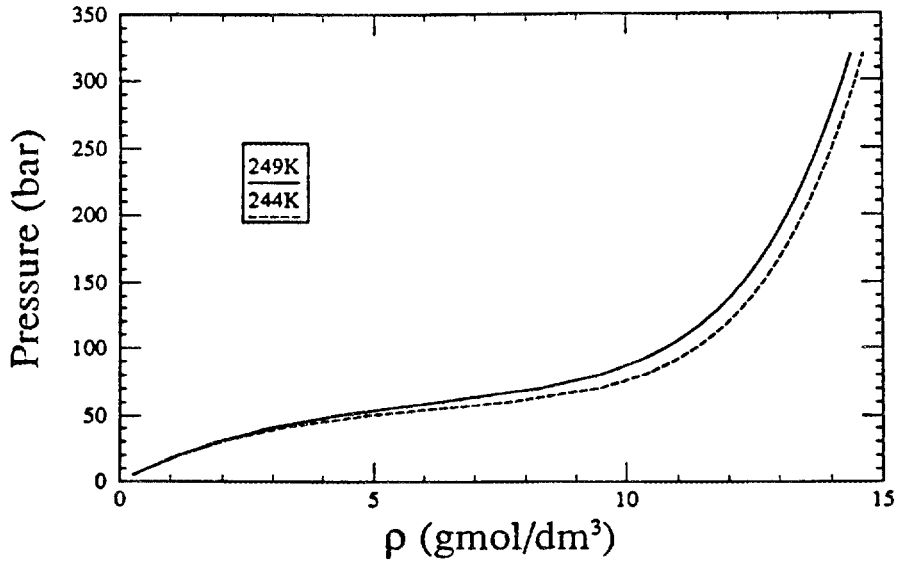

Fig. 5.2. CF_4 density vs. pressure.

$(\partial y_i/\partial T)_P = 0$. The crossover point is a function of the vapor pressure of the solute. For pressures above the critical point of the solvent up to a specific pressure (estimated to be between 60 and 70 bar), the solubility decreases as temperature increases because at lower temperature the solvent is more dense. Above that pressure the solubility increases with increasing temperature because the increase in vapor pressure overwhelms the decrease in solvent density. Because $(\partial\rho/\partial P)$ is greater in the low pressure region, a solubility crossover point could not be determined as most data was taken above 67 bar.

In Figure 5.3 the same data have been replotted with the solubility as a function of the CF_4 density rather than pressure. The equation of state developed by Rubio et al. (1985) was used to calculate CF_4 density utilizing the Strobridge equation. It has been reported that the density calculation is reliable to within 0.4% outside the critical region, and to within 2% near the critical point. The isotherms have taken on an almost linear characteristic. These graphs confirm that the solvent power of a supercritical fluid is directly related to its density.

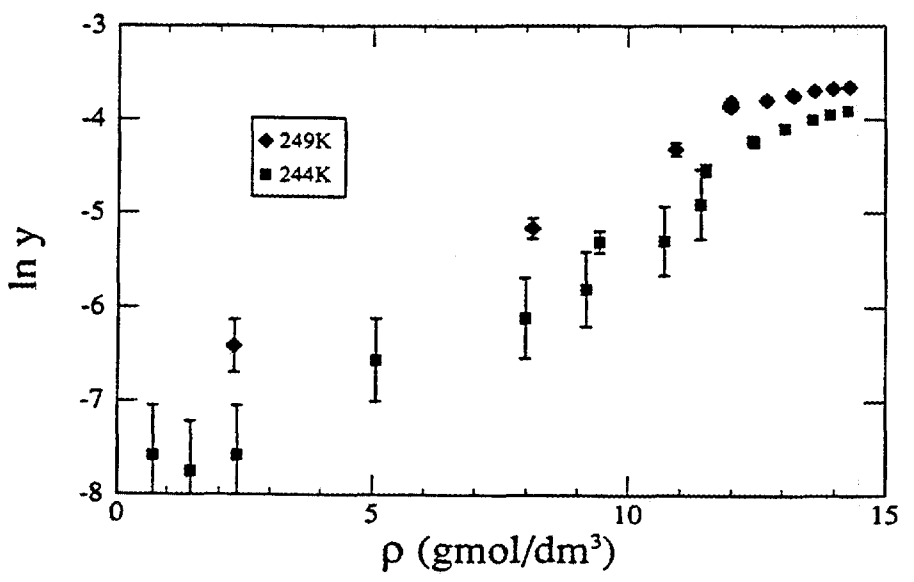

Fig. 5.3. Mole fraction of CCl_4 vs. density at 244K and 249K.

To show the extent to which pressure enhances the solubility of CCl_4 in supercritical CF_4, it is convenient to define an enhancement factor

$$E = y_{exp}P/p^{sat} \tag{5-1}$$

The enhancement factor, E, is the extent to which pressure enhances the solubility of a solid in the gas compared to the solubility calculated from the ideal gas expression $y_{ideal} = p^{sat}/P$. The enhancement factor was calculated using equilibrium vapor pressure for solid CCl_4 from the *International Critical Tables*, 1933. Substitution of equation (5-1) into equation (3-5) gives

$$E = \frac{1}{\phi_i^f} \exp\left[\frac{v_i^s \left[P - p_i^{sat}\right]}{RT}\right] \tag{5-2}$$

The logarithm of E is plotted versus density of supercritical CF_4 in Figures 5.4 and 5.5 from data in Table 5.1. At a given density (or pressure) the differences in the enhancement

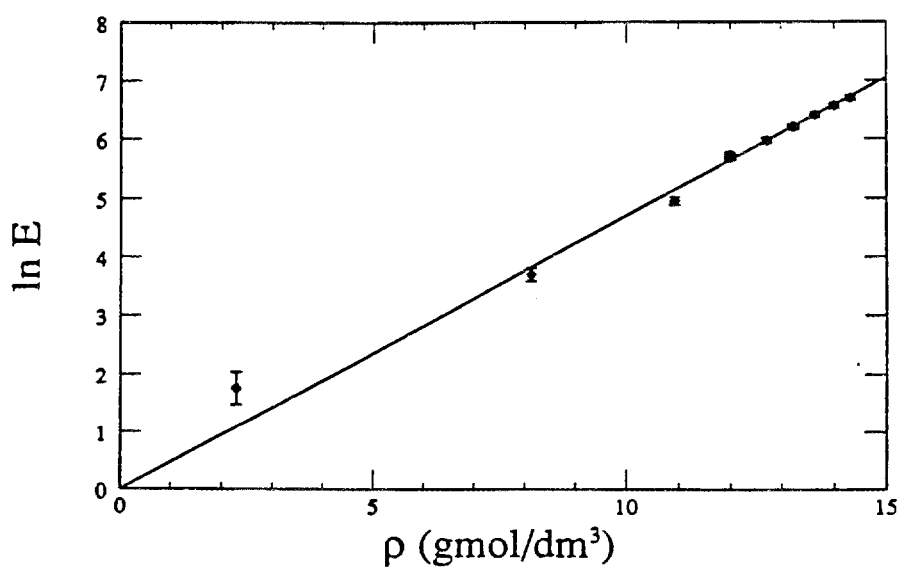

Fig. 5.4. ln E vs. density at 249K.

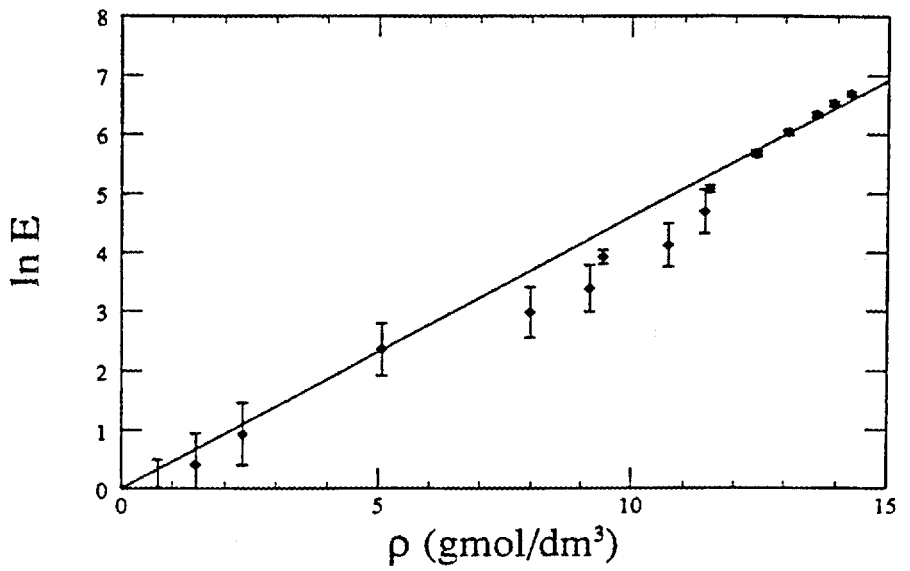

Fig. 5.5. ln E vs. density at 244K.

factors are primarily because of the difference in the fugacity coefficient, which is a function of temperature. The appearance of the isotherm curves take on a linear characteristic over the entire range of density. These figures show that CCl_4 can dissolve in supercritical CF_4 at concentrations up to 10^3 times greater than predicted solely by the ideal gas law.

5.2 Modeling

The solubility data were correlated to express the solubility behavior of the system with two models - the Peng-Robinson compressed gas model and the Kirkwood-Buff local composition model. The two models are compared for any computational or correlative advantages.

The first approach utilized the P-R compressed gas model. In this approach the solubility y_2 of a pure solid in a supercritical fluid is expressed by

$$y_i = \frac{p_i^{sat}}{P} \frac{\phi_i^{sat}}{\phi_i^f} \exp\left[\frac{v_i^s \left[P - p_i^{sat}\right]}{RT}\right] \tag{5-3}$$

For the estimation of ϕ_2^f the P-R equation of state was used because it requires only the critical properties (T_c,P_c) and the acentric factor ω for application to a solid fluid system. The binary interaction parameter (k_{ij}) was regressed by minimizing the average absolute deviation (AAD) for y_2 vs. pressure data.

$$AAD = \frac{1}{N} \sum Abs \left[\frac{y_{cal} - y_{exp}}{y_{exp}}\right] \tag{5-4}$$

The computer program used to determine the binary interaction parameter is presented in Appendix C.

For the 244K isotherm, the low pressure data taken on 02/27/89 deserved scrutiny because the MS pressure was operated 2-3 times greater than for any other data to increase peak height. As mentioned, an increase in MS pressure was not linear with respect to ion current and a significant correction factor was required. In addition the superficial velocity that approaches equilibrium solubility ($\bar{v}_0 < 0.2$ cm/sec) is exceeded below 70 bar.

The results of these calculations are presented in Table 5.2. Since the effect of temperature on solubility is due to its effect on intermolecular interaction as well as vapor pressure and density, it was thought that the binary interaction parameter may show some temperature dependence. From the modeling efforts shown in Figure D.5 of Appendix D, a plot of regressed k_{ij} values showed a near linear temperature dependence. The mole fraction vs. pressure isotherms predicted by the Peng-Robinson model are plotted in Figures 5.6 and 5.7. As has been found for many other systems, the values of the interaction parameter were also found to range from 0 to 0.20 (*Walas*, 1985).

Table 5.2. P-R CG Modeling Correlations

Isotherm(s) Regressed	k_{ij}	AAD%	Remarks
249K	0.131	10.8	
249K+244K	0.136	34.7	
249K+244K	0.135	13.1	minus 2/27/89 data
244K	0.145	43.5	
244K	0.142	6.2	minus 2/27/89 data
All isotherms	0.157	49.85	see Table D.1 for 234K/239K isotherm data

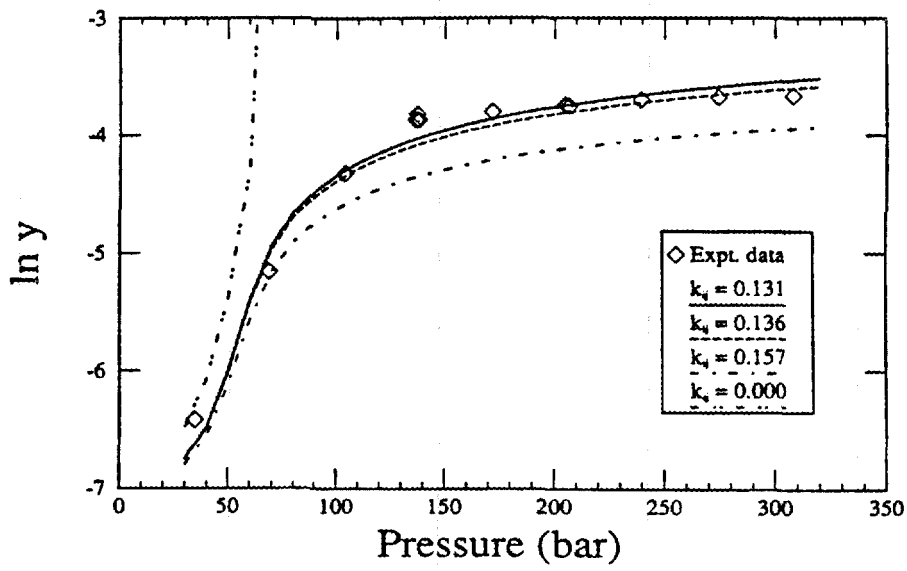

Fig. 5.6. P-R Modeling at 249K.

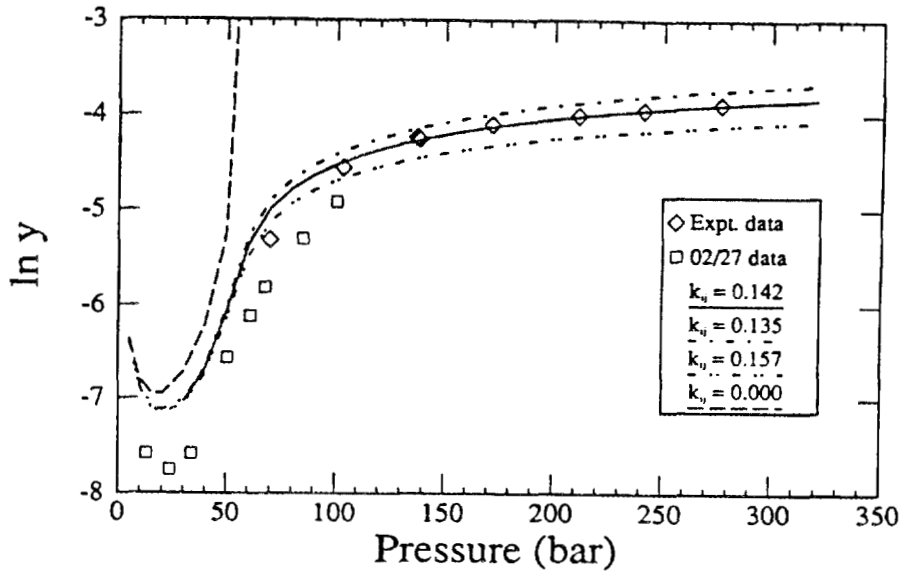

Fig. 5.7. P-R Modeling at 244K.

Some observations can be made from these tables and figures.

(1) The AAD resulted from well established critical properties, solid density, and particularly the vapor pressure of the solute. It implies that the data were consistent for the conditions under which they were obtained.

(2) When the low pressure data of 02/27/89 are included in the regression of the 244K isotherm, the AAD increases from 6.2% to 43.5%. Likewise, when both isotherms are regressed, the AAD increases from 13.1% to 34.7%. Similar poor results in the low pressure region have been found in many other systems with the compressed gas model (*Bae* et al., 1987). There is very little difference in the calculated mole fraction as there is virtually no difference in their respective k_{ij} values. Poor results in the low pressure region may imply that

(a) the P-R (or other cubic) EOS does not describe the critical region well; and

(b) the k_{ij} value is unable to compensate for the inadequacy of the model in that region.

(3) As shown in Figure 5.7, as pressure (P_r<2.0) approaches the critical pressure, the effect of k_{ij} on the calculated mole fraction diminishes. This observation helps support paragraph (2) above.

(4) A better correlation is obtained when k_{ij} is treated as temperature-dependent.

Overall the P-R compressed gas model did an excellent job in fitting the high pressure data.

The second approach to modeling utilized the Kirkwood-Buff local composition model. In this approach the solubility y_2 of a pure solid in a supercritical fluid is expressed by

$$\ln E = \ln Z_j^0 - \alpha_{ij} \ln(f_j^0 V_j^0/RT) + (v_i^s + V_{ij}\exp(b_0 + b_1/T) - V_{ij})(P - p_i^{sat})/RT \qquad (5\text{-}5)$$

The principle advantage for the local composition model in this case is that two of the three parameters, b_0 and b_1 , regressed from the data account for the solubility dependence on temperature. The computer program used to determine V_{12} , b_0 and b_1 , is presented in Appendix C. The results are shown in Table 5.3 and Figures 5.8 and 5.9.

Table 5.3. K-B LC Modeling Correlations

Case	Isotherm(s) Regressed	V_{12}	b_0	b_1	AAD%	Remarks
(a)	249K	327	5.39	-1239	13.8	
(b)	249K+244K	301	5.39	-1219	40.7	
(c)	249K+244K	312	5.39	-1226	19.7	minus 2/27/89 data
(d)	244K	271	5.38	-1184	37.0	
(e)	244K	286	5.33	-1185	12.2	minus 2/27/89 data

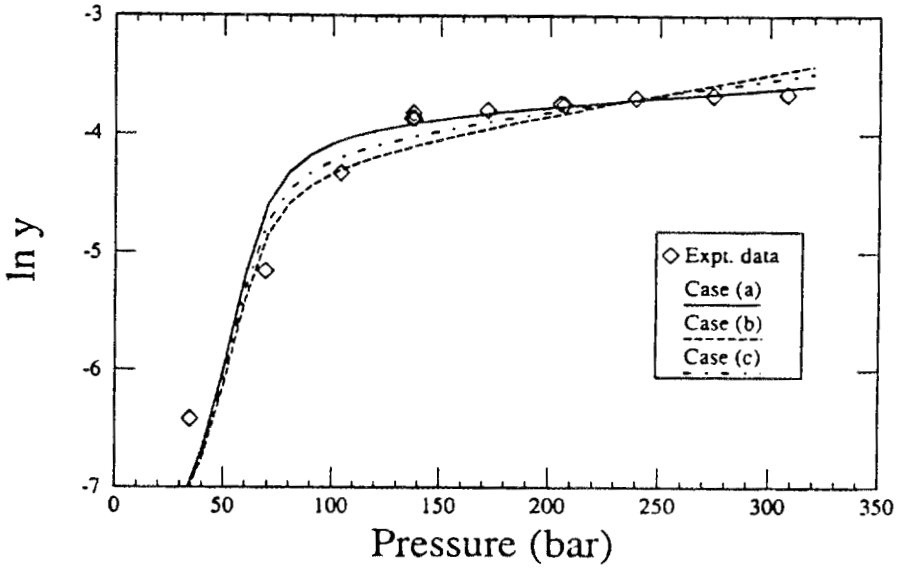

Fig. 5.8. K-B Modeling at 249K.

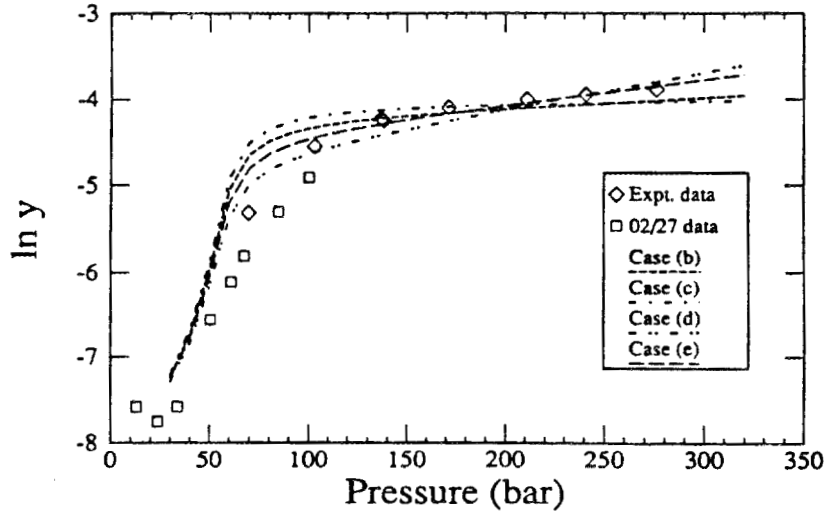

Fig. 5.9. K-B Modeling at 244K.

Some observations can be made from these tables and figures.

(1) The low AAD resulted from well established critical properties, solid density, and particularly the accurate EOS for the density of CF_4.

(2) The K-B local composition model appears more sensitive to the inclusion of the low pressure data of 02/27/89 than the P-R compressed gas model. As in the compressed gas model, an increase in AAD is also observed and the low pressure region does not correlate well.

(3) A better correlation is obtained when the parameters are treated as being temperature dependent.

Overall, the K-B model did an excellent job of correlating the data.

A comparison of the models is presented in Table 5.4. There appears to be no computational advantage and no significant improvement in correlation of the data by either model. For this system when the 02/27/89 data is excluded, the AAD of both models were equal to or less than the average AAD reported in the literature which for the P-R CG model is 26.4 % and for the K-B LC model is 18.4% (*Pfund* et al., 1988).

In regards to the low pressure data of 02/27/89, neither model correlated the data well. These data can be viewed with less than full confidence because they were taken outside the normal MS operating conditions at a superficial velocity which exceeds the equilibrium flow rate.

Table 5.4. Model Correlation Comparison

Isotherm	Model	NR. Isotherms Regressed	NR. Parameters	AAD%	Remarks
244K	K-B	2	3	40.7	
and	K-B	2	3	19.7	minus 2/27/89 data
249K	P-R	2	1	34.7	
	P-R	2	1	13.1	minus 2/27/89 data
249K	K-B	1	3	13.8	
	P-R	1	1	10.8	
244K	K-B	1	3	37.0	
	K-B	1	3	12.2	minus 2/27/89 data
	P-R	1	1	43.5	
	P-R	1	1	6.2	minus 2/27/89 data

5.3 Data Reliability

5.3.1 Summary of Error Analysis

The accumulated error was determined and applied to the 244K and 249K isotherms. As can be graphically seen in Figure 5.3, the accumulated error for high pressure data (> 136 bar) was less than 5% while the low pressure data (< 70 bar) was approximately 50%. The major variables in determining the accumulated error were:

(1) the accuracy of the calibration curve

(2) the interpretation of ion current strip chart values

(3) the correction for the MS pressure

(4) the accuracy of temperature and pressure measurements

Each data point was treated as the example in Appendix B.

5.3.2 Summary of Data Validation

Special care was taken to ensure the reliability of the 244K and 249K isotherms. The reproducibility of selected data (≈ 136 bar at 244K and 249K) thrice within 1.5% (less than the accumulated error) indicates that the sampling procedure was consistent and representative sampling had occurred. Appendix D discusses critical concerns regarding temperature uniformity and attainment of steady state equilibrium and their impact on data validity. Appendix D also addresses two isotherms (234K and 239K) at which data were inconsistent.

CHAPTER VI

CONCLUSIONS AND RECOMMENDATIONS

6.1 Conclusions

This study was concerned with the solubility of solid CCl_4 in supercritical CF_4 to broaden the database for current and future supercritical modeling. This particular solute-solvent system was chosen because both molecules can be approximated as being spherically symmetric, easing theoretical interpretation and because in their relative molecular size and interaction energy, they are different from previously studied systems..

The objectives of the study were met with great success. The apparatus capably demonstrated a simple means to directly couple mass spectrometry to SCFE for relatively volatile solutes. The 244K and the 249K isotherms are considered to be valid solubility measurements with the possible exception of 244K data taken 02/27/89. The 234K and 239K isotherms cannot be said with confidence to have reached equilibrium because of poor mass transfer and temperature equilibration. The accumulated error for the system was approximately 5% for high pressure data while the error increased to approximately 50% for the low pressure data of 02/27/89.

The objectives for modeling were also met with great success. The models effectively accounted for the small difference in molecular size and the large difference in intermolecular attraction of the system. Both the P-R compressed gas model and the K-B local composition model performed well. The AAD for both models were lower than the average AAD

reported in the literature. In this study there was no significant computational or correlative advantage to the Kirkwood-Buff local composition model when compared to the simpler P-R compressed gas model.

6.2 Recommendations

The results of this work lead to several recommendations regarding further solubility studies and data modeling.

6.2.1 Future Solubility Studies

This study has fulfilled it goals. Before any further studies are undertaken the equipment should be modified. Conditions should be optimized to achieve equilibrium at higher flow rates. Listed are several 'add on' improvements short of a complete equipment design.

(1) add another extraction cell in order to operate at higher superficial velocity rates and still approach equilibrium mole fractions

(2) mount the circulating fan external to the temperature enclosure

(3) replace the control meter valve stem with a finer tapered stem

With these changes and careful handling of inorganic fluorides such as MoF_6 in a dry box, these inorganic fluorides-CF_4 systems could again be studied with this apparatus.

6.2.2 Future Modeling

The success of the P-R compressed gas model and the Kirkwood-Buff local composition model indicates that the 244K and 249K isotherms lend themselves to further modeling.

It would be interesting to test the following models (among many) on the data:

(1) the Kirkwood-Buff excluded volume model

(2) the Carnahan-Starling van der Waals (CSVDW) hard sphere model

It is hoped that the K-B excluded volume model will be tested in the near future.

LIST OF REFERENCES

LIST OF REFERENCES

1. Adachi, Y. and C. Y. Benjamin, "Supercritical Fluid Extraction with Carbon Dioxide and Ethylene," *Fl. Ph. Equilib.*, **14**, 147 (1983).

2. Bae, H. K., S. S. Kim, and D. H. Han, "Estimation of the Equilibrium Concentration of Less-Volatile Substances in Supercritical Gases," *Int. Chem. Eng.*, **27**, 132 (1987).

3. Bamberger, T., J. C. Erickson, C. L. Cooney, and S. K. Kumar, "Measurement and Model Prediction of Solubilities of Pure Fatty Acids, Pure Triglycerides, and Mixtures of Triglycerides in Supercritical Carbon Dioxide," *J. Chem. Eng. Data*, **33**, 327 (1988).

4. Bienkowski, P. R., D. D. Lee, and C. H. Byers, "Evaluation of Separation and Purification in the Antibiotic Industry," *Applied Biochem. & Biotechnol.*, **18**, 262 (1988).

5. Billoni, N., J. Jose, and J. C. Merlin, "Solubility of Heavy Components in Supercritical CO_2 Using Directly Coupled Supercritical Fluid Extraction-High Performance Liquid Chromatography," *Proc. Int. Symp. on Supercritical Fluids*, **2**, 373 (1988).

6. Brennecke, J. F., and C. A. Eckert, "Fluoresence Spectroscopy Studies of Intermolecular Interactions in Supercritical Fluids," *Am. Chem. Soc., Symp. Ser.*, **406**, 14 (1989).

7. Brownlee, K. A., *Industrial Experimentation*, Chemical Publishing Co., Inc., Brooklyn, N. Y. (1948).

8. Bucher, E. H., "Solubilities of Organic Compounds in Supercritical CO_2," *Physik. Chem.*, **5**, 665 (1906).

9. Carnahan, N. F., and K. E. Starling, "Intermolecular Repulsions and the Equation of State for Fluids," *AIChE J.*, **18**, 1184 (1972).

10. Cochran, H. D., E. Johnson, and L. L. Lee, "Molecular Theory of Ternary Supercritical Solutions. I. Theory and Methods of Calculation," *J. Supercrit. Fluids*, submitted (1990).

11. Cochran, H. D., L. L. Lee, and D. M. Dfund, "Application of the Kirkwood-Buff Theory of Solutions to Dilute Supercritical Mixtures," *Fluid Phase Equilibria*, **34**, 219 (1987).

12. Cochran, H. D., L. L. Lee, and D. M. Dfund, "Theoreticl Models of Thermodynamic Properties of Supercritical Solutions," *Separation Science and Technology*, **23(12&13)**, 2031 (1988).

13. Cochran, H. D., R. S. Wu, and L. L. Lee, "Molecular Clustering in Supercritical Solutions," *I&EC Res.*, in press (1990).

14. Cornu, A., and R. Massot, *Compilation of Mass Spectral Data*, Vol. 1, Heyden and Son, Inc. (1975).

15. Czubryt, J. J., M. N. Myers, and J. C. Giddings, "Solubility Phenomena in Dense Carbon Dioxide in the Range 270-1900 Atmospheres," *J. Phys. Chem.*, **74**, 4269 (1970).

16. Dimitrelis, D., and J. M. Prausnitz, "Comparison of Two Hard-Sphere Reference Systems for Perturbation Theories for Mixtures," *Fluid Phase Equilibria*, **31**, 1 (1986).

17. Eckert, C. A., D. H. Ziger, K. P. Johnston, and T. K. Ellison, "The Use of Partial Molar Volume Data to Evaluate Equations of State for Supercritical Fluid Mixtures," *Fluid Phase Equilibria*, **14**, 167 (1983).

18. Eckert, C. A., D. H. Ziger, K. P. Johnston, and S. Kim, "Solute Partial Molal Volumes in Supercritical Fluids," *J. Phys. Chem.*, **90**, 2738 (1986).

19. Giddings, J. C., M. N. Myers, and J. W. King, "Dense Gas Chromatography at Pressures up to 2000 Atmospheres," *J. Chrom. Sci.*, **7**, 67 (1968).

20. Hannay, J. B. and J. Hogarth, "On the Solubility of Solid in Gases," *Proc. Royal Soc London*, **A29**, 324 (1879).

21. Haselow, J. S., S. J. Han, R. A. Greenkorn, and K. C. Chao, "Equation of State for Supercritical Extraction," *Am. Chem. Soc., Symp. Ser.*, **300**, 156 (1985).

22. Hawthorne, S. B., and D. J. Miller, "Directly Coupled Supercritical Fluid Extraction-Gas Chromatographic Analysis of Polycyclic Aromatic Hydrocarbons and Polychlorinated Biphenyls from Environmental Solids," *J. Chrom.*, **403**, 63 (1987).

23. Hubert, P. and O. G. Vitzthum, "Fluid Extraction of Hops, Spices and Tobacco with Supercritical Gases," *Ang. Chem. Int. Ed.*, **17**, 710 (1978).

24. *International Critical Tables of Numerical Data, Physics, Chemistry, and Technology*, Vol. 3, 215, McGraw-Hill Book Co. (1933).

25. Johnston, K. P., "New Directions in Supercritical Fluid Science and Technology," *Am. Chem. Soc., Symp. Ser.*, **400**, 1 (1989).

26. Johnston, K. P. and C. A. Eckert, "An Analytical Carnahan-Starling-van der Waals Model for Solubility of Hydrocarbon Solids in Supercritical Fluids," *AIChE J.*, **27**, 773 (1981).

27. Johnston, K. P., D. G. Peck and S. Kim, "Modeling Supercritical Mixtures: How Predictive Is It?," *Ind. Eng. Chem. Res.*, **28**, 1115 (1989).

28. Johnston, K. P., and J. M. Penninger, Eds., *Supercritical Fluid Science and Technology*, Am. Chem. Soc., Symp. Ser. 406, American Chemical Society: Washington, DC (1989).

29. Joshi, D. K. and J. M. Prausnitz, "Supercritical Fluid Extraction with Mixed Solvents," *AIChE J.*, **30(3)**, 522 (1984).

30. Kirkwood, J. G., and F. P. Buff, "The Statistical Theory of Solutions," *J. Chem. Phys.*, **19**, 774 (1951).

31. Kumar, S K., U. W. Suter, and R C. Reid, "A Statistical Mechanical Based Lattice Model Equation of State," *Ind. Eng. Chem. Res.*, **26**, 2532 (1987).

32. Lira, C. T., "Physical Chemistry of Supercritical Fluids: A Tutorial," *Am. Chem. Soc., Symp. Ser.*, **366**, 1 (1988).

33. Mackay, M. E., and M. E. Paulaitis, "Solid Solubilities of Heavy Hydrocarbons in Supercritical Solvents," *Ind. Eng. Chem. Fundam.*, **18**, 149 (1979).

34. Mansoori, G. A., N. F. Carnahan, K. E. Starling, and T. W. Leland, "Equilibrium Thermodynamic Properties of the Mixture of Hard Spheres," *J. Chem. Phys.*, **54**, 1523 (1971).

35. McHugh, M. A. and M. E. Paulaitis, "Solid Solubilities of Naphthalene and Biphenyl in Supercritical Carbon Dioxide," *J. Chem. Eng. Data*, **25**, 326 (1980).

36. McHugh, M. A., A. J. Seckner, and T. J. Yogan, "High Pressure Phase Behavior of Octacosane And Carbon Dioxide," *Ind. Eng. Chem. Fundam.*, **23**, 493 (1984).

37. McHugh, M. A., and V. J. Krukonis, *Supercritical Fluid Extraction: Principles and Practice*, Butterworth Publishers, Boston (1986).

38. Mitra, S., J. W. Chen, and D. S. Viswanath, "Solubility and Partial Molar Volumes of Heavy Hydrocarbons in Supercritical CO_2," *J. Chem. Eng. Data*, **33**, 35 (1988).

39. Moradinia, I. and A. S. Teja, "Solubilities of *n*-Octacosane, *n*-Triacontane, and *n*-Dotriacontane in Supercritical Ethane," *Fl. Ph. Equilib.*, **28**, 199 (1986).

40. Paulaitis, M. E., V. J. Krukonis, R. T. Kurnik, and R. C. Reid, "Supercritical Fluid Extraction," *Reviews in Chemical Engineering*, **1(2)**, 179 (1983).

41. Peng, D. Y. and D. B. Robinson, "A New Two-Constant Equation of State," *Ind. Eng. Chem. Fund.*, **15**, 1, 59 (1976).

42. Pfund, D. M., L. L. Lee and H. D. Cochran, "Application of the Kirkwood-Buff Theory of Solutions to Dilute Supercritical Mixtures. II. The Excluded Volume and Local Composition Models," *Fluid Phase Equil.*, **39**, 161 (1988).

43. Prausnitz, J. M., R. N. Lichtenthaler, and E. G. de Azevedo, *Molecular Thermodynamics of Fluid Phase Equilibria*, 2nd Edition, Prentice-Hall Pub. Co., Englewood Cliffs, New Jersey, 1986.

44. Renon, H., and J. M. Prausnitz, "Local Compositions in Thermodynamic Excess Functions for Liquid Mixtures," *AIChE J.*, **14**, 135 (1968).

45. Reynolds, W. C., *Thermodynamic Properties in SI: Graphs, Tables, and Computational Equations for Fourty Substances*, Standford University Mechanical Engineering Department: Stanford, CA (1979).

46. Schneider, G. M., "Physicochemical Principles of Extraction with Supercritical Gases," *Agnew. Chem. Int. Ed. Engl.*, **17**, 716 (1978).

47. Schneider, G. M., "Extraction of Fluid Mixtures at High Pressures — Basis of Supercritical Fluid Technology," *Proc. of the Int. Symp. on Supercritical Fluids*, **1**, 1 (1988).

48. Schneiderman, M. A., A. K. Shara, and D. C. Locke, "Determination of Anthraquinone in Paper and Wood Using Supercritical Fluid Extraction and High-Performance Liquid Chromatography with Electrochemical Detection," *J. Chrom.*, **409**, 343 (1987).

49. Shing, K. S., and S.T. Chung, "Computer Simulation Methods for the Calculation of Solubility in Supercritical Extraction Systems," *J. Phys. Chem.*, **91**, 1674 (1987).

50. Shoemaker, D. P., and C. W. Garland, *Experiments in Physical Chemistry*, McGraw-Hill Book Co., Inc. (1962).

51. Simnick, J. J., C. C. Lawson, H. M. Lin, and K. C. Chao, "Vapor-liquid Equilibrium of Hydrogen/Tetralin System at Elevated Temperatures and Pressures," *AIChE J.*, **23**, 469 (1977).

52. Smith, R. D., H. T. Kalinoski, and H. D. Udseth, "Fundamentals and Practice of Supercritical Fluid Chromatography-Mass Spectrometry," *Mass Spectrometry Reviews*, **6**, 445 (1987a).

53. Smith, R. D., H. R. Udseth, B. W. Wright, and C. R. Yonkers, "Solubilities in Supercritical Fluids," *Separation Science and Technology*, **22(2)**, 1065 (1987b).

54. Smith, R. D., B. W. Wright, and C. R. Yonker, " Supercritical Fluid Chromatrography: Current Status and Progress," *Anal. Chem.*, **60(23)**, 1323 (1988).

55. Squires, T. G. and M. E. Paulaitis, Eds., *Supercritical Fluids: Chemical and Engineering Principles and Applications*, Am. Chem. Soc. Symp. Ser. 329, American Chemical Society: Washington, DC (1987).

56. Stahl, E., E. Schutz, and H.K. Mangold, "Extraction of Seed Oils with Liquid and Supercritical Carbon Dioxide," *J. Agric. Food Chem.*, **28**, 1153 (1980).

57. Streett, W. B., "Gas-Gas Equilibrium: High Pressure Limits," *Can. J. Chem. Eng.*, **52**, 92 (1974).

58. Todd, D. B. and J.C. Elgin, "Phase Equilibria in Systems with Ethylene above Its Critical Temperature," *AIChE J.*, **1**, 20 (1955).

59. Van Leer, R. A., and M. E. Paulaitis, "Solubilities of Phenol and Chlorinated Phenols in Supercritical Carbon Dioxide," *J. Chem. Eng. Data*, **25**, 257 (1980).

60. Villard, P., "Solubility of Liquids and Solids in Gas," *J. Phys.*, **5**, 455 (1896).

61. Williams, D. F., "Extraction with Supercritical Gases," *Chem. Eng. Sci.*, **36**, 1769 (1981).

62. Willson, R. C., and C. L. Cooney, "Use of Supercritical and Near Critical Solvents for Recovery of Fermentation Products," Preprints -Chicago ACS Meeting, September 1985.

63. Wolkomir, R.,"Supercritical Potatoe Chips Breakthrough," *Omni*, **6**, 28 (1984).

64. Wong, J. M., and K. P. Johnston, "Solubilization of Biomolecules in Carbon Dioxide Based Supercritical Fluids," *Biotech. Prog.*, **2**, 29 (1986).

65. Wong, J. M., R. S. Pearlman, and K. P. Johnston, "Supercritical Fluid Mixtures: Prediction of the Phase Behavior," *J. Phys. Chem.*, **89**, 2671 (1985).

66. Zhuze, T. P., "Compressed Hydrocarbon Gases as a Solvent," *Petroleum*, **23**, 289 (1960).

67. Zosel, K., "Separation with Supercritical Gases: Practical Applicatons," *Angew. Chem. Int. Ed. Engl.*, **17**, 702 (1978).

APPENDICES

APPENDIX A

RAW DATA

234K ISOTHERM							
Date (M/D/Y)	Pres. (bar)	FR (l/min)	I (10^{-12}A)	MS Pres. (10^{-6}torr)	I_{corr} (10^{-12}A)	y	Notes (#)
03/01/89	68.95	.045	0.87	2.330	0.354	.00367	
03/01/89	86.18	.045	1.26	2.340	0.511	.00513	
03/01/89	102.73	.040	1.55	2.330	0.631	.00622	
03/01/89	135.48	.060	1.50	2.315	0.616	.00609	
03/03/03	103.42	.045	1.52	2.360	0.605	.00597	
03/10/89	136.86	.050	1.31	2.465	0.503	.00505	(1)
03/19/89	271.65	.025	1.13	2.175	0.512	.00514	(2)
03/22/89	274.06	.060	1.63	2.950	0.466	.00471	(3)
03/23/89	273.72	.040	1.05	2.120	0.496	.00499	(4)
03/23/89	206.84	.030	1.16	2.090	0.557	.00555	
03/23/89	136.86	.030	1.75	2.575	0.610	.00603	
03/23/89	275.00	.030	1.72	2.550	0.607	.00601	
03/27/89	273.03	.030	1.86	2.680	0.612	.00605	
04/05/89	274.41	.035	1.50	2.280	0.627	.00618	
04/05/89	205.46	.030	1.58	2.255	0.675	.00662	
04/05/89	136.86	.035	1.47	2.280	0.614	.00606	
04/12/89	102.73	.040	1.14	2.200	0.505	.00507	(5)
04/12/89	171.68	.030	1.08	2.100	0.518	.00520	(5)
04/12/89	243.73	.045	1.07	2.085	0.519	.00520	(5)
04/24/89	239.24	.030	1.10	1.975	0.586	.00581	(6)

Notes:

(1) abnormal experimental conditions - high Δ T across column, increase in pressure resulted in decrease in mole fraction observed

(2) abnormal experimental conditions - high Δ P across column and plugging observed

(3) temperature was low - 233.3K

(4) abnormal experimental conditions - erratic flow rate

(5) inconsistent with any other data

(6) abnormal experimental conditions - high Δ P across column and plugging observed, erratic flow rate

239K ISOTHERM							
Date (M/D/Y)	Pres. (bar)	FR (l/min)	I (10^{-12}A)	MS Pres. (10^{-6}torr)	I_{corr} (10^{-12}A)	y	Notes (#)
04/25/89	67.64	.025	0.95	2.120	0.448	.00455	
04/25/89	136.51	.035	2.06	2.125	0.972	.00934	
04/25/89	205.94	.020	2.10	2.120	0.991	.00952	
04/26/89	205.12	.020	1.75	1.930	0.984	.00945	
04/26/89	273.12	.025	1.77	1.930	0.995	.00956	
04/28/89	135.20	.035	1.72	2.150	0.800	.00775	
04/28/89	274.75	.030	1.75	2.057	0.884	.00852	
05/02/89	136.17	.040	1.60	2.150	0.744	.00724	
05/02/89	273.72	.035	1.69	2.050	0.853	.00823	
05/03/89	67.57	.030	0.72	2.020	0.370	.00382	
05/03/89	136.51	.050	1.52	2.070	0.742	.00722	
05/03/89	204.43	.045	1.74	2.200	0.771	.00749	
05/03/89	275.79	.040	1.83	2.145	0.851	.00822	
05/23/89	136.51	.020	2.16	2.100	1.037	.00998	(1)
05/23/89	137.55	.025	2.05	2.070	1.000	.00963	(1)
05/23/89	136.51	.040	1.62	2.020	0.827	.00800	(1)
05/23/89	136.17	.060	1.39	2.095	0.673	.00662	(1)
05/23/89	136.17	.085	1.32	2.060	0.667	.00656	(1)
05/23/89	136.17	.125	1.20	2.075	0.586	.00583	(1)
05/25/89	136.51	.025	1.75	2.105	0.840	.00812	(2)

239K ISOTHERM							
Date (M/D/Y)	Pres. (bar)	FR (l/min)	I (10^{-12}A)	MS Pres. (10^{-6}torr)	I_{corr} (10^{-12}A)	y	Notes (#)
06/07/89	138.24	.035	2.03	2.030	1.043	.01050	(3)
06/07/89	137.55	.085	1.65	1.970	0.873	.00844	(3)
06/09/89	137.20	.040	1.40	1.900	0.791	.00769	(4)
06/21/89	135.82	.030	1.71	1.970	0.911	.00880	(5,6)

Notes:

(1) flow rate experiment data

(2) abnormal experimental conditions - high Δ P across column and plugging observed

(3) abnormal experimental conditions - temperature erratic, loss of temperature control

(4) abnormal experimental conditions - temperature and flow rate erratic, loss of fine control

(5) abnormal experimental conditions - plugging observed

(6) Cu block installed

244K ISOTHERM							
Date (M/D/Y)	Pres. (bar)	FR (l/min)	I (10^{-12}A)	MS Pres. (10^{-6}torr)	I_{corr} (10^{-12}A)	y	Notes (#)
01/18/89	240.90	.050	1.44	1.120	1.938	.01938	
01/18/89	276.13	.050	1.49	1.120	2.006	.02006	
01/24/89	275.10	.040	1.70	1.380	1.700	.01700	(1)
01/24/89	138.24	.040	1.43	1.400	1.429	.01429	
01/31/89	67.57	.030	0.15	1.100	0.206	.00223	(2)
02/07/89	210.98	.030	1.78	1.345	1.831	.01831	
02/08/89	171.33	.045	1.62	1.345	1.667	.01667	
02/08/89	103.08	.040	1.11	1.390	1.102	.01063	
02/08/89	69.70	.050	0.49	1.380	0.490	.00495	
02/10/89	137.55	.020	1.27	1.270	1.448	.01448	(3)
02/10/89	137.55	.130	1.18	1.390	1.172	.01133	(3)
02/10/89	136.86	.065	1.40	1.390	1.386	.01386	(3)
02/10/89	136.86	.220	0.70	1.390	0.695	.00682	(3)
02/17/89	42.75	.045	0.35	1.900	0.202	.00219	(4)
02/17/89	51.16	.040	0.40	1.775	0.253	.00270	(4)
06/22/89	136.86	.025	1.30	1.300	1.461	.01461	(5)
07/20/89	136.86	.170	1.00	1.380	1.000	.00963	(3,5)
07/20/89	136.86	.125	1.17	1.380	1.170	.01131	(3,5)
07/20/89	135.82	.025	2.00	1.370	2.040	.02040	(1,3,5)

244K ISOTHERM							
Date (M/D/Y)	Pres. (bar)	FR (l/min)	I (10^{-12}A)	MS Pres. (10^{-6}torr)	I_{corr} (10^{-12}A)	y	Notes (#)
02/27/89	12.96	.030	0.20	3.720	0.044	.00051	(6)
02/27/89	23.78	.030	0.17	3.725	0.037	.00043	(6)
02/27/89	33.78	.025	0.20	3.725	0.044	.00056	(6)
02/27/89	50.67	.025	0.57	3.725	0.126	.00141	(6)
02/27/89	61.02	.025	1.10	4.150	0.203	.00220	(6)
02/27/89	67.58	.025	1.52	4.130	0.282	.00299	(6)
02/27/89	84.81	.025	2.62	4.090	0.495	.00500	(6)
02/27/89	100.32	.030	4.20	4.200	0.759	.00740	(6)

Notes:

(1) abnormal experimental conditions - high Δ P across column and plugging observed

(2) contaminated sample - contaminated by isopropanol

(3) flow rate experiment data

(4) column temperature was high - 244.5K

(5) Cu block installed

(6) high vacuum chamber pressure of MS was outside normal experimental operating conditions - large pressure correction factor applied

249K ISOTHERM							
Date (M/D/Y)	Pres. (bar)	FR (l/min)	I (10^{-12}A)	MS Pres. (10^{-6}torr)	I_{corr} (10^{-12}A)	y	Notes (#)
06/27/89	274.06	.025	2.52	1.379	2.555	.02550	
06/29/89	136.51	.025	2.06	1.370	2.101	.02101	
06/29/89	103.76	.030	1.35	1.380	1.350	.01329	
06/29/89	68.95	.025	0.58	1.400	0.576	.00574	
06/29/89	34.47	.030	0.15	1.420	0.147	.00163	
07/06/89	307.85	.025	2.58	1.380	2.580	.02580	
07/06/89	206.49	.025	2.36	1.375	2.360	.02360	
07/06/89	239.24	.025	2.49	1.380	2.490	.02490	
07/06/89	171.68	.025	2.25	1.380	2.250	.02250	
07/12/89	204.77	.020	2.38	1.385	2.380	.02380	
07/13/89	137.89	.020	2.10	1.380	2.100	.02100	
07/14/89	137.55	.015	2.10	1.375	2.100	.02100	
07/18/89	136.51	.170	1.60	1.390	1.589	.01589	(1)
07/18/89	137.27	.015	2.20	1.380	2.200	.02200	(1)
07/18/89	136.86	.090	2.00	1.380	2.000	.02000	(1)
07/18/89	137.55	.035	2.12	1.390	2.102	.02102	(1)
07/18/89	136.17	.105	1.98	1.380	1.980	.01980	(1)

Notes:

(1) flow rate experiment data

Comment: Cu block installed for all data

CALIBRATION DATA					
Date	x (10^{-2})	I_{exp} (10^{-12}A)	MS Pres. (10^{-6}Torr)	I_{corr} (10^{-12}A)	cal. error (%)
08/02/89	0.544±0.5%	0.550±.025	1.375	0.550±4.55%	±5.05
08/10/89	1.400±1.0%	1.400±.025	1.380	1.400±1.79%	±2.79
08/11/89	1.408±1.0%	1.420±.025	1.390	1.410±1.79%	±2.79
08/14/89	0.355±2.0%	0.320±.025	1.380	0.320±7.81%	±9.81
08/23/89	0.710±1.0%	0.730±.025	1.375	0.730±3.42%	±4.42
08/24/89	1.054±1.3%	1.090±.025	1.375	1.090±2.30%	±3.60

APPENDIX B

ERROR ANALYSIS

It is important to determine the experimental uncertainty in each of the measurements to evaluate the accuracy of the experimental solubility. An estimate of the error of the reported experimental solubility data is discussed using a mathematical error analysis (*Shoemaker* and *Garland*, 1962). The accumulated error in the measurements such as ion current intensity, pressure, and temperature is used to determine the error for the reported experimental solubility data.

Consider a function f with several variables,

$$f = f(x_1, x_2, ..., x_n) \tag{B-1}$$

The total derivatives of f is given as

$$df = \left[\frac{\partial f}{\partial x_1}\right]_{x \neq x_1} dx_1 + ... + \left[\frac{\partial f}{\partial x_n}\right]_{x \neq x_n} dx_n \tag{B-2}$$

If the change in the independent variable is assumed to be small, the equation (B-2) can be expressed by

$$df = \Delta f = \left[\frac{\partial f}{\partial x_1}\right]_{x \neq x_1} \Delta x_1 + ... + \left[\frac{\partial f}{\partial x_n}\right]_{x \neq x_n} \Delta x_n \tag{B-3}$$

This is equivalent to a Taylor expansion in which only the first-power terms have been retained.

As an example of the accumulated error associated with CCl_4 in supercritical CF_4, the condition of 249K and 137.55 bar on 06/22/89 was used.

The variables that effect the total accumulated error are as follows:

(1) T = 249.0 ± 0.2 K (the column temperature deviated from the isotherm temperature up to ± 0.2K)

(2) P = 137.55 ± 0.345 bar (the outlet Heise pressure gauge was accurate to ± 0.345 bar)

(3) I_{CCl_4} = 2.100 ± 0.025 (the error accounts for the strip chart interpretation error and any MS pressure correction error)

(4) Accuracy of calibration I = ±2.79% (results from the uncertainty of mass delivery (± 0.1μl) to the calibration cylinder and the strip chart interpretation error)

Thus, the accumulated error in general terms is

acc. error = (calibration + ion current + pressure + temperature) error

The calibration error is computed from two areas of uncertainty - the mass of CCl_4 delivered to the calibration cylinder and the inaccuracy of reading the strip chart recorder. Then, the total relative error is equal to the mass error plus the ion current error.

Mass error:

$$n_{CCl_4} = \frac{(20 \pm .1ml)(10^{-3})(1.584g/ml)}{153.82g/mol} = .00020595 \pm .00000206\ moles$$

$$n_{CF_4} = \frac{(2.6+14.7/14.7)(0.3034)}{(0.08205)(300)} = .01450589\ moles \qquad \text{(assumed ideal gas law)}$$

$$x_{CCl_4} = \frac{n_{CCl_4}}{n_{CF_4} + n_{CCl_4}} = .01400 \pm .00014\ (\approx 1.0\%\ \text{error})$$

Calibration ion current error:

$$I_{corr} = 1.4000 \pm 0.025\ (\approx 1.79\%\ \text{error})$$

calibration error = 1.0% + 1.79% = ±2.79%

The ion current measurement error accounts for the inaccuracy in interpretating the strip

chart peak height and the MS pressure correction, which was significant at MS pressures of 10^{-6} Torr (up to 36%).

$$I_{corr} = 2.100 \pm .025$$

then $y_2 = (2.10 \pm .025\ I)(.01 - I)$

$$= .02100 \pm .00025\ (\approx 1.19\%\ \text{error})$$

The uncertainty of the system temperature and pressure influence the value of the solubility

$$y_2 = f\ (T, P) \tag{B-4}$$

Therefore

$$dy_2 = \Delta y_2 = \left[\frac{\partial y_2}{\partial T}\right]_P \Delta T + \left[\frac{\partial y_2}{\partial P}\right]_T \Delta P \tag{B-5}$$

To solve the equation (B-5) the partial derivatives, $(\partial y_2/\partial T)_P$ and $(\partial y_2/\partial P)_T$, must be determined. These values can be obtained in two ways, a graphical method and an analytical method. The partial derivatives, $(\partial y_2/\partial T)_P$ and $(\partial y_2/\partial P)_T$ are just the slopes of the tangent lines. The graphical differentiation would be difficult because of the number of data points and isotherms, and also inaccurate because of the questionable values of the 234 and 239K isotherms. For the analytical method, the Peng-Robinson model can be used to approximate the values of the partial derivatives.

$$y_2 = \frac{p_2^{sat}}{P}\ \frac{1}{\phi_2^f}\ \left[\frac{v_2^s\ \left[P - p_2^{sat}\right]}{RT}\right] \tag{B-6}$$

In this work the approximate values of partial derivatives were calculated using equation (B-6) at 138 bar.

P (bar)	y_2 (P-R EOS)
138	0.01560128
136	0.01545050

Thus

$$\left|\frac{\Delta y_2}{\Delta P}\right|_{249K} = \frac{|.01560128 - .01545050|}{138 - 136} = 0.000075 bar^{-1}$$

and at 249K

T (K)	y_2 (P-R EOS)
249K	0.01560128
248K	0.01533285

Thus

$$\left|\frac{\Delta y_2}{\Delta T}\right|_{138bar} = \frac{|.01560128 - .01533285|}{249 - 248} = 0.000268\ K^{-1}$$

Therefore the accumulated error in the solubility of the solid CCl_4 at 249K and 137.55 bar is given by

$$\varepsilon = \left|\left[\frac{\partial y_2}{\partial T}\right]_P \Delta T + \left[\frac{\partial y_2}{\partial P}\right]_T \Delta P\right| + \left|\left[\frac{\partial y_2}{\partial I}\right]\right| \Delta I_{calibration} + \left|\left[\frac{\partial y_2}{\partial I}\right]\right| \Delta I_{measured}$$

$$= (7.5\times10^{-5})(0.345) + (2.68\times10^{-4})(0.2) + (.0586)(.01) + (.025)(.01)$$

$$= \pm\ 9.155\times10^{-4}$$

Therefore the reported value of the solubility is

$y_2 = 0.02100 \pm .00092$ (≈ 4.38% error) at 249K and 137.55 bar.

Likewise, the uncertainity of the experimental solubility data was determined for the remaining data on the 244K and 249K isotherms.

APPENDIX C

COMPUTER PROGRAMS

```
      PROGRAM TBNTEST
C-----------------------------------------------------------------------------
C
C     TOM BARBER 3/12/90
C
C     MAIN DRIVER FOR DOING NONLINEAR REGRESSION WITH NL2SOL
C
C     CALCULATES KIJ, CALCULATES PX CURVE FOR P-R EOS
C

      IMPLICIT DOUBLE PRECISION (A-H,O-Z)
      INTEGER UIPARM,IV(100),NP,NF
      DIMENSION R(100),V(1000)
      DOUBLE PRECISION KIJ(2), CONS(3), XTOL(2), CONSF(3)
      DIMENSION  Z(2), FUG(2), XF(4), YCALC(100), YEXP(100), VSAT(2)
      DIMENSION P(100), TEMP(100), TC(2), PC(2), ACEN(2), TB(2)
      DIMENSION PSAT(100), PSA(10)
      CHARACTER*30 FNAME(10), FNAME1, FNAME2, FNAME3
      CHARACTER*78 SS1, SS2, SS3, SS4

      EXTERNAL ERR3PN,ERR3N
      COMMON /EXPTAL/ P, YCALC, YEXP, TEMP,  NC, PSAT
      COMMON /CRPROP/ TC, PC, ACEN, TB, VSAT
      COMMON /FIN/ IFIN ,ICON

      CALL DFAULT(IV,V)
      UIPARM = 0

C     NUMBER OF COMPONENTS  NC = 2

      NC = 2
C
C     READ THE FILE TEST.FIL AND GET THE FILE NAMES THAT CONTAIN THE
C      PROPERTIES OF THE COMPONENTS
C     FNAME1 - PROPERTIES OF CF4
C     FNAME2 - PROPERTIES OF CCL4
C     IPSAT -  FLAG TO INDICATE HOW PSAT IS TO BE CALCULATED
C      IPSAT = 1      PSAT TO BE CALCULATED USING THE LEE-KESSLER CORR.
C      IPSAT = 2      PSAT TO BE READ IN FROM A FILE
C
C      IPSAT = 3      PSAT TO BE CALCULATED FROM ANTOINES EQN
C      Note that IPSAT = 3 has not been implemented yet
C                IPSAT = 1 will not be used
C
C     ICON  -  FLAG TO INDICATE HOW MANY CONSTANTS ARE BEING REGRESSED
C      ICON = 1       KIJ TO BE REGRESSED
C      ICON = 3       KIJ AND PSAT TO BE REGRESSED
C
C      ICON = 2       ONLY PSAT TO BE REGRESSED
C      Note that ICON = 2 has not been implemented yet
C                     = 3 will not be used either
C
      OPEN (UNIT=20,FILE='TBNTEST.FIL',STATUS='OLD')
      READ (20,'(A)') FNAME1
      READ (20,'(A)') FNAME2
      READ (20,*) ICON
      READ (20,*) IPSAT
C     IF (IPSAT.EQ.3) READ (20,'(A)') FNAME3 (IPSAT = 3 not used)
      CLOSE (UNIT=20)

      OPEN (UNIT=25,FILE='TBNTEST.DAT',STATUS='OLD')
      DO 50 I = 1,10
             READ (25,'(A)',ERR=55) FNAME(I)
50    CONTINUE
55    NFDATA = I - 1
```

```
      CLOSE (UNIT=25)

      OPEN (UNIT=30,FILE=FNAME1,STATUS='OLD')
      READ (30,'(A)') SS1
      READ (30,*) PC(1)
      READ (30,*) TC(1)
      READ (30,*) ACEN(1)
      CLOSE (UNIT=30)

      OPEN (UNIT=40, FILE=FNAME2,STATUS='OLD')
      READ (40,'(A)') SS2
      READ (40,*) PC(2)
      READ (40,*) TC(2)
      READ (40,*) ACEN(2)
      READ (40,*) TB(2)
      READ (40,*) VSAT(2)
      CLOSE (UNIT=40)

C     This portion not used
C     IF (IPSAT.EQ.3) THEN
C             OPEN (UNIT=50,FILE=FNAME3,STATUS='OLD')
C             READ (50,*)ANTA
C             READ (50,*)ANTB
C             READ (50,*)ANTC
C     ENDIF
C
C     This portion used when acentric factor not known, used for Ko's thesis  C
C     CALCULATE THE ACENTRIC FACTOR OF PENICILLIN
C
C     TBR = TB(2)/TC(2)
C     A = -DLOG(PC(2)/1.01325D0) -5.97214D0 + 6.09648D0/TBR +
C    $        1.28862*DLOG(TBR) - 0.169347D0*TBR**6
C     B = 15.2518 - 15.6875D0/TBR - 13.4721*DLOG(TBR) +
C    $        0.43577D0*TBR**6
C     ACEN(2) = A/B

      OPEN (UNIT=78,FILE='NTEST.OUT',STATUS='UNKNOWN')
C      CALL APPEND(78)
      OPEN (UNIT=100,FILE='NTEST.RES',STATUS='UNKNOWN')
C      CALL APPEND(100)
      WRITE (78,*)'*************************************************',
     $ '*****************'
      WRITE (100,*)'*************************************************',
     $ '*****************'

      ND = 0
      JJ = 1
      DO 70 J = 1,NFDATA
          OPEN (UNIT=10,FILE=FNAME(J),STATUS='OLD')
          K = 1
          DO 110 I = ND+1,200
              IF ((K.EQ.1).AND.(IPSAT.EQ.2)) THEN
                  READ (10,*,ERR=115)P(I),YEXP(I),TEMP(I),PSAT(I)
                  PSA(JJ) = PSAT(I)
              ELSE
                  READ (10,*,ERR=115)P(I),YEXP(I),TEMP(I)
C
C  This part used if all choices of IPSAT where available
C                 IF (IPSAT.EQ.1) THEN
C                     TR = TEMP(I)/TC(2)
C                     PSAT(I) = DEXP(TBR/(1.D0-TBR)*(1.D0-1.D0/TR)
C    $                   *DLOG(PC(2)/1.01325D0))
C                 ELSE IF (IPSAT.EQ.2) THEN
C                     PSAT(I) = PSAT(I-1)
C                 ELSE IF (IPSAT.EQ.3) THEN
C                     PSAT(I) = DEXP(ANTA - ANTB/(TEMP(I)+ANTC))
```

```
C                   ENDIF

                PSAT(I) = PSAT(I-1)
                ENDIF
                WRITE (78,95)P(I),YEXP(I),TEMP(I),PSAT(I)
95      FORMAT(1X,F10.2,5X,1P,E12.5,5X,0P,F10.2,5X,1P,E12.5)
                K = K + 1
110         CONTINUE
115         ND  = I - 1
            JJ = JJ + 1
            CLOSE (UNIT=10)
70      CONTINUE


        OPEN (UNIT=55,FILE='NL2GUEST.DAT',STATUS='OLD')
C       Initial Kij guess
        READ (55,*) CONS(1)
C       Only Kij to be regressed
C       READ (55,*) CONS(2)
C       READ (55,*) CONS(3)
C       No tolerances levels set
C       READ (55,*) XTOL(1)
C       READ (55,*) XTOL(2)
C       READ (55,*) XTOL(3)
        WRITE (78,*) SS1
        WRITE (78,*)' PROPERTIES OF COMPONENT 1 (CF4) '
        WRITE (78,*) 'CRITICAL PRESSURE ',PC(1),' bar.'
        WRITE (78,*) 'CRITICAL TEMPERATURE ',TC(1),' K.'
        WRITE (78,*) 'ACENTRIC FACTOR ',ACEN(1)

        WRITE (78,*) SS2
        WRITE (78,*)' PROPERTIES OF COMPONENT 2 (CCL4) '
        WRITE (78,*) 'CRITICAL PRESSURE ',PC(2),' bar.'
        WRITE (78,*) 'CRITICAL TEMPERATURE ',TC(2),' K.'
        WRITE (78,*) 'ACENTRIC FACTOR ',ACEN(2)
        WRITE (78,*) 'BOILING POINT ',TB(2),' K.'
        WRITE (78,*) 'SATURATED MOLAR VOLUME ',VSAT(2),' cm^3/gmol.'


C       IV(1) = 12 MEANS THAT DFAULT HAS BEEN CALLED INITIALLY
C
        IV(1) = 12

C
C       IV(15) CORRESPONDS TO THE COVARIANCE MATRIX OUTPUT
C        = 1 IMPLIES SIGMA*H**-1*(J**T*J)*H**-1
C        = 2 IMPLIES SIGMA*H**-1
C        = 1 IMPLIES SIGMA*(J**T*J)**-1
C
        IV(15) = 2
C
C       V(32) = V(RCTOL)        DEFAULT MAX( 10^-10, MACHEP^(2/3))
C       V(33) = V(XCTOL)        DEFAULT 100*MACHEP
C       V(34) = V(XFTOL)        DEFAULT 100*MACHEP
C       BY SETTING V(32) = 1.2D-16 WE ARE TRYING TO USE THE X-CONVERGENCE
C        CRITERION.
C
C       V(32) = 1.2D-16
c       IV(39) = 1
C MINEXP                        -1024
C MAXEXP                         1023
C EPS             1.110223024625157E-016
C EPSNEG                  1.110223024625157E-016
C XMIN            5.562684646268003E-309
C XMAX            8.988465674311579E+307
```

```
      IV(24) = 0
C     V(34) = 1.11d-10
C     IF (ICON.EQ.3) NP = 2 not used
C     IF (ICON.EQ.2) NP = 2 not used
      IF (ICON.EQ.1) NP = 1

      UIPARM = 0
      CALL NL2SNO(ND, NP, CONS, ERR3N, IV, V, UIPARM, URPARM, UFPARM)

      IFIN = 1
      CALL ERR3N(ND, NP, CONS, NF, R, UIPARM, URPARM, UFPARM)


      IFIN = 2
      PINIT = 30.D0
      TEMPER = TEMP(1)
      ND = 30
      DELP = 10.D0
      DO 250 I=1,50
              P(I) = PINIT + DBLE(I-1)*DELP
              TEMP(I) = TEMPER
C
C     Used for Lee-Keesler Correlation
C                 IF ((ICON.EQ.1).AND.(IPSAT.EQ.1)) THEN
C                     TR = TEMP(I)/TC(2)
C                     PSAT(I) = DEXP(TBR/(1.D0-TBR)*(1.D0-1.D0/TR)
C    $                   *DLOG(PC(2)/1.01325D0))
C                 ELSE
            IF ((ICON.EQ.1).AND.(IPSAT.EQ.2)) THEN
            PSAT(I) = PSAT(I-1)
C                 ELSE IF ((ICON.EQ.1).AND.(IPSAT.EQ.3)) THEN (not used)
C                     PSAT(I) = DEXP(ANTA - ANTB/(TEMP(I)+ANTC))
            ENDIF
C                 IF (ICON.EQ.3) PSAT(I) = DEXP(CONS(2)) (not used)
C             WRITE (*,*)P(I),TEMP(I)
250   CONTINUE
      CALL ERR3N(ND, NP, CONS, NF, R, UIPARM, URPARM, UFPARM)
900   CONTINUE

      STOP
      END

      SUBROUTINE ERR3N (ND, NP, CONS, NF, R, UIPARM, URPARM, UFPARM)

C-----------------------------------------------------------------------
C
C     VINOD SHAH 2/27/90
C     THIS SUBROUTINE IS USED BY NL2SOL OR NL2SNO TO CALCULATE THE RESIDUAL
C      VECTOR R(I) FOR I = 1,N EXPERIMENTS TO BE USED FOR NONLINEAR
C      REGRESSION.
C
C
      IMPLICIT REAL*8 (A-H,O-Z)
      INTEGER N,NP,NF,UIPARM
      DOUBLE PRECISION R(100), X(10), KIJ(2), K1(2),
     $ PROP(20), YCALC(100),YEXP(100),XTOL(2),KF(2),PE(100),K2(2),
     $ TEMP(100),P(100),TC(2),PC(2),ACEN(2),TB(2),VSAT(2),PSAT(100)
      COMMON /EXPTAL/ P, YCALC, YEXP, TEMP,  NC, PSAT
      COMMON /CRPROP/ TC, PC, ACEN, TB, VSAT
      COMMON /FIN/ IFIN ,ICON

      EXTERNAL ERR3PN

      CALL ERR3PN (R,ND,CONS,NF,UIPARM)
      RETURN
      END
```

```
      SUBROUTINE ERR3PN (R,ND,CONS,NF,UIPARM)
*-----------------------------------------------------------------------
*
*       1 = FLUID        2 = SOLID
*       THE FOLLOWING PROCEDURE IS FOLLOWED
*
*       1. CALCULATE THE MIXTURE PARAMETERS AM AND BM
*
*       2. CALCULATE THE ROOTS OF THE CUBIC EOS
*
*       3. CALCULATE THE FUGACITY IN THE SUPERCRITICAL PHASE
*
*       4. CALCULATE THE FUGACITY IN THE SOLID PHASE
*
*-----------------------------------------------------------------------

      IMPLICIT DOUBLE PRECISION (A-H,O-Z)
      INTEGER UIPARM
      DOUBLE PRECISION PC(2),YEXP(100),P(100),TEMP(100),TC(2),TB(2)
      DOUBLE PRECISION AIJ(2,2),A(2),B(2),SSA,YCALC(100),ACEN(2),
     $            OA(2),OB(2),Z(2),CONS(3),COEFF(4),XF(4),VSAT(2)
      DOUBLE PRECISION ROOTS(4),RR(4),K,FUG(4),PSAT(100),R(100)
      COMPLEX*16 RT(3)
      LOGICAL FAIL
      COMMON /EXPTAL/ P, YCALC, YEXP, TEMP, NC, PSAT
      COMMON /CRPROP/ TC, PC, ACEN, TB, VSAT
      COMMON /FIN/ IFIN ,ICON

C     RG = 83.1439 bar*cm^3/mol/K
      PARAMETER (RG = 0.0831439D+3)
      SQRT2 = DSQRT(2.D0)
      NC = 2
      ERR1 = 0.0
C     CALCULATE PURE COMPONENT PARAMETERS A,B,OB,OA
      KK = 0

      IF (CONS(1).GT.0.80) THEN
              NF = 0
              RETURN
      ENDIF

      IF (CONS(1).LT.-0.10) THEN
              NF = 0
              RETURN
      ENDIF

C  Only one cons regressed
C     IF (DABS(CONS(2)).GT.700.D0) THEN
C             NF = 0
C             RETURN
C     ELSEIF (CONS(2).GT.0.001) THEN
C             NF = 0
C             RETURN
C     ENDIF

      DO 999 LL = 1,ND
              PRESS = P(LL)
              TEMPP = TEMP(LL)
          DO 200 I = 1,2
              OW = ACEN(I)
              TR = TEMPP/TC(I)
              B(I) = 0.07780D0*RG*TC(I)/PC(I)
              FW = (0.37464D0 + 1.54226D0*OW - 0.26992D0*OW**2)
              TMP1 = (1.D0+FW*(1.D0-DSQRT(TR)))**2
```

```
                A(I) = 0.45724D0*RG*RG*TC(I)*TC(I)/PC(I)*TMP1
200         CONTINUE
                ICOUNT = 0
                XF(2) = 1.D-8
                XF(1) = 1.D0 - XF(2)

C       CALCULATE THE MIXTURE PARAMETER AM

C       FIRST CALCULATE Aij
C
C       Aij = (1 - KIJ)*SQRT(Ai*Aj)
C
                DO 1500 II = 1,100
                        DO 310 I = 1,2
                                DO 310 J = 1,2
                                        IF (I.EQ.J) THEN
                                        AIJ(I,J) = A(I)
                                        ELSE
                        AIJ(I,J) = (1.D0 - CONS(1))*DSQRT(A(I)*A(J))
                                ENDIF
310                     CONTINUE

                        AM = 0.0
                        DO 330 I = 1,2
                                DO 330 J = 1,2
                                        AM = XF(I)*XF(J)*AIJ(I,J) + AM
330                     CONTINUE

                        OAM = AM*PRESS/RG**2/TEMPP**2

C       CALCULATE THE MIXTURE PARAMETER BM
                        BM = 0.D0
                        DO 350 I = 1,NC
                                BM = BM + XF(I)*B(I)
350                     CONTINUE

                        OBM = BM*PRESS/RG/TEMPP

C  Call to DPOLYG to evaluate the roots to the cubic equation
C
                COEFF(1) = 1.D0
                COEFF(2) = -(1.D0 - OBM)
                COEFF(3) = (OAM - 3.d0*OBM**2 - 2.D0*OBM )
                COEFF(4) = -( OAM*OBM - OBM**2 - OBM**3)
                NDEG = 3
                CALL DPOLYG (COEFF, NDEG, RT, FAIL)

                IF (FAIL.EQV..TRUE.) THEN
                        INFO = -1
                        RETURN
                ENDIF
                RMAX = -1.D+10
                RMIN = +1.D+10
                IND = 0
        DO 100 I = 1,NDEG
                        IF (DIMAG(RT(I)).EQ.0.0) THEN
                                RRI = DBLE(RT(I))
                                IF (RRI.GT.0.0) THEN
                                        RR(I) = RRI
                                ELSE
                                        RR(I) = +1.D+10
                                ENDIF
                                RMAX = DMAX1 (RMAX, RR(I))
                        RMIN = DMIN1 (RMIN, RR(I))
                                IND = IND + 1
                        ENDIF
```

```
100             CONTINUE

        IF (IND.EQ.1) THEN
                ROOTS(2) = RMAX
                INFO = 2
        ELSEIF (IND.GE.2) THEN
                ROOTS(1) = RMIN
                ROOTS(2) = RMAX
                INFO = 1
        ENDIF

C       DETERMINE THE CORRECT ROOT BASED ON INPUT INFORMATION

        IF (INFO.LT.0) RETURN

        ZM = ROOTS(2)
        FUG(1) = ZM
C       CALCULATE THE FUGACITY
C

        F1 = DLOG((ZM - OBM*0.414D0)/(ZM + OBM*2.414D0))
        SSA = XF(1)*AIJ(1,2) + XF(2)*AIJ(2,2)

        F2 = (2.D0*SSA/AM - B(2)/BM)*OAM/2.D0/SQRT2/OBM*F1
        F3 = B(2)/BM*(ZM - 1.D0) - DLOG(ZM - OBM) + F2
        FUG(2) = DEXP(F3)
        FUGV = FUG(2)

C       CALCULATE THE FUGACITY OF SOLID COMPONENT IN THE SOLID PHASE
C       PRINT *,XF(4),XF(2)

C     Only ICON 1 used
C             IF ((ICON.EQ.2).OR.(ICON.EQ.3)) THEN
C                PSAT2 = DEXP(CONS(2))
C             ELSE
        PSAT2 = PSAT(LL)
C             ENDIF

        FUGS = PSAT2*DEXP(VSAT(2)*(PRESS-PSAT2)/RG/TEMPP)
        XF(4) = FUGS/PRESS/FUGV
        XERR = DABS((XF(4)-XF(2))/XF(2))
        ICOUNT = ICOUNT + 1
        IF (XERR.LT.1.D-4) THEN
                GO TO 2000
        ELSE
                XF(2) = XF(4)
                XF(1) = 1.D0 - XF(2)
        ENDIF
1500    CONTINUE

2000    CONTINUE
        YCALC(LL) = XF(4)
        IF (IFIN.NE.2) THEN
                R(LL) = (YCALC(LL)-YEXP(LL))
                EE = DABS((YCALC(LL)-YEXP(LL))/YEXP(LL))
555     FORMAT(1X,4(3X,G13.5))
                ERR1 = ERR1 + EE
        ENDIF
999     CONTINUE
        ERR3P1 = ERR1/DBLE(ND)

557     FORMAT(1X,4(G13.5,A),G13.5)

        IF (IFIN.EQ.1) WRITE (78,556)TEMPP,CONS(1),PSAT2,ERR3P1
        IF (IFIN.EQ.1) WRITE (100,556)TEMPP,CONS(1),PSAT2,ERR3P1
556     FORMAT(1X,' TEMPERARTURE ',F7.2,2X,' KIJ ',F5.3,3X,' PSAT ',
```

```
     $          G12.5,' bar ERROR ',G12.5)
        IF (IFIN.EQ.2) THEN
                DO 1000 I = 1,ND
        WRITE (78,558)P(I),CHAR(09),YCALC(I),CHAR(09),TEMPP
        WRITE (100,558)P(I),CHAR(09),YCALC(I),CHAR(09),TEMPP
        WRITE (*,558)P(I),CHAR(09),YCALC(I),CHAR(09),TEMPP
558     FORMAT (1X,F8.2,A,1P,E13.6,A,0P,F8.2)

1000    CONTINUE
        ENDIF
        RETURN
        END
```

```
C       PROGRAM KBTEST3
C-----------------------------------------------------------------------------
C
C       VINOD SHAH 2/23/90 as modified by Tom Barber 3/17/90
C
C       MAIN DRIVER FOR DOING NONLINEAR REGRESSION WITH NL2SOL
C
C       This version of the program regresses all the three parameters
C        of the Kirkwood Buff LC model
C

        IMPLICIT DOUBLE PRECISION (A-H,O-Z)
        INTEGER UIPARM,IV(100),NP,NF
        INTEGER*4 ITIME
        DIMENSION R(100),V(1000)
        DOUBLE PRECISION KIJ(2), CONS(3), XTOL(2), CONSF(3), VC(2)
        DIMENSION  Z(2), FUG(2), XF(4), YCALC(100), YEXP(100), VSAT(2)
        DIMENSION P(100), TEMP(100), TC(2), PC(2), ACEN(2), TB(2)
        DIMENSION PSAT(100),PSA(10)
        CHARACTER*30 FNAME(10), FNAME1, FNAME2, FNAME3
        CHARACTER*78 SS1, SS2, SS3, SS4

        EXTERNAL ERR3KB,ERR3N
        COMMON /EXPTAL/ P, YCALC, YEXP, TEMP,  NC, PSAT
        COMMON /CRPROP/ TC, PC, ACEN, TB, VSAT ,VC
        COMMON /FIN/ IFIN ,ICON

        CALL DFAULT(IV,V)
        UIPARM = 0

C       NUMBER OF COMPONENTS  NC = 2

        NC = 2

C       FNAME1 - PROPERTIES OF CF4
C       FNAME2 - PROPERTIES OF CCL4

        OPEN (UNIT=20,FILE='KBTEST3.FIL',STATUS='OLD')
        READ (20,'(A)') FNAME1
        READ (20,'(A)') FNAME2
        READ (20,*) ICON
        READ (20,*) IPSAT
        CLOSE (UNIT=20)

        OPEN (UNIT=25,FILE='KBTEST3.DAT',STATUS='OLD')
        DO 50 I = 1,10
                READ (25,'(A)',ERR=55) FNAME(I)
50      CONTINUE
55      NFDATA = I - 1
        CLOSE (UNIT=25)

        OPEN (UNIT=30,FILE='FNAME1.TXT',STATUS='OLD')
        READ (30,'(A)') SS1
        READ (30,*) PC(1)
        READ (30,*) TC(1)
        READ (30,*) ACEN(1)
        READ (30,*) VC(1)
        CLOSE (UNIT=30)

        OPEN (UNIT=40, FILE='FNAME2.TXT',STATUS='OLD')
        READ (40,'(A)') SS2
        READ (40,*) PC(2)
        READ (40,*) TC(2)
        READ (40.*) ACEN(2)
        READ (40,*) TB(2)
```

```
      READ (40,*) VSAT(2)
      CLOSE (UNIT=40)

      OPEN (UNIT=78,FILE='KBTEST3.OUT',STATUS='UNKNOWN')
C      CALL APPEND (78) use if IBM
      OPEN (UNIT=99,FILE='KBTEST3.RES',STATUS='UNKNOWN')
C      CALL APPEND (100) use if IBM
      WRITE (78,*)'                                                  '
      WRITE (78,*)'                                                  '
      WRITE (78,*)'*************************************************'
     $          ,'*********************************'
      WRITE (100,*)'                                                 '
      WRITE (100,*)'                                                 '
      WRITE (100,*)'*************************************************'
     $          ,'*********************************'
      WRITE (100,*)' KBTEST3 '

      ND = 0
      JJ = 1
      DO 70 J = 1,NFDATA
          OPEN (UNIT=10,FILE=FNAME(J),STATUS='OLD')
          K = 1
          DO 110 I = ND+1,200
              IF ((K.EQ.1).AND.(IPSAT.EQ.2)) THEN
                  READ (10,*,ERR=115)P(I),YEXP(I),TEMP(I),PSAT(I)
                  PSA(JJ) = PSAT(I)
              ELSE
                  READ (10,*,ERR=115)P(I),YEXP(I),TEMP(I)
                  PSAT(I) = PSAT(I-1)
              ENDIF
              WRITE (78,95)P(I),YEXP(I),TEMP(I),PSAT(I)
              WRITE (*,95)P(I),YEXP(I),TEMP(I),PSAT(I)
95    FORMAT(1X,F10.2,5X,1P,E12.5,5X,0P,F10.2,5X,1P,E12.5)
              K = K + 1
110       CONTINUE
115       ND  = I - 1
          JJ = JJ + 1
          CLOSE (UNIT=10)
70    CONTINUE

      OPEN (UNIT=55,FILE='KBGUESS.DAT',STATUS='OLD')
      READ (55,*) CONS(1)
      READ (55,*) CONS(2)
      READ (55,*) CONS(3)

      WRITE (78,*) SS1
      WRITE (78,*)' PROPERTIES OF COMPONENT 1 (CF4) '
      WRITE (78,*) 'CRITICAL PRESSURE ',PC(1),' bar.'
      WRITE (78,*) 'CRITICAL TEMPERATURE ',TC(1),' K.'
      WRITE (78,*) 'ACENTRIC FACTOR ',ACEN(1)

      WRITE (78,*) SS2
      WRITE (78,*)' PROPERTIES OF COMPONENT 2 (CCL4) '
      WRITE (78,*) 'CRITICAL PRESSURE ',PC(2),' bar.'
      WRITE (78,*) 'CRITICAL TEMPERATURE ',TC(2),' K.'
      WRITE (78,*) 'ACENTRIC FACTOR ',ACEN(2)
      WRITE (78,*) 'BOILING POINT ',TB(2),' K.'
      WRITE (78,*) 'SATURATED MOLAR VOLUME ',VSAT(2),' cm^3/gmol.'

      ICC = 1

      UIPARM = 2
C     IV(1) = 12 MEANS THAT DFAULT HAS BEEN CALLED INITIALLY
C
      IV(1) = 12
```

```
C
C       IV(15) CORRESPONDS TO THE COVARIANCE MATRIX OUTPUT
C        = 1 IMPLIES SIGMA*H**-1*(J**T*J)*H**-1
C        = 2 IMPLIES SIGMA*H**-1
C        = 1 IMPLIES SIGMA*(J**T*J)**-1
C
        IV(15) = 2
C
C       V(32) = V(RCTOL)        DEFAULT MAX{ 10^-10, MACHEP^(2/3)}
C       V(33) = V(XCTOL)        DEFAULT 100*MACHEP
C       V(34) = V(XFTOL)        DEFAULT 100*MACHEP
C       BY SETTING V(32) = 1.2D-16 WE ARE TRYING TO USE THE X-CONVERGENCE
C        CRITERION.
C
C       V(32) = 1.2D-16
C       IV(39) = 1
C MINEXP                        -1024
C MAXEXP                         1023
C EPS             1.110223024625157E-016
C EPSNEG                  1.110223024625157E-016
C XMIN            5.562684646268003E-309
C XMAX            8.988465674311579E+307

        IV(24) = 0
C       V(34) = 1.11d-10
        NP = 3
        UIPARM = 0
        CALL NL2SNO(ND, NP, CONS, ERR3N, IV, V, UIPARM, URPARM, UFPARM)

        IFIN = 1
        UIPARM = 1
        CALL ERR3N(ND, NP, CONS, NF, R, UIPARM, URPARM, UFPARM)


        IFIN = 2
        TEMPER = 239.D0
        DO 900 KK = 1,NFDATA
        PINIT = 30.D0
        TEMPER = TEMPER + 5.D0
        ND = 28
        DELP = 10.D0
        DO 250 I=1,50
                P(I) = PINIT + DBLE(I-1)*DELP
                TEMP(I) = TEMPER
                PSAT(I) = PSA(KK)

C               WRITE (*,*)P(I),TEMP(I),PSAT(I)
250     CONTINUE
        CALL ERR3N(ND, NP, CONS, NF, R, UIPARM, URPARM, UFPARM)
900     CONTINUE

        STOP
        END

       SUBROUTINE ERR3N (ND, NP, CONS, NF, R, UIPARM, URPARM, UFPARM)

C-----------------------------------------------------------------------------
C
C       VINOD SHAH 5/18/879
C       THIS SUBROUTINE IS USED BY NL2SOL OR NL2SNO TO CALCULATE THE RESIDUAL
C        VECTOR R(I) FOR I = 1,N EXPERIMENTS TO BE USED FOR NONLINEAR
C        REGRESSION.
C
C
       IMPLICIT REAL*8 (A-H,O-Z)
```

```
      INTEGER N,NP,NF,UIPARM
       DOUBLE PRECISION R(100), X(10), VC(2) , PC(2), TC(2), ACEN(2),
     $ PROP(20), YCALC(100),YEXP(100),XTOL(2),KF(2),P(100),K2(2),
     $ TEMP(100),PSAT(100), TB(2), VSAT(2)
       COMMON /EXPTAL/ P, YCALC, YEXP, TEMP,  NC, PSAT
       COMMON /CRPROP/ TC, PC, ACEN, TB, VSAT, VC
       COMMON /FIN/ IFIN ,ICON

       EXTERNAL ERR3KB

       CALL ERR3KB (R,ND,CONS,NF,UIPARM)
       RETURN
       END


      SUBROUTINE ERR3KB(R,ND,BETA,NF,UIPARM)
*-----------------------------------------------------------------------------
*
*       1 = FLUID        2 = SOLID
*
*-----------------------------------------------------------------------------

        IMPLICIT DOUBLE PRECISION (A-H,O-Z)
        INTEGER NF,NP,ND,UIPARM

        DOUBLE PRECISION YEXP(100),P(100),TEMP(100), PSAT(100),ACEN(2)
        DOUBLE PRECISION YCALC(100),R(100),BETA(3),VC(2),TC(2),PC(2)
        DOUBLE PRECISION VSAT(2), TB(2)
        COMMON /EXPTAL/ P, YCALC, YEXP, TEMP,  NC, PSAT
        COMMON /CRPROP/ TC, PC, ACEN, TB, VSAT ,VC
        COMMON /FIN/ IFIN ,ICON

        PARAMETER (RG = 0.0831439D+3, RGM = 0.00831439D0)

C       R = 83.1439 bar*cm^3/mol/K
        NC = 2

        IF (BETA(2).LT.0.0) THEN
                NF = 0
                RETURN
        ENDIF
        IF (DABS(BETA(2)).GT.600.0) THEN
                NF = 0
                RETURN
        ENDIF
        ERR1 = 0.0
        ERR2 = 0.0

        DO 999 LL = 1,ND

        PRESS = P(LL)
C
C Call to subroutine ZCF4DG which returns the density, Z & Fug of pure CO2
C
        CALL ZCF4DG(PP,TEMP(LL),D,Z,F)

        TMP1 = DLOG(PSAT(LL)/PRESS) + DLOG(Z)
        A12 = BETA(1)/VC(1)*DSQRT(TC(2)/TC(1))
        TMP2 = A12*DLOG(F/D/RGM/TEMP(LL))
        TTMP = (BETA(2) + BETA(3)/TEMP(LL))
        IF (TTMP.GT.500.D0) THEN
                NF = 0
                RETURN
        ENDIF
        TMP3 =(VSAT(2) + BETA(1)*DEXP(BETA(2) + BETA(3)/TEMP(LL))-BETA(1))
```

```
     $          *(PRESS-PSAT(LL))/RG/TEMP(LL)

        YLY = TMP1 - TMP2 + TMP3
        IF (YLY.GT.500.D0) THEN
                NF = 0
                RETURN
        ENDIF

        YCALC(LL) = DEXP(YLY)
        IF (IFIN.NE.2) THEN
                EE = (YCALC(LL)-YEXP(LL))
                R(LL) = EE
        IF (UIPARM.EQ.1) WRITE (78,555)PRESS,TEMP(LL),YEXP(LL),
     $          YCALC(LL),PSAT(LL)
        IF (IFIN.EQ.1) WRITE (87,559)YEXP(LL)/PSAT(LL)*PRESS
     $          ,char(09),RHO/10.634D0
        IF (IFIN.EQ.1) WRITE (*,559)YEXP(LL)/PSAT(LL)*PRESS
     $          ,char(09),RHO/10.634D0
559     format(1x,g13.5,a,g13.5)
        IF (UIPARM.EQ.1) WRITE (*,555)PRESS,TEMP(LL),YEXP(LL),
     $          YCALC(LL),PSAT(LL)
555     FORMAT(1X,5(3x,G13.5))
                ERR1 = ERR1 + EE**2
                ERR2 = ERR2 + DABS(EE)/YEXP(LL)
        ENDIF
999     CONTINUE
        ERR1P1 = ERR1
        ERR1P2 = ERR2/DBLE(ND)*100.D0
        IF (IFIN.EQ.2) THEN
                DO 1000 I = 1,ND
                WRITE (*,558)P(I),CHAR(09),YCALC(I),CHAR(09),TEMP(I)
                WRITE (100,558)P(I),CHAR(09),YCALC(I),CHAR(09),TEMP(I)
558     FORMAT(1X,2(G13.5,A),G13.5)
1000            CONTINUE
        ENDIF

        IF (UIPARM.EQ.1) WRITE (78,556)BETA(1),BETA(2),BETA(3),
     *          ERR1P1,ERR1P2
        IF (UIPARM.EQ.1) WRITE (*,556)BETA(1),BETA(2),BETA(3),
     *          ERR1P1,ERR1P2
556     FORMAT(1X,' V21 ',G13.5,2X,' B0 ',G13.5,2X,' B1 ',G13.5,2X,
     $          ' SSE ERROR ',G13.5,' AARD %',G13.5)
        RETURN
        END
```

```
SUBROUTINE ZCF4DG (P,T,D,Z,F)
IMPLICIT REAL*8(A-H,O-Z)

C-----------------------------------------------------------------------------
C
C   CALCULATES D, Z, & F OF CF4 USING the EOS from
C
C               RUBIO; J. PHYS. CHEM., 89, 4637 (1985).
C
C   UNITS (EXCEPT WHERE NOTED OTHERWISE):
C               P (bar)
C               T (K)
C               D (GMOL/DM3)
C
C   CODED BY T.A. BARBER   3-18-90
C
C-----------------------------------------------------------------------------

C     CONSTANTS OF RUBIO EOS

      A1=0.041
      A2=1.76
      A3=-1947
      A4=1.347E+05
      A5=4.835E+08
      A6=0.53E-02
      A7=-0.337
      A8=4.0E-05
      A9=5846.E+01
      A10=-1.102E+07
      A11=6.566E+08
      A12=-28.6
      A13=7970.0
      A14=-1.2011E+06
      A15=4.749E-05
      A16=-0.0040
      R=0.083144

C     CALCULATE COEFFICIENTS IN EOS

      B1=R*T
      B2=A1*R*T + A2 + A3/T +A4/(T**2) + A5/(T**4)
      B3=A6*R*T + A7
      B4=A8*T
      B6=A15

      C1=A9/(T**2) + A10/(T**3) + A11/(T**4)
      C2=A12/(T**2) + A13/(T**3) + A14/(T**4)

C     BEGINNING DENSITY FOR ITERATION

      IF (P.LT.35.0) THEN
          D=1.0D0
        ELSE IF (P.LT.70.0) THEN
          D=2.0D0
        ELSE D=9.0D0
      ENDIF

100   D=D+0.002D0

      E=EXP(A16*(D**2))

C     CALCULATE PCALC FROM P AND T AND D GUESS

      PCALCb = B1*D + B2*(D**2) + B3*(D**3) + B4*(D**4) + B6*(D**6)
      PCALC = PCALCb + C1*E*(D**3) + C2*E*(D**5)
```

```
C     COMPARE PCALC AND P AND ITERATE D

      PDIFF = DABS((PCALC -P)/P)
      IF (PDIFF.LT.0.001) THEN GOTO 100

C     CALCULATE Z-COMPRESSIBLITY

      Z=P/(D*R*T)

      WRITE (*,*)'P=',P,'D=',D,'Z=',Z

C     CALCULATE FUG
C     F=LN(FUGACITY/D*R*T)=Z-1+[(Z-1)/D]dD

      F=B2*D/(R*T)
      F=F+B3*(D**2)/(2.*R*T)
      F=F+B4*(D**3)/(3.*R*T)
      F=F+B6*(D**5)/(5.*R*T)
      F=F+C1*E/(2.*A16*R*T)
      F=F+C2*E*(A16*(D**2)-1)/(2.*R*T*A16**2)
      F=F+Z-1

      FUG = D*R*T*DEXP(F)
      F=FUG

      END
```

```
      PROGRAM PRCALCY
C-----------------------------------------------------------------------
C
C     TOM BARBER 3/12/90
C     CALCULATES Y FROM P & T
C
C
C

      IMPLICIT DOUBLE PRECISION (A-H,O-Z)
      DIMENSION R(100),V(1000)
      DOUBLE PRECISION KIJ(2), CONS(3), CONSF(3)
      DIMENSION  Z(2), FUG(2), XF(4), YCALC(100), VSAT(2)
      DIMENSION P(100), TEMP(100), TC(2), PC(2), ACEN(2), TB(2)
      DIMENSION PSAT(100), PSA(10)
      CHARACTER*30 FNAME(10), FNAME1, FNAME2
      CHARACTER*78 SS1, SS2

      EXTERNAL ERR3PN
      COMMON /EXPTAL/ P, YCALC, TEMP,  NC, PSAT
      COMMON /CRPROP/ TC, PC, ACEN, TB, VSAT

C     NUMBER OF COMPONENTS NC=2
      NC = 2

      OPEN (UNIT=20,FILE='TBNTEST.FIL',STATUS='OLD')
      READ (20,'(A)') FNAME1
      READ (20,'(A)') FNAME2
      CLOSE (UNIT=20)
C
      OPEN (UNIT=25,FILE='TEST.DAT',STATUS='OLD')
      DO 50 I = 1,10
              READ (25,'(A)',ERR=55) FNAME(I)
50    CONTINUE
55    NFDATA = I - 1
      CLOSE (UNIT=25)

      OPEN (UNIT=30,FILE=FNAME1,STATUS='OLD')
      READ (30,'(A)') SS1
      READ (30,*) PC(1)
      READ (30,*) TC(1)
      READ (30,*) ACEN(1)
      CLOSE (UNIT=30)

      OPEN (UNIT=40, FILE=FNAME2,STATUS='OLD')
      READ (40,'(A)') SS2
      READ (40,*) PC(2)
      READ (40,*) TC(2)
      READ (40,*) ACEN(2)
      READ (40,*) TB(2)
      READ (40,*) VSAT(2)
      CLOSE (UNIT=40)

      OPEN (UNIT=78,FILE='TEST.OUT',STATUS='UNKNOWN')

      OPEN (UNIT=100,FILE='TEST.RES',STATUS='UNKNOWN')

      WRITE (78,*)'*************************************************',
     $ '*****************'
      WRITE (100,*)'*************************************************',
     $ '*****************'

      ND = 0
      JJ = 1
      DO 70 J = 1,NFDATA
```

```
          OPEN (UNIT=10,FILE=FNAME(J),STATUS='OLD')
          K = 1
          DO 110 I = ND+1,200
                READ (10,*,ERR=115)P(I),TEMP(I),PSAT(I)
                PSA(JJ) = PSAT(I)
            WRITE (78,95)P(I),TEMP(I),PSAT(I)
            WRITE (100,95)P(I),TEMP(I),PSAT(I)
95      FORMAT(1X,F10.2,5X,1P,E12.5,5X,1P,E12.5)
            K = K + 1
110       CONTINUE
115       ND  = I - 1
          JJ = JJ + 1
          CLOSE (UNIT=10)
70      CONTINUE

        OPEN (UNIT=55,FILE='KIJ.DAT',STATUS='OLD')
        READ (55,*) CONS

        WRITE (78,*) SS1
        WRITE (78,*)' PROPERTIES OF COMPONENT 1 (CF4) '
        WRITE (78,*) 'CRITICAL PRESSURE ',PC(1),' bar.'
        WRITE (78,*) 'CRITICAL TEMPERATURE ',TC(1),' K.'
        WRITE (78,*) 'ACENTRIC FACTOR ',ACEN(1)

        WRITE (78,*) SS2
        WRITE (78,*)' PROPERTIES OF COMPONENT 2 (CCL4) '
        WRITE (78,*) 'CRITICAL PRESSURE ',PC(2),' bar.'
        WRITE (78,*) 'CRITICAL TEMPERATURE ',TC(2),' K.'
        WRITE (78,*) 'ACENTRIC FACTOR ',ACEN(2)
        WRITE (78,*) 'BOILING POINT ',TB(2),' K.'
        WRITE (78,*) 'SATURATED MOLAR VOLUME ',VSAT(2),' cm^3/gmol.'

        CALL ERR3PN  (CONS,ND)

        STOP
        END


        SUBROUTINE ERR3PN (CONS,ND)

*-----------------------------------------------------------------------------
*
*       1 = FLUID        2 = SOLID
*       THE FOLLOWING PROCEDURE IS FOLLOWED
*
*       1. CALCULATE THE MIXTURE PARAMETERS AM AND BM
*
*       2. CALCULATE THE ROOTS OF THE CUBIC EOS
*
*       3. CALCULATE THE FUGACITY IN THE SUPERCRITICAL PHASE
*
*       4. CALCULATE THE FUGACITY IN THE SOLID PHASE
*
*-----------------------------------------------------------------------------

        IMPLICIT DOUBLE PRECISION (A-H,O-Z)

        DOUBLE PRECISION PC(2),P(100),TEMP(100),TC(2)
        DOUBLE PRECISION AIJ(2,2),A(2),B(2),SSA,YCALC(100),ACEN(2),
     $          OA(2),OB(2),Z(2),CONS(3),COEFF(4),XF(4),VSAT(2)
        DOUBLE PRECISION ROOTS(4),RR(4),K,FUG(4),PSAT(100),R(100)
        COMPLEX*16 RT(3)
        LOGICAL FAIL
        COMMON /EXPTAL/ P, YCALC, TEMP, NC, PSAT
```

```
      COMMON /CRPROP/ TC, PC, ACEN, TB, VSAT

C     RG = 83.1439 bar*cm^3/mol/K
      PARAMETER (RG = 0.0831439D+3)
      SQRT2 = DSQRT(2.D0)
      NC = 2
      ERR1 = 0.0
C     CALCULATE PURE COMPONENT PARAMETERS A,B,OB,OA
      KK = 0

      DO 999 LL = 1,ND
              PRESS = P(LL)
              TEMPP = TEMP(LL)
          DO 200 I = 1,2
              OW = ACEN(I)
              TR = TEMPP/TC(I)
              B(I) = 0.07780D0*RG*TC(I)/PC(I)
              FW = (0.37464D0 + 1.54226D0*OW - 0.26992D0*OW**2)
              TMP1 = (1.D0+FW*(1.D0-DSQRT(TR)))**2
              A(I) = 0.45724D0*RG*RG*TC(I)*TC(I)/PC(I)*TMP1
200       CONTINUE
              ICOUNT = 0
              XF(2) = 1.D-2
              XF(1) = 1.D0 - XF(2)

C     CALCULATE THE MIXTURE PARAMETER AM

C     FIRST CALCULATE Aij
C
C     Aij = (1 - KIJ)*SQRT(Ai*Aj)
C
              DO 1500 II = 1,100
                      DO 310 I = 1,2
                              DO 310 J = 1,2
                                      IF (I.EQ.J) THEN
                                      AIJ(I,J) = A(I)
                                      ELSE
                      AIJ(I,J) = (1.D0 - CONS(1))*DSQRT(A(I)*A(J))
                              ENDIF
310                   CONTINUE

                      AM = 0.0
                      DO 330 I = 1,2
                              DO 330 J = 1,2
                                      AM = XF(I)*XF(J)*AIJ(I,J) + AM
330                   CONTINUE

                      OAM = AM*PRESS/RG**2/TEMPP**2

C     CALCULATE THE MIXTURE PARAMETER BM
                      BM = 0.D0
                      DO 350 I = 1,NC
                              BM = BM + XF(I)*B(I)
350                   CONTINUE

                      OBM = BM*PRESS/RG/TEMPP

C  Call to DPOLYG to evaluate the roots to the cubic equation
C
              COEFF(1) = 1.D0
              COEFF(2) = -(1.D0 - OBM)
              COEFF(3) = (OAM - 3.d0*OBM**2 - 2.D0*OBM )
              COEFF(4) = -( OAM*OBM - OBM**2 - OBM**3)
              NDEG = 3
              CALL DPOLYG (COEFF, NDEG, RT, FAIL)
```

```
                IF (FAIL.EQV..TRUE.) THEN
                        INFO = -1
                        RETURN
                ENDIF
                RMAX = -1.D+10
                RMIN = +1.D+10
                IND = 0
        DO 100 I = 1,NDEG
                        IF (DIMAG(RT(I)).EQ.0.0) THEN
                                RRI = DBLE(RT(I))
                                IF (RRI.GT.0.0) THEN
                                        RR(I) = RRI
                                ELSE
                                        RR(I) = +1.D+10
                                ENDIF
                                RMAX = DMAX1 (RMAX, RR(I))
                        RMIN = DMIN1 (RMIN, RR(I))
                                IND = IND + 1
                        ENDIF
100             CONTINUE

        IF (IND.EQ.1) THEN
                ROOTS(2) = RMAX
                INFO = 2
        ELSEIF (IND.GE.2) THEN
                ROOTS(1) = RMIN
                ROOTS(2) = RMAX
                INFO = 1
        ENDIF

C       DETERMINE THE CORRECT ROOT BASED ON INPUT INFORMATION

        IF (INFO.LT.0) RETURN

        ZM = ROOTS(2)
        FUG(1) = ZM
C       CALCULATE THE FUGACITY
C

        F1 = DLOG((ZM - OBM*0.414D0)/(ZM + OBM*2.414D0))
        SSA = XF(1)*AIJ(1,2) + XF(2)*AIJ(2,2)

        F2 = (2.D0*SSA/AM - B(2)/BM)*OAM/2.D0/SQRT2/OBM*F1
        F3 = B(2)/BM*(ZM - 1.D0) - DLOG(ZM - OBM) + F2
        FUG(2) = DEXP(F3)
        FUGV = FUG(2)

C       CALCULATE THE FUGACITY OF SOLID COMPONENT IN THE SOLID PHASE
C       PRINT *,XF(4),XF(2)

        PSAT2 = PSAT(LL)

        FUGS = PSAT2*DEXP(VSAT(2)*(PRESS-PSAT2)/RG/TEMPP)
        XF(4) = FUGS/PRESS/FUGV
        XERR = DABS((XF(4)-XF(2))/XF(2))
        ICOUNT = ICOUNT + 1
        IF (XERR.LT.1.D-4) THEN
                GO TO 2000
        ELSE
                XF(2) = XF(4)
                XF(1) = 1.D0 - XF(2)
        ENDIF
1500    CONTINUE

2000    CONTINUE
```

```
      YCALC(LL) = XF(4)

555   FORMAT(1X,4(3X,G13.5))

999   CONTINUE

557   FORMAT(1X,4(G13.5,A),G13.5)

      DO 1000 I = 1,ND
      WRITE (78,558)P(I),CHAR(09),YCALC(I),CHAR(09),TEMPP
      WRITE (100,558)P(I),CHAR(09),YCALC(I),CHAR(09),TEMPP
      WRITE (*,558)P(I),CHAR(09),YCALC(I),CHAR(09),TEMPP
558   FORMAT (1X,F8.2,A,1P,E13.6,A,0P,F8.2)

1000  CONTINUE

      RETURN
      END
```

```
1 '*****************************************************************************
2 '
3 '  PROGRAM CF4RHO CONVERTS PRESSURE TO DENSITY AT A SPECIFIC TEMPERATURE
4 '
5 '  USES THE EOS FROM RUBIO; J. PHYS. CHEM., 89, 4637 (1985)
6 '
7 '*****************************************************************************
10 ' A constants of Rubio EOS
20 A1=.041
30 A2=1.76
40 A3=-1947!
50 A4=134700!
60 A5=4.835E+08
70 A6=.0053
80 A7=-.337
90 A8=.00004
100 A9=58460!
110 A10=-1.102E+07
120 A11=6.566E+08
130 A12=-28.6
140 A13=7970!
150 A14=-1201100!
160 A15=4.749E-05
170 A16=-.004
180 R=.083144
190 ' input T(K) and P(bar)
200 TC=227.6
210 INPUT "temperature (K)";T
290 ' calc powers temp
300 T1=T
310 T2=T1*T1
320 T3=T2*T1
330 T4=T3*T1
340 T5=T4*T1
350 ' calc Bi terms of Rubio EOS
351 B1=R*T
360 B2=A1*R1+A2+A3/T+A4/T2+A5/T4
370 B3=A6*B1+A7
380 B4=AR*T
390 C1=A9/T2+A10/T3+A11/T4
391 C2=A12/T2+A13/T3+A14/T4
400 B6=A15
409 DIM RHO(30)
410 F=0!
411 DIM P(30)
412 DATA 30, 40, 50, 60, 70, 80, 90, 100, 110, 120
413 DATA 130, 140, 150, 160, 170, 180, 190, 200, 210, 220
414 DATA 230, 240, 250, 260, 270, 280, 290, 300, 310, 320
420 FOR I = 1 TO 30
421 READ P(I)
422 NEXT I
430 OPEN "RHO.DAT" FOR OUTPUT AS #1
440 FOR K = 1 TO 30
441 P = P(K)
442 IF P < 50 THEN DEN =1
443 IF P => 50 AND P < 90 THEN DEN = 3
444 IF P => 90 AND P < 120 THEN DEN = 8
445 PRINT "P",P
446 IF P => 120 AND P < 200 THEN DEN = 9
447 IF P => 200 THEN DEN = 11
460 ' calc powers of density
470 'start of loop
471 DEN = DEN +.002
480 RR=DEN
```

```
491 RR3=RR2*RR
500 RR4=RR2*RR2
510 RR5=RR2*RR3
520 RR6=RR3*RR3
530 ' calc P=PCALC from rubio EOS
540 PCALCB=B1*RR+B2*RR2+B3*RR3+B4*RR4+B6*RR6
550 PCALC=PCALCB+(C1*EXP(A16*RR2)*RR3)
560 PCALC=PCALC+(C2*EXP(A16*RR2)*RR5)
570 ' calc Z
580 Z=PCALC/(R*T*RR)
590 ' compare PCALC from Rubio EOS with input value
600 IF ABS(PCALC-P)/P > .001 THEN 471
605 RHO(K) = DEN
610 PRINT #1 , USING "##.###,";RHO(K)
620 NEXT K
630 END
```

```
1 '*****************************************************************************
10 ' PROGRAM ENHANCE.BAS CALCULATES FACTOR E FOR EXPERIMENTAL DATA
20 ' PRESSURE IN BAR --- E = X*P/PSAT
21 '*****************************************************************************
30 P$ = "P="
40 X$ = "X="
50 E$ = "E="
60 OPEN "ENH.OUT" FOR OUTPUT AS #1
70 INPUT "PSAT (BAR)=";PSAT
71 ' COMMENT OUT DATA THAT DOESN'T APPLY FOR EACH ISOTHERM,ADJUST FOR LOOPS
80 DIM X (18)
90 'DATA .003669, .005129, .005939, .006059, .005548, .006164
100 'DATA.00455, .00934, .00945, .00952, .00956, .00382, .00775, .00724, .00722,
         .00749, .00823, .00852, .00822
110  DATA .00051, .00043, .00051, .00141, .00220, .00299,
          .00495, .00490, .00733, .01063, .01463, .01448, .01429, .01667,
          .01938, .01831, .01920, .02006
120 'DATA .00163, .00574, .01329, .02101, .02200, .02100, .02100,
          .02250, .02380, .02360, .02490, .02550, .02580
121 FOR I = 1 TO 18
122 READ X(I)
123 NEXT I
130 DIM E (18)
140 DIM P(18)
150 'DATA 68.95, 86.18, 103.42, 136.86, 206.84, 274.41
160 'DATA 67.64, 136.51, 205.12, 205.94, 273.72, 67.57, 135.20, 136.17, 136.51,
          204.43, 273.72, 274.75, 275.79
170 DATA 12.96, 23.78, 33.78, 50.67, 61.02, 67.58, 69.70, 85.84,
         101.35, 103.08, 136.86, 137.55, 138.24, 171.33, 240.90, 210.97,
         238.21, 276.13
180 'DATA 34.47, 68.95, 103.76, 136.51, 137.27, 137.55, 137.89,
          171.68, 204.77, 206.49, 239.23, 274.06, 308.85
181 FOR I = 1 TO 18
182 READ P(I)
183 NEXT I
190 ' CALC E LOOP
200 FOR I = 1 TO 18
220 E(I) = X(I)*P(I)/PSAT
230 WRITE #1, P$,P(I),X$,X(I),E$,E(I)
231 PRINT P$;P(I);X$;X(I);E$;E(I)
232 LPRINT P$;P(I);X$;X(I);E$;E(I)
240 NEXT I
300 END
```

```
1 '*****************************************************************************
2 '
3 '              CALCULATES MOLE FRACTION FROM ION CURRENT
4 '
5 '      BASED ON POLYNOMIAL EQN I=A0+A1*X+A2*X^2+A3*X^3 WHERE A0=0
6 '
7 '*****************************************************************************
10 INPUT "enter I";I
100 IF I<= .2 THEN X=0
110 IF I<.4 AND I > .2 THEN X=.0015
120 IF I<.6 AND I >= .4 THEN X=.0035
130 IF I<.8 AND I >= .6 THEN X=.0055
140 IF I<1! AND I>= .8 THEN X=.0075
150 IF I<1.2 AND I>= 1! THEN X=.0095
160 IF I<1.4 AND I>= 1.2 THEN X=.0115
170 IF I<1.6 AND I>= 1.4 THEN X=.0135
180 IF I<1.8 AND I>= 1.6 THEN X=.0155
190 IF I<2! AND I>= 1.8 THEN X=.0175
200 IF I>2! THEN X=.0195
500 X=X+.000001
510 A1= 84.49*X
520 A2= 3857*X^2
530 A3= -194500!*X^3
540 INEW = A1+A2+A3
550 PRINT "inew=";INEW
560 IF ABS( (I-INEW)/I) > .002 THEN 500
570 PRINT "x=";X
1000 END
```

INTENSITY AS A FUNCTION OF PRESSURE LINSTAT.SSF

Intensity I	Pressure P(x)	I/P (y)	x**2	y**2
1.00	1.12	0.89286	1.2544	0.797
1.40	1.37	1.02190	1.8769	1.044
2.05	1.70	1.20588	2.8900	1.454
7.27	3.90	1.86410	15.2100	3.475
2.03	1.69	1.20118	2.8561	1.443
1.42	1.39	1.02158	1.9321	1.044
6.80	3.93	1.73028	15.4449	2.994
		*		
	15.100	8.93779	41.4644	12.251
	2.157	1.276827		

y-bar	1.276827
x-bar	2.157
Sum (x-x-bar)**2	8.892
Sum (y-y-bar)**2	0.839
Sum (x-x-bar)(y-y-bar)	2.690
r**2	0.683
r	0.826
sigma**2	0.053
sigma r	0.231
95%L	0.224
b	0.303
a-b*x-bar	0.624

(sigma ri)**2 = (sigma r)**2[1 + |xi-x-bar|**2/(Sum(x-x-bar)**2]

I/P = 0.62424 + 0.30253P
I= 0.62424P + 0.30253P**2

xy	Calculated I	INPUT P	CAL I FROM INPUT P	95 % C. I. const. sig r
1.0000	1.079	3.720	6.509	0.834
1.4000	1.423	3.725	6.523	0.835
2.0500	1.936	3.725	6.523	0.835
7.2700	7.036	3.725	6.523	0.835
2.0300	1.919	4.150	7.801	0.930
1.4200	1.452	4.130	7.738	0.926
6.8000	7.126	4.090	7.614	0.917
		4.200	7.958	0.941
21.9700		1.380	1.438	0.309

var. of I/P by eq.	std. dev.in I	95 % C. I. (better)	I(1.38)/I(x)	95 % C. I.
0.068	1.696	1.647	0.221	0.076
0.068	1.701	1.652	0.220	0.076
0.068	1.701	1.652	0.220	0.076
0.068	1.701	1.652	0.220	0.076
0.077	2.165	2.103	0.184	0.066
0.077	2.141	2.080	0.186	0.066
0.076	2.094	2.034	0.189	0.067
0.078	2.226	2.162	0.181	0.065
0.057	0.343	0.333	1.000	0.328

I (exp)	I (exp error)	I (corr)	I (corr err)
0.200	0.025	0.044	0.016
0.170	0.025	0.037	0.014
0.200	0.025	0.044	0.016
0.570	0.025	0.126	0.043
1.100	0.025	0.203	0.072
1.520	0.025	0.282	0.100
2.620	0.025	0.495	0.175
4.200	0.025	0.759	0.271

APPENDIX D

DATA VALIDATION

The 244K and 249K isotherms presented in Chapter 5 were only two of four isotherms obtained. Data at 234K and 239K were also taken. These data are presented in Table D.1 and Figure D.1. The broad scatter in the data cannot be easily explained as random sampling error. An attempt to "quantify" the accuracy of the data is presented.

There were two major experimental areas of concern for all isotherms - temperature uniformity and mass transfer which approaches an equilibrium condition.

D.1 Column Temperature Uniformity

As discussed in the experimental section, a small fan internal to the enclosure was utilized to circulate the cold air bath. The volume of air moved and its turbulence were often insufficient to keep a uniform temperature throughout the enclosure. During early experimental runs the exit temperature of the column was maintained at the recorded isothermal temperature with an average Δ T along the columns axis of 1.5K. This problem was alleviated by the addition of the copper cylinder around the column, keeping the entire column at a uniform temperature. Selected data from previously taken isotherms were duplicated (136.86 bar @ 244K) to within 1.5% (less than accumulated error). It was concluded that previous data were valid with respect to column temperature and that the scatter in the data was probably not attributable to column temperature variations. It should be noted that some of the raw data has been excluded for loss of temperature control due to equipment malfunction as annotated in Appendix A.

Table D.1. Solubility Isotherms of CCl_4 in Supercritical CF_4 at 234K and 239K

239K				234K			
P (bar)	y (-)	ρ (gmol/l)	E (-)	P (bar)	y (-)	ρ (gmol/l)	E (-)
67.57	0.00382	10.31	55.21	68.95	0.00367	11.31	80.18
69.67	0.00455	10.31	65.82	86.18	.00513	12.04	140.10
135.20	0.00775	12.79	224.13	102.73	0.00622	12.52	202.53
136.17	0.00724	12.81	210.88	102.73	0.00507	12.52	165.08
136.51	0.00722	12.82	210.82	103.42	0.00594	12.53	194.68
136.51	0.00934	12.82	272.73	135.48	0.00609	13.20	261.51
204.43	0.00749	13.83	327.53	136.86	0.00603	13.22	261.57
205.12	0.00945	13.84	414.63	136.86	0.00606	13.22	262.83
205.94	0.00952	13.85	419.37	171.68	0.00520	13.74	282.96
273.72	0.00823	14.52	481.86	205.46	0.00662	14.14	431.11
273.72	0.00956	14.52	559.74	206.84	0.00555	14.16	363.85
274.75	0.00852	14.53	500.72	243.73	0.00520	14.52	387.80
275.79	0.00822	14.54	484.92	273.03	0.00605	14.77	523.56
				274.41	0.00618	14.78	537.51
				275.00	0.00601	14.79	523.85

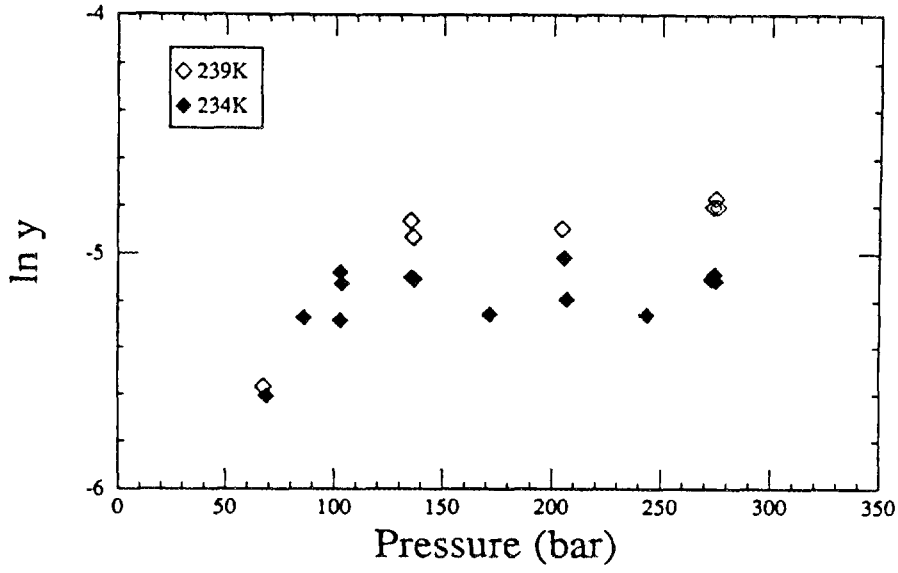

Fig D.1. Mole fraction of CCl_4 vs. Pressure at 234K and 239K.

D.2 Mass Transfer Equilibrium

In a dynamic apparatus, the critical factors in reaching a mass transfer condition approaching equilibrium are the residence time of the SCF (determined by the volumetric flow rate) and the surface area contact between the solute and SCF. The column was packed with fine, irregularly shape particles of CCl_4 with the average load being approximately 62% of the column volume. Experiments were run in order to determine the maximum superficial velocity, $\bar{v}_0$, that approached equilibrium conditions and operate in that region. Figure D.2 shows the effect of $\bar{v}_0$ on three isotherms from the data in Table D.2. As previously displayed in the experimental chapter (Figure 4.5) as a function of volumetric flow rate, the 244K and the 249K isotherms appear to approach equilibrium at $\bar{v}_0 < 0.2$

Table D.2. Flow Rate Experiment Results

Isotherm	Date	P	FR	I/P	$\bar{v}_0$	$\bar{v}(\varepsilon=.4)$
249K	06/29	136.51	0.025	1.522	0.151	0.377
	07/13	137.89	0.020	1.522	0.121	0.301
	07/14	137.55	0.015	1.522	0.090	0.226
	07/18	136.86	0.090	1.449	0.542	1.356
	07/18	137.55	0.035	1.525	0.211	0.527
	07/18	136.17	0.170	1.151	1.020	2.560
244K	01/24	138.24	0.040	1.036	0.233	0.582
	02/10	137.55	0.020	1.049	0.116	0.291
	02/10	137.55	0.130	0.849	0.756	1.891
	02/10	136.86	0.065	1.004	0.378	0.946
	02/10	136.86	0.220	0.504	1.280	3.200
	06/22	136.86	0.025	1.058	0.145	0.364
239K	05/23	136.51	0.020	0.751	0.113	0.282
	05/23	137.55	0.025	0.725	0.141	0.353
	05/23	136.51	0.040	0.599	0.226	0.564
	05/23	136.17	0.060	0.488	0.339	0.846
	05/23	136.17	0.085	0.483	0.480	1.200
	05/23	136.17	0.125	0.424	0.705	1.763

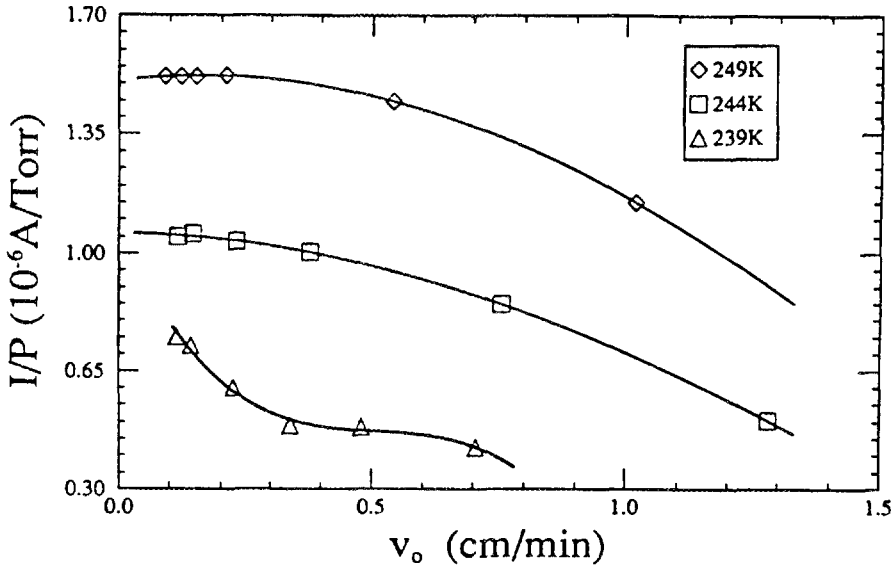

Fig. D.2. I/P vs. superficial velocity results.

cm/min. In distinct contrast the 239K isotherm appears to be much more sensitive to $\bar{v}_0$ in approaching equilibrium. A rapid drop in mole fraction occurs between 0.11 and 0.35 cm/min. This velocity region is where most of the 234K and 239K data were recorded. It should also be noted that the superficial velocity required to approach equilibrium for the 244K and 249K isotherms were considerably less than anticipated.

Table D.3 and Figure D.3 illustrate how the mean velocity, $\bar{v}$, of the SCF varies with temperature through the column under the following conditions: the column void space is 40% and the exiting low pressure volume of CF_4 is 0.05 l/min. Three points can be made:

(1) the velocity at 239K is slightly slower than 244K because of increased density;

(2) the velocity profile tends to flatten out at pressure twice the critical pressure of CF_4, 65 bar, which means the residence time is roughly the same in all cases; and

(3) the velocity is such that if the flow was through a smooth pipe, it would be laminar with a Reynold's number estimated to be approximately 120. The Ergun equation also supports the estimation of a Reynold's number between 1 and 1000.

Table D.3. Column Velocities at Different Pressures

	244K		239K	
P(bar)	$\bar{v}_0$(cm/min)	$\bar{v}$(cm/min)	$\bar{v}_0$(cm/min)	$\bar{v}$(cm/min)
30	1.85	4.62	1.75	4.38
40	1.18	2.95	1.07	2.69
50	0.75	1.86	0.60	1.49
60	0.47	1.18	0.39	0.97
70	0.39	0.97	0.35	0.87
80	0.35	0.89	0.33	0.82
90	0.34	0.84	0.32	0.79
100	0.32	0.80	0.31	0.77
120	0.31	0.76	0.29	0.74
140	0.29	0.73	0.28	0.71
180	0.28	0.69	0.27	0.68
240	0.26	0.66	0.26	0.64
280	0.26	0.66	0.25	0.63

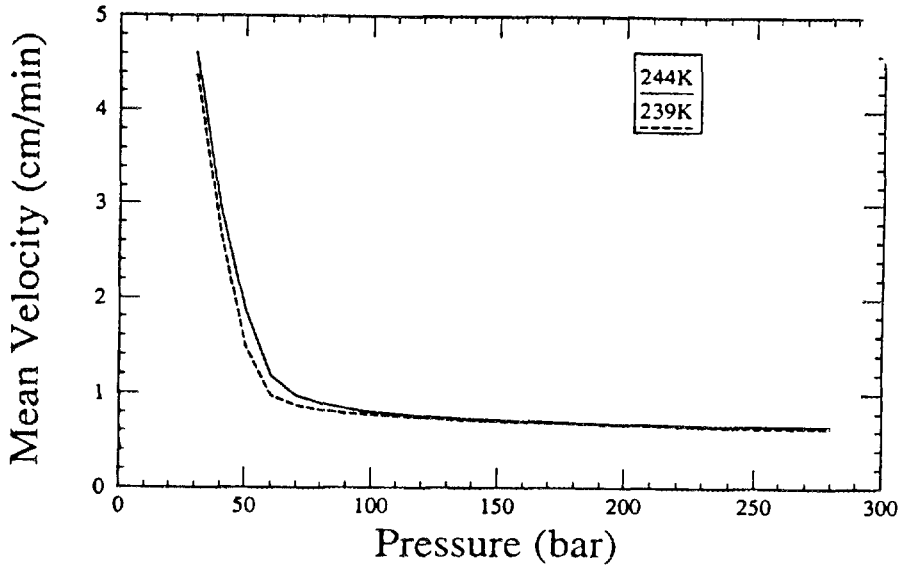

Fig. D.3. Column mean velocity profile.

The low mass transfer coefficient observed is undoubtedly influenced by channeling in the extraction column. Channeling at the wall surface where the packing is less dense provides a quick path for the SCF through the column. This essentially forms a 'plug' of solute where the effective surface area is greatly reduced and the velocity of CF_4 is much greater than the mean velocity.

If one assumes that (1) each column was packed equally well and presented approximately the same surface area for all isotherms and (2) the flow rates actually favor equilibrium at lower temperatures, then the effect of temperature probably reflects some physical change to the column or packing which enhances channeling.

During the operations of three of the four isotherms, an increase in Δ P with a decrease in flow rate was observed. This often resulted in complete blockage of flow or 'plugging'. One of the major disadvantages to a flow type apparatus is the inability to

observe if any phase changes are occurring in the equilibrium cell. It is possible that a third (liquid) phase was formed and later froze into a solid inhibiting the passage of the SCF. Other plausible explanations include:

(1) rapid expansion of the solute rich SCF phase condenses CCl_4 on the metering valve outlet to form a plug

(2) local temperature variation within the column causing regions of higher solubility which condense CCl_4 when passing through a colder temperature region.

Without building a static apparatus to determine any phase changes, the question as to why plugging occurred will remain unanswered.

D.3 234K and 239K Isotherms Validity

As discussed, the $\bar{v}_0$ at which these data were recorded cannot be said with confidence to have approached equilibrium; but, do the data have any validity?

With the use of the P-R compressed gas model and the following assumptions:

(1) the 239K isotherm approached equilibrium at a superficial velocity of 0.112 cm/min.; and

(2) the I/P vs. $\bar{v}_0$ curve for the 234K isotherm would be similar to the 239K isotherm

one can propose that the data are within certain limits of the projected equilibrium value.

D.3.1 239K Isotherm Data Validity

It was observed that the 239K isotherm contained essentially two different data sets

distinguished by the flow rate at which they were taken. Data taken on 04/24-25/89 had a $\overline{v}_0$ of 0.141 cm/min whereas data taken between 04/28/9 and 05/03/89 had an average $\overline{v}_0$ of 0.197 cm/min. With respect to Figure D.3 the 04/24-25/89 data closely approached the equilibrium superficial velocity.

Figure D.4 presents the P-R modeling of each set of data. An excellent correlation was found in both cases with an AAD < 6%. Figure D.5 is a plot of k_{ij} parameters regressed from each individual isotherm. The plot shows that the k_{ij} parameter appears to have a near linear dependence on temperature.

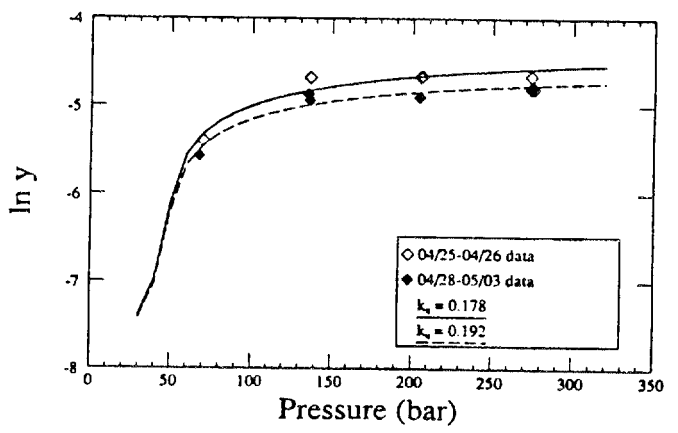

Fig. D.4. P-R Modeling at 249K.

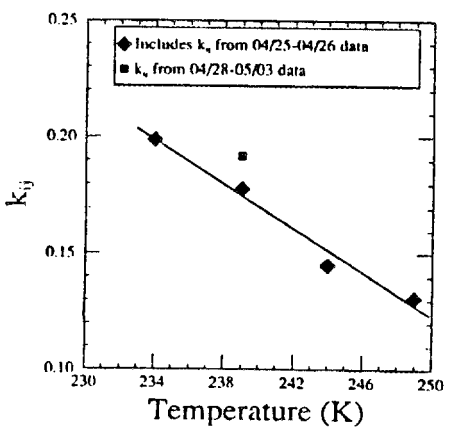

Fig. D.5. Temperature Dependence of k_{ij}.

Based on the k_{ij} of the 04/25-04/26 data and the superficial velocity at which the data were taken, these data closely represent the solubility at equilibrium. By looking at the ratio of I/P values at $\bar{v}_0$ = 0.112 and $\bar{v}_0$ = 0.141 cm/min, one can estimate that the 04/25-04/26 data were within 95% of the equilibrium mole fraction.

D.3.2 234K Isotherm Data Validity

The "validation" of the 234K data becomes even more questionable in the absence of superficial velocity vs. I/P data.

Figure D.6 presents the P-R modeling of the data. With an AAD of 11.4%, the model supports that the data are consistent for the condition under which they were taken. By applying the assumption that the I/P vs. $\bar{v}_0$ profiles for 234K and 239K would be similar and the average $\bar{v}_0$ was 0.2 cm/min., then one can estimate that the 234K isotherm was within 85% of the equilibrium mole fraction.

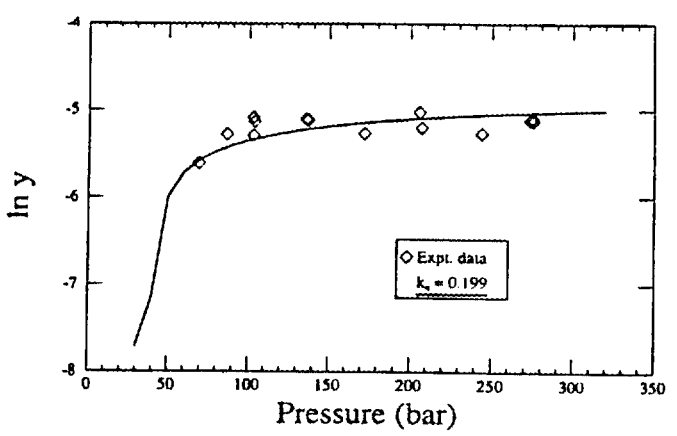

Fig. D.6. P-R Modeling at 234K.

INTERNAL DISTRIBUTION

1. T. A. Barber
2. J. M. Begovich
3. J. T. Bell
4. C. H. Brown
5. C. H. Byers
6. H. D. Cochran
7. E. D. Collins
8. A. G. Croff
9. W. Fulkerson
10. R. K. Genung
11. J. R. Hightower
12. E. K. Johnson
13. T. H. Row
14. C. D. Scott
14. M. G. Stewart
15. Central Research Library

16–17. Laboratory Records

18. Laboratory Records, RC
19. ORNL Y-12 Technical Library
    Document Reference Section
20. ORNL Patent Section

EXTERNAL DISTRIBUTION

21. Office of Assistant Manager for Energy Research and Development, DOE-ORO, Oak Ridge, TN 37831
22. R. L. Gordon, Office of Basic Energy Sciences, DOE, Room G-339/GTN, Washington, D.C. 20454
23. F. Dee Stevenson, Office of Basic Energy Sciences, DOE, Room G-341/GTN, Washington, D.C. 20454
24. P. R. Bienkowski, Department of Chemical Engineering, University of Knoxville, Knoxville, Tennessee 37916

25–31. D. M. Pfund, 1751 Chester, Lansing, MI 48913

32–41. Office of Scientific and Technical Information, P.O. Box 62, Oak Ridge, TN 37831